Using Parameters Space Analysis Techniques for Diagnostic Purposes in the Framework of Empirical Model Validation

A Report of Task 22, Subtask A
Building Energy Analysis Tools
December 2002

USING PARAMETERS SPACE ANALYSIS TECHNIQUES FOR DIAGNOSTIC PURPOSES IN THE FRAMEWORK OF EMPIRICAL MODEL VALIDATION

THEORY, APPLICATIONS AND COMPUTER IMPLEMENTATION

Elena PALOMO DEL BARRIO
LEPT-ENSAM UMR 8508
Esplanade des Arts et Métiers
F-33405 Talence Cedex

Gilles GUYON
Electricité de France
Direction des Etudes et Recherches
Les Renardières, BP 1
F-77250 Moret-sur-Loing

Preface

INTRODUCTION TO THE INTERNATIONAL ENERGY AGENCY

BACKGROUND

The International Energy Agency (IEA) was established in 1974 as an autonomous agency within the framework of the Economic Cooperation and Development (OCDE) to carry out a comprehensive program of energy cooperation among its 25 member countries and the Commission of the European Communities.

An important part of the Agency's program involves collaboration in the research, development and demonstration of new energy technologies to reduce excessive reliance on imported oil, increase long-term energy security and reduce greenhouse gas emissions. The IEA's R&D activities are headed by the Committee on Energy Research and Technology (CERT) and supported by a small Secretariat staff, headquartered in Paris. In addition, three Working Parties are charged with monitoring the various collaborative energy agreements, identifying new areas for cooperation and advising the CERT on policy matters.

Collaborative programs in the various energy technology areas are conducted under Implementing Agreements, which are signed by contracting parts (government agencies or entities designated by them). There are currently 42 Implementing Agreements covering fossil fuel technologies, renewable energy technologies, efficient energy end-use technologies, nuclear fusion science and technology, and energy technology information centers.

SOLAR HEATING AND COOLING PROGRAM

The Solar Heating and Cooling program was one of the first IEA Implementing Agreements to be established. Since 1977, its 21 members have been collaborating to advance active solar, passive solar and photovoltaic technologies and their application in buildings.

The members are:

Australia	Finland	Norway
Austria	France	Portugal
Belgium	Italy	Spain
Canada	Japan	Sweden
Denmark	Mexico	Switzerland
European Commission	Netherlands	United Kingdom
Germany	New Zealand	United States

A total of 30 Tasks have been initiated, 21 of which have been completed. Each Task is managed by an Operating Agent from one of the participating countries. Overall control of the program rests with an Executive Committee comprised of one representative from each contracting party to the

Implementing Agreement. In addition, a number of special ad hoc activities – working groups, conferences and workshops – have been organised.

The Tasks of the IEA Solar Heating and Cooling Programme, both completed and current, are as follows:

Completed Tasks

Task 1	Investigation of the Performance of Solar Heating and Cooling Systems
Task 2	Coordination of Solar Heating and Cooling R&D
Task 3	Performance Testing of Solar Collectors
Task 4	Development of an Insolation Handbook and Instrument Package
Task 5	Use of Existing Meteorological Information for Solar Energy Application
Task 6	Performance of Solar Systems Using Evacuated Solar Collectors
Task 7	Central Solar Heating Plants with Seasonal Storage
Task 8	Passive and Hybrid Solar Low Energy Buildings
Task 9	Solar Radiation and Pyranometry Studies
Task 10	Solar Materials R&D
Task 11	Passive and Hybrid Solar Commercial Buildings
Task 12	Building Energy Analysis and Design Tools for Solar Applications
Task 13	Advance Solar Low Energy Buildings
Task 14	Advanced Active Solar Energy Systems
Task 16	Photovoltaics in Buildings
Task 17	Measuring and Modelling Spectral Radiation
Task 18	Advanced Glazing and Associated Materials for Solar and Building Applications
Task 19	Solar Air Systems
Task 20	Solar Energy in Buildings Renovation
Task 21	Daylight in Buildings
Task 23	Optimisation of Solar Energy Use in Large Buildings

Completed Working Groups

CSHPSS
ISOLDE
Materials in Solar Thermal Collectors
Evaluation of Task 13 Houses

Current Tasks

Task 22	Building Energy Analysis Tools
Task 24	Solar Procurement
Task 25	Solar Assisted Cooling Systems for Air Conditioning of Buildings
Task 26	Solar Combisystems
Task 27	Performance of Solar Façade Components
Task 28	Solar Sustainable House
Task 29	Solar Crop Drying
Task 31	Daylighting Buildings in the 21st Century
Task 32	Advanced Storage Concepts for Solar Thermal Systems in Low Energy Buildings (Task Definition Phase)
Task 33	Solar Heat for Industrial Process (Task Definition Phase)

Current Working Groups

PV/Thermal Systems

TASK 22 : BUILDING ENERGY ANALYSIS TOOLS

Goal and Objectives of the task

The overall goal of the task 22 is to establish a sound technical basis for analysing solar, low-energy buildings with available and emerging energy analysis tools. This goal will be pursued by accomplishing the following objectives:

- Assess the accuracy of available building energy analysis tools in predicting the performance of widely used solar and energy efficiency concepts;
- Collect and document engineering models of widely used solar and low-energy concepts for use in the next generation building energy analysis tools; and
- Assess and document the impact (value) of improved building analysis tools in analysing solar, low-energy buildings, and widely disseminate research results tools, industry associations and government agencies.

Scope of the task

This Task will investigate the availability and accuracy of building energy analysis tools and engineering models to evaluate the performance of solar and low-energy buildings. The scope of the Task is limited to whole building energy analysis tools, including emerging modular type tools, and to widely used solar and low-energy design concepts. Tool evaluation activities will include analytical, comparative and empirical methods, with emphasis given to blind empirical validation using measured data from test rooms or full scale buildings. Documentation of engineering models will use existing standard reporting formats and procedures. The impact of improved building energy analysis tools will be assessed from a building owner perspective.

The audience for the results of the Task is building energy analysis tool developers. However, tool users, such as architects, engineers, energy consultants, product manufacturers, and building owners and managers, are the ultimate beneficiaries of the research, and will be informed through targeted reports and articles.

Means

In order to accomplish the stated goal and objectives, the Participants will carry out research in the framework of two Subtasks:

Subtask A: Tool evaluation

Subtask B: Model Documentation

Participants

The participants in the Task are: Finland, France, Germany, Spain, Sweden, Switzerland, United Kingdom, and United States. The United States serves as Operating Agent for this Task, with Michael Holtz of Architectural Energy Corporation providing Operating Agent services on behalf the U.S. Department of Energy.

This report includes works carried out under the Subtask A.3, Empirical Validation.

CONTENTS

Chapter 1

MODEL VALIDATION MEANINGS AND STATE-OF-THE-ART

The word "validation" is often misunderstood and has certainly been used in different senses in the past. First section in this chapter includes a structured discussion on the different model validation meanings, from conceptual models validation to empirical operational models validation. Our attention is then focussed on empirical model validation. A state of the art in this matter is presented in the last section.

1.1. MODEL VALIDATION MEANINGS

Modelling environments and simulation codes have been used for building thermal analysis for many decades now. Many simulation programs have over the years been checked to some extent, and it is not uncommon for the developers to claim that they have "validated" them. The word "validation" is often misunderstood and has certainly been used in different senses in the past. It is often taken to mean a once and for all time check of the absolute accuracy of a program. In practice, the thermal performance of a building is dependent on a very large number of parameters. It would be quite impossible to test all feasible combinations of these parameters in order to ensure that the model/program is correct, even if the true building performance was known.

Although it is not possible to validate a model or a simulation code for all kinds of applications, correct and carefully performed validation will increase confidence in both. It may also give an indication of their reliability, at least for more common cases. In addition, validation plays a dual role for the modeller: firstly, as a modelling aid, guiding the choice of an effective model structure and associated numerical values with respect to the model specific utilisation; and secondly, as an aid to model reuse, by simplifying access to models by a third party.

Different studies have been carried out in the past with the attempt to establish a methodology for model validation. The first study, undertaken by the US Solar Energy Research Institute [1] had resulted in a three part methodology including analytical tests, inter-model comparisons, and empirical validation. This methodology has further been refined and extended in the second study carried out by four British research teams - the University of Nottingham, Leicester Polytechnic, the Rutherford Appleton Laboratory and the Building Research Establishment [2]. The methodology comprises: theory and source code checking, analytical tests, inter-model comparison, sensitivity analysis, and empirical validation. This was the methodology reviewed and accepted at the commencement of the CEC Concerted Action PASSYS [3]. In the second phase of PASSYS main emphasis was devoted to empirical model validation. The complete description of the resulting methodology can be found in [4] and more condensed in [5, 6].

A better understanding on what model validation involves can be obtained using the "semiological grid" proposed in [7] as a tentative conceptual tool for an efficient and useful

description of the modelling process. The "semiological grid" (see Fig. 1.1) is a five layer structure (worlds) describing the main phases of a model development process:

- **Technical world**. It is ordinarily here that system is conceptualised, where appearances of reality are symbolised. For instance, in a project building, this is where components, identifiers and technical questions to be answer have to be specified.
- **Physical world**. It is a theoretical layer dealing with physics, where the previous technical description is translated into a physical one. It is here that the scale of the analysis, the physical phenomena taking place in the system, the laws governing them and the constitutive materials laws, etc. has to be specified.
- **Mathematical world**. We step down to a more rigorous mathematical formulation. Equations governing the space-time evolution of the system state have to be written. A qualitative understanding of the processes, relations and structures involved is now accessible.
- **Numerical world**. This layer is devoted to computation methods allowing numerical solutions of the problem, especially when analytical solutions are not available. It is a very specific world, half between mathematics and computers, which was for a long time considered as a sub-layer of the previous one.
- **Computer world**. The output of the deepest layer is a computerised model allowing simulations, data production in general.

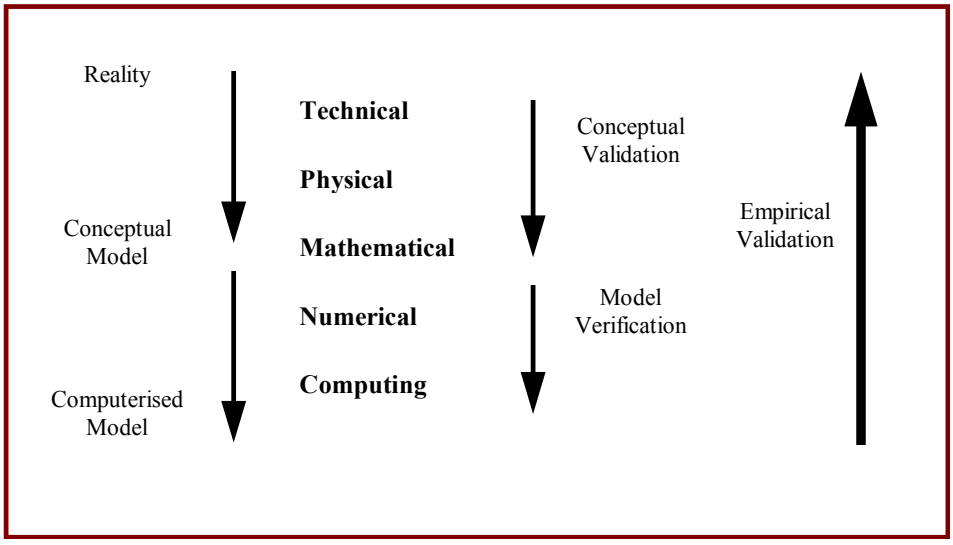

Figure 1.1. *Main stages in model credibility assessment.*

Going from reality to a conceptual model (see Fig.1.1) means stepping down from the technical world to the mathematical one. Similarly, translating the conceptual model into a computerised one, implies to move down from the mathematical world to the computing one.

According to the five layers structure before (see Fig.1.1), three main stages in models credibility assessment can be recognised:

- **Conceptual Model Validation**. Analysis of the adequacy of the conceptual model to provide a "reasonable" representation of the system for the intended use of the model. This process is usually accomplished by analysis and review of the theories and assumptions underlying the conceptual model. It mainly tests the coherence between the conceptual model and the image of reality the modeller has, that is, the passage from the technical to the mathematical world.
- **Computerised Model Verification**. Substantiation that the computerised model represents the conceptual model within specified limits of accuracy. In essence, model verification is for insuring that the computer programming and implementation of the conceptual model is

correct. Computer scientists have been devoting a great deal of effort to develop design and management techniques that minimise coding errors (e.g. structured programming, top-down design, chief programming, etc.). Recently, rigorous (formal) design and implementation techniques allow for program correctness proof [8]. Analytical test and inter-model comparisons are also applied at this stage, as well as special simulation based tests as the ones described in [9].

- **Empirical Operational Model Validation**. Empirical validation should in principle compare a true model derived from experiments with a computerised model. It is not, as analytical validation, limited to isolated processes in simple constructions, but deals with real world complexity comparable to situations as encountered when the simulation code is used in design studies. Empirical validation is, therefore, the most widely used technique for validating transient simulation programs. Beyond any technical consideration, it provides a guarantee of users confidence, and enables the modeller to improve his understanding on the system he is modelling and to improve the model itself. However, it involves experiments, with the risk that the question regarding the reliability of the predictions cannot be answered due to the un-reliability of the measurements.

Model assessment should be performed throughout the model development process. In this way, the risk of observing model deficiencies due to an improperly conceptual model implementation should be negligible when performing empirical model validation, the measurements/simulations differences reflecting essentially the conceptual model inadequacy.

We will focus our attention on empirical validation, whose aim is two-fold:

- **Checking model validity**. Firstly, one needs to detect if the model is capable of describing the reality correctly, that is, to check whether the analysed model satisfies some *a priori* validation criteria.
- **Modelling errors diagnosis**. Secondly, the causes of the observed discrepancies between measured and predicted values must be identified in order to indicate how to improve the analysed model, if required.

This is, however, a non-trivial task to perform, as it requires expertise in experimental design, modelling principles and simulations techniques, as well as in special mathematical methods involving sensitivity analysis, identification techniques, spectral analysis, and so on.

1.2. STATE OF THE ART IN EMPIRICAL MODEL VALIDATION

Comparison between measured and predicted values has often been performed in a very subjective way by e.g. comparing a curve showing the measured values with a curve showing the predicted values and then by looking at this, stating whether the agreement is satisfactory or not. This kind of comparison gives only little information on model validity and on what may cause deviations between measurements and predictions. It is necessary to apply more sophisticated techniques in order to increase the quality and the confidence in the validation result and to obtain valuable information about the model.

Several mathematical techniques exist for comparison between measured and predicted values, testing the goodness of different aspects of the model and trying to identify the causes of unsatisfactory model behaviour.

Checking model validity

The most commonly used validation criterion is the verification of whether model/data discrepancy is smaller than a threshold taking into account of measurements noise and model input

data uncertainties. It implies the estimation of the so called "overall uncertainty bands", which are a measure of the influence that the variations in the model parameters have on the model outputs. Three kinds of sensitivity analysis techniques have been used in the past to estimate them: differential sensitivity analysis, Monte Carlo methods, and stochastic sensitivity analysis. See e.g. [10] for an analysis of their corresponding advantages and drawbacks.

The agreement between simulations and measurements is stated to be good if the measured values fit within the overall uncertainty bands. The advantage of this method is that it is very clear when good agreement is obtained, the disadvantage is that it only compare measurements and simulations in the low frequency area (daily or less). It does not test the highly dynamic behaviour (hourly) of the model.

Within the CEC funded PASSYS program, some frequency domain analyses on the residuals (differences between measurements and simulations) were proposed in order to establish a validation criterion for the dynamic behaviour. The most interesting one is based on the analysis of the residuals density power spectrum. This statistic represents the residuals variance distribution over frequencies. It shows in which frequency ranges the problems in the model mainly appear. When compared with the so called "qualifying density power spectrum", which represents the allowed upper bound for the residuals density power spectrum, frequency areas where the model shows an unsatisfactory behaviour are revealed. However a reliable validation criterion should encompass both a measure of the measurements noise and a measure of the model expected accuracy including model input data uncertainty.

Modelling errors diagnosis

Two significant techniques using linear analysis tools have been proposed in the past for diagnostic purposes.

The first one consist in a direct comparison of the system global physical parameters (first time constant and static gains) estimated from measurements with the ones calculated by means of the analysed model [4, 11]. To obtain such information from experimental data, identification techniques can be applied. A dynamic linear model, in state space form [4] or in a black-box form [11], is identified on data, and then reduced to its characteristic time constant and its static gains. To get such information from the "knowledge" model the use of spectral decomposition techniques has been proposed in [11], and a different technique based on simulations in [4].

The second technique deals with residuals analysis and was first proposed in [5]. Because model simulation aims at reproducing the effect of the external influences that drive the experiment, one expects a part of the residuals to be sensitive to these inputs. Hence, the proposed technique seeks to quantify the contribution of each input to the residuals. Such information helps modellers to sort the inputs and to target the one responsible of the major part of the error. Efforts to improve the model should then focus the way model takes into account this particular input.

The technique proposed in [4, 5] is based on residuals non-parametric spectral analysis. The contribution of each input to the residuals is analysed by means of the squared partial coherence functions. The squared partial coherence for the i^{th} input is a normalised measure at frequency ω of the linear cross-correlation existing between residuals and input i after allowance is made for the effect of the other input variables. It takes values from 0 to 1. Zero values mean that no correlation exists between the i^{th} input and the residuals, unity values mean that residuals could be completely recovered from this input, and values between 0 and 1 correspond to situations where residuals can be partially predicted from the i^{th} input. Such information helps modellers to sort the inputs and to target the one responsible of the major part of the error over a given frequency area. This is the method reviewed and accepted in [12, 13], where spectra and partial coherence functions are simultaneously used to quantify the contribution of each model input to the residuals variance.

The technique proposed in [14] is slightly different, although it also deals with residuals analysis. A dynamic linear and stationary MISO (Multiple Inputs Single Output) model is identified on the residuals/input data. Such model is intended to predict the residuals time evolution, and it is then used to estimate the contribution of each model input to the total variance of the residuals. This error disaggregating technique, dealing with the total residuals variance, does not allow separating time-scales (frequency ranges). It does not provide so rich information than the previous ones.

Residuals analysis techniques have been widely used in the 90's, especially in the framework of a British-French collaboration - the Building Research Establishment and Électricité de France. Although they revealed capable of diagnosing some of the modelling errors, the authors believe them to suffer some limitations. The main important ones are:

- They are based on linear analysis tools. Hence, they cannot be applied for non-linear models studies.
- They can be qualified as black-box approximations to the diagnosis for they are mainly based on the analysis of the causal relationships between the residuals and the model inputs. Any direct information is supplied concerning the modelling hypothesis to be reviewed and the parts to be modified. Frequently, no indications on how to improve models are given by means of residuals analysis. For instance, which parts in a test cells model must be modified when a strong coherence has been detected between the outdoor temperature and the residuals: thermal bridges, convective coefficients, indoor air stratification hypothesis, etc.? Residuals analysis brings any answer about.

These limitations lead us to propose another kind of approach for models diagnostic purposes. It is based on the analysis of the correlation existing between the different model parameters and the residuals observed. The aim of the method is to identify the amplitude of variations in parameters allowing significant residuals reduction. The comparisons of such results with the knowledge we have about the actual system and the modelling hypothesis will help us to know the reasons of the observed modelling errors, and to propose model improvements.

Chapter 2

INTERNATIONAL ENERGY AGENCY EMPIRICAL MODEL VALIDATION APPROACH : THEORY AND COMPUTER IMPLEMENTATION

The methodology and the underlying methods we are proposing for empirical model validation purposes are presented in this chapter. It first includes a general overview of the methodology, from checking model validity to diagnosis. Thermal models for buildings are presented in the second section, as well as measurements and uncertainty matters. The third section describes the mathematical tools that have been chosen for testing the model validity. Our main contribution however concerns diagnosis. A new approach based on the model parameter space analysis has been developed. It is described in the two next sections. A simple example of application is presented and discussed in the last by one section and last section includes some computer implementation matters.

2.1. GENERAL OVERVIEW OF THE METHODOLOGY

As pointed out in the previous chapter, the aim of empirical validation is two-fold. Firstly, it intends to test the model performances by identification of significant disagreements between measurements and simulations (checking model validity). Secondly, it tries to explain such disagreements (model diagnosis). This means going up from the observed differences between simulations and measurements to the modelling hypothesis that must be modified to improve the model.

Checking model validity

Testing model validity is based on comparisons between simulations and measurements. Different studies have been carried out in the past with the attempt to establish methods for rigorous model validity test. In the framework of the IEA Task 22, checking model validity involves:

- A systematic analysis of the residuals comprising non-stationary patterns detection, mean and standard deviation calculation and spectral density function analysis.

- A comparison between measurements and simulations that takes into account both the measurements noise and the model input data uncertainties. The agreement between model and reality is stated to be good when a significant overlapping is observed between simulations and measurements uncertainty bands. This is today a standard way for model/data comparisons (cf. [10, 4]).

– The estimation of the spectral domain of application of the model. It defines the frequency ranges of excitation where no significant differences between model simulations and measurements are expected.

Model diagnosis

The diagnosis approach we are proposing is based on the analysis of the model parameters space. The main objective is to identify the changes in parameters values that are required for a significant model behaviour improvement. Diagnosis is then provided by comparison of such results with the knowledge we have about both the actual system and the model itself.

As stated before, residuals analysis aims to target the model inputs responsible of the major part of the differences measures/simulations observed. Contrary to such techniques, parameter space analysis focuses its attention on physical phenomena and modelling hypothesis. It must be noticed that parameters are the elements of a computerized model that are closest to the represented physical phenomena, as well as to the assumed modelling hypothesis. Consequently, it is expected that this new approach supplies better information for diagnosis than residuals analysis. In addition, it can be applied to both linear and non-linear models.

Two main stages can be recognized in the methodology that we are proposing (see Fig. 2.1):

(a) **Active model parameters identification and preliminary diagnosis.** This is a preliminary and fundamental step toward diagnosis. It aims to identify the physical phenomena and the parts of the model that can be really tested on the available experimental data. As it is shown later (section 2.2), sensitivity analysis is the main mathematical tool for this purpose. It involves: a) calculation of the model outputs sensitivity to every model parameter; b) active model parameters identification and correlation analysis; and c) sensitivities principal components analysis.

Active model parameters are those to which model outputs are sensitive enough. They are related to the mathematical representation of the dominant parts and phenomena in the model. Unfortunately, active model parameters are often correlated among each other. Such correlations introduce some additional limitations for validation purposes as well as some ambiguities for diagnosis. Generally, active model parameters must be grouped and validation and diagnosis conclusions will only refer to such groups. There is no way of making distinction among parameters in a same group.

Some useful information concerning diagnosis can also be obtained at this step. As we will se later, principal components analysis is the main tool for this purpose. It gives some preliminary indications on how active model parameters can be modified to improve model performances.

(b) **Optimisation and diagnosis.** Parameters estimation techniques are the main mathematical tool we are proposing to guide model diagnosis. Free model parameters values allowing significant residuals reduction are here identified by fitting the model on the available data. Diagnosis mainly involves comparisons between estimated and nominal model parameters values. Large differences are expected for parameters related to the physical phenomena that are not correctly represented in the model. Different algorithms for optimisation have been considered and tested (see section 2.3).

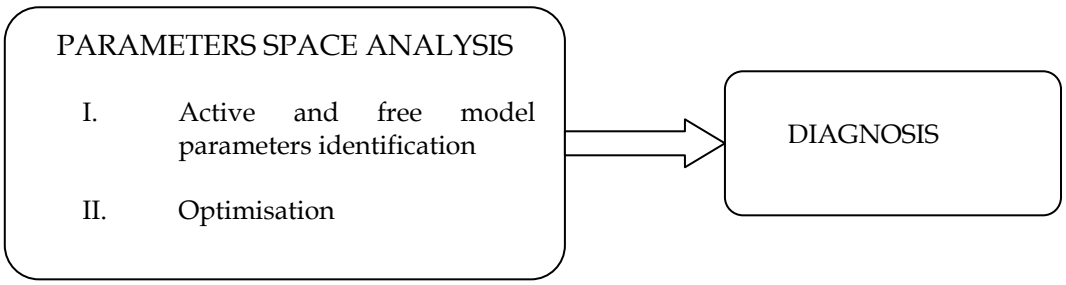

Figure 2.1. *The main steps toward diagnosis in the proposed methodology.*

2.1. MODELS, MEASUREMENTS AND UNCERTAINTIES

Thermal models for buildings

A building is an open and non-adiabatic thermodynamic system that exchanges mass and energy with its environment. It can be seen as an ensemble of solid elements (walls, doors, windows, etc.) that separate a volume of air from the outdoor environment. The main physical processes contributing to the definition of the building thermal state are:

- heat conduction in the matrix of the solid elements;
- long-wave radiation exchanges among the indoor surfaces, and between the outdoor surfaces and the environment;
- solar radiation transmission and absorption;
- convective heat transfer at the surface-air interfaces; and
- convective heat transfer by air mass transport among building zones, and between every zone and the building environment.

Thermal models for buildings can be usually described by finite-dimensional models of the general form:

$$\begin{aligned} \dot{T}(t) &= \mathsf{F}(T(t),U(t),\theta) \\ Y(t) &= \mathsf{G}(T(t),U(t),\theta) \end{aligned} \tag{2.1}$$

where $T(t)$ is a n-dimensional vector containing the so-called state space variable (e.g. temperatures at the nodes of the discretisation mesh), $Y(t)$ is a q-dimensional vector including the observation variables or outputs, and $U(t)$ is the inputs or excitations vector. θ is the p-dimensional vector of models parameters, and F and G two matrices of time-dependent non-linear functions. A particular model thus corresponds to specification of functions in matrices F and G, as well as the parameters vector θ.

For envelope models, linearity is usually assumed. Model (2.1) then becomes:

$$\begin{aligned} \dot{T}(t) &= A(\theta)T(t) + B(\theta)U(t) \\ Y(t) &= J(\theta)T(t) + G(\theta)U(t) \end{aligned} \tag{2.2}$$

where A $(n \times n)$ is the so-called state matrix, B $(n \times r)$ is the inputs matrix, J $(q \times n)$ is the outputs matrix and G $(q \times r)$ is the direct gains matrix.

Typical model inputs in building thermal analysis are the outdoor dry temperatures, the solar irradiance on the different building facades, and the heating power injected in the different zones of the building. Most of the time, the model user is not interested on predicting the time evolution of the whole building temperature field. The "mean" air temperature and/or the "mean radiant" temperature at the building zones usually form the outputs vector.

Concerning model parameters, we can split them in several categories:

- Geometrical parameters: volumes, surfaces dimensions, walls orientation and inclination, thickness of the wall layers, etc.
- Themophysical parameters: thermal conductivity, density, and specific heat capacity of the different materials in the building.
- Optical parameters: solar transmittance, absorptance and reflectance for transparent elements; solar absoptance for the opaque elements; surfaces emissivities; etc.
- Convective parameters: parameters in the phenomenological laws representing the heat exchanges taking place at the solid-air interfaces.
- Air exchange parameters: parameters involving the infiltrations and ventilation processes representation.
- Others: parameters related to heating/cooling control, shading devices operation, ventilation strategies, etc.

Measurements

Empirical model validation requires good quality and informative enough data concerning the building behaviour. The design of a validation experiment includes several choices, such as which signals to measure and when to measure them and which signals to manipulate and how to manipulate them. It also includes some more practical aspects, such as sensors accuracy and location.

High quality experiments for empirical model validation purposes are scarce. The better ones has been carried out in specific and well characterised experimental devices (e.g. test rooms). In such cases, measurements sampling time generally goes from 1 minute to 1 hour and the experiment duration is several times larger than the first time constant of the system.

Measurements must provide good enough information about the time evolution of both the forcing functions and the quantities involved in the definition of the outdoor environment. That is, the solar radiation (at least, its diffuse and its direct components), the temperature and the humidity of the different ambiances surrounding the system, the wind speed and the wind direction, the heating or cooling power supplied to the different zones of the system, etc.

Measurements describing the thermal behaviour of the system generally concern the time evolution of the air temperature at different places, the black globe temperature, the temperature and the heat flux at the indoor wall surfaces, etc. However, measurements involving heat flux or surface temperatures are not reliable enough in practice.

Uncertainties

A keyword in empirical model validation is uncertainty. Uncertainty involves measured data, model parameters or/and structure, and model response:

Measurements uncertainty

Data are always associated with some uncertainty, if only because of the finite precision of the sensors used to collect them. The approach most commonly used to characterize such uncertainty

consists in assuming that data are corrupted by additive random noise, whose probability density function is known. While very popular, this approach is not immune to criticism. The probability density function assumed for the noise is not always based upon any sound prior information, and one does not necessarily have enough data to test it. Moreover there are situations where the main contribution to error is not of a random nature and therefore not suitably described by random noise.

An attractive alternative to the stochastic characterization of errors is characterization by upper and lower bounds only. Let $Y^*(t) = \left\{ y_k^*(t), k = 1, \cdots, q \right\}$ be the q-dimensional vector of observed quantities. Measured bounded-error data at time *t* are thus represented by the intervals:

$$\forall k \qquad \left[y_{k,\min}^*(t) \quad y_{k,\max}^*(t) \right] \tag{2.3}$$

Most sensors manufacturers provide rules for computing the maximum and minimum possible measurement errors at any given range of operation, allowing $y_{k,\min}^*(t)$ and $y_{k,\max}^*(t)$ to be computed. Structural errors (such as bias introduced by the location of a sensor within a inhomogeneous medium) may however lead one to choose more pessimistic bounds than those obtained by this method. These bounds can then be viewed as the extreme values of the error between system and model outputs that are considered acceptable by the experimenter.

Model parameters uncertainty

The uncertainty in model parameters is generally not of a random nature. It can reflect:

- an imperfect knowledge of the system geometry or even composition;
- the lack of measured data for parameters;
- the uncertainty due to the finite precision of the sensors and methods used for measuring system properties;
- the uncertainty associated to the system exploitation, which is generally related to an unpredictable behaviour of the future users;
- and the imperfect knowledge we have about the physical processes taken place in the system.

Hence, as data before, model parameters uncertainties will be characterised by upper and lower bounds. Let $\theta = \left\{ \theta_i(t), i = 1, \cdots, p \right\}$ be the p-dimensional vector of model parameters. Parameters uncertainty is thus described by the intervals:

$$\forall i \qquad \theta_i \in \left[\theta_{i,\min} \quad \theta_{i,\max}(t) \right] \tag{2.5}$$

or in a more compact way, by

$$\Theta \equiv \bigtimes_{i=1}^{p} \left[\theta_{i,\min} \quad \theta_{i,\max} \right] \tag{2.6}$$

which is the Cartesian product of the previous p intervals. The box Θ will be called parameters set.

When checking model validity, intervals (2.5) generally represent parameters uncertainty due to the finite precision of the sensors and methods used to estimate them (see section 2.2). For diagnosis purposes, they can be larger than the previous ones, as they represent the domain of variation where we are looking for suitable parameters values (see section 2.4).

Model response uncertainty

Model outputs uncertainty results from the uncertainties of the model parameters. The uncertainty in the model response at time t, associated to the parameter set Θ, can be characterized by the intervals

$$\left[y_{k,\min}(t) \quad y_{k,\max}(t)\right], \qquad k=1,\cdots,q \tag{2.7}$$

so that $\forall\theta\in\Theta$ the probability for $y_k(t,\theta)\notin\left[y_{k,\min}(t) \quad y_{k,\max}(t)\right]$ is less than α (e.g. 0.01). If $\alpha=0$, then (2.7) represents the intervals of minimum width, so as

$$\forall\theta\in\Theta, \quad \forall t, \quad \forall k, \qquad y_{k,\min}(t)\le y_k(t,\theta)\le y_{k,\max}(t) \tag{2.8}$$

Such intervals are the result of an application from the parameters space to the outputs space that is defined through the model equations. Methods for calculating them are presented in next section. They are usually referred as "β % simulations uncertainty bands", where $\beta=(1-\alpha)\times 100$.

2.2. CHECKING THE MODEL VALIDITY

Checking the model validity is based on comparisons between measurements and simulations. The simplest way to compare them is just to depict the trace of the simulated values together with measured values. This is important and should never be overlooked. However, it is often not the best way to characterize the differences observed between measurements and simulations. Others methods have, therefore, also been applied. This section describes some of the mathematical tools available for rigorous checking of the model validity.

Relevant characteristics of the residuals

Residuals are defined as the difference between measurements and simulations*:

$$e(t)=y_{measured}(t)-y_{simulated}(t)$$

Relevant characteristics of residuals can be investigated by analysing trends, mean and standard deviation values, as well as spectral properties. This section introduces the statistics we are using as well as some comments on their meaning and their potential use for model validation purposes.

- Stationarity. A stochastic process is said to be strictly stationary if its properties are unaffected by a change of time origin; that is, the joint distribution of any set of observations must be unaffected by shifting all the times of observations forward or backward by any integer amount. It is said to be stationary up to the order m if all its joint moments up to the order m are independent of the absolute time. Usually, the term stationary is applied to a stationary process up to order 2. Different methods exist to detect non-stationarity: 1) depict residuals; 2) estimate mean and variance over different time periods; 3) analyse the autocorrelation function. Systematic changes in the level of a time series (trends) is a typical kind of non-stationarity. In the framework of model validation, residuals trends usually reveal changes in the causes of deficient model behaviour.

- Mean and variance. The mean value is the first statistic that can be used to characterise residuals. A mean value far from zero means that the model does not represent adequately the

* This is perhaps a little misleading since the term residuals most often is used for the deviations between an estimated model and the measurements (the so-called prediction error). This convention has been adopted here although there is a conceptual difference between simulation and prediction errors.

static behaviour of the actual system. The residuals variance measures the fluctuations of the residuals around their mean value. It can be used as a first indication of the ability of the model to describe the dynamic behaviour of the system.

– Spectrum. The power spectrum is defined as the Fourier transform of the residuals auto-covariance function. It shows how the residuals variance is distributed with frequency. In the framework of model validation, the spectrum can be used to determine at which frequencies the problems of the model mainly appear. In other words, it is a frequency check on the dynamic performances of the model. As it is shown later, the spectrum will allow us to estimate the domain of applicability for the model.

Simulations-measurements consistency analysis

Let

$$\Theta = \left[\theta_{1,\min} \quad \theta_{1,\max}\right] \times \left[\theta_{2,\min} \quad \theta_{2,\max}\right] \times \cdots \times \left[\theta_{p,\min} \quad \theta_{p,\max}\right]$$

be the so-called parameter set, where $\left[\theta_{i,\min} \quad \theta_{i,\max}\right]$ $(i = 1, \cdots, p)$ represent the uncertainty intervals for model parameters. We note

$$\left[y_{k,\min}(t) \quad y_{k,\max}(t)\right], \qquad k = 1, \cdots, q \tag{2.9}$$

the model outputs bounds over Θ. They are also called "model outputs uncertainty" or "β % simulations uncertainty bands". They have been defined in section 2.1. As pointed out before, measured bounded-error data are characterised by the intervals

$$\left[y^*_{k,\min}(t) \quad y^*_{k,\max}(t)\right], \qquad k = 1, \cdots, q \tag{2.10}$$

In the following, we will assumed that 99% simulation uncertainty bands (eq. 2.9) are not too large compared with the uncertainty bands associated with measurements (eq. 2.10). In other words, we suppose that the model is accurate enough for validation purposes.

Some judgement about the validity of the model can be get by comparing measurements with the 99% simulations uncertainty bands:

– The model is stated to be good enough compared with data uncertainties when the following condition is verified

$$\forall t, \ \forall k \qquad y^*_{k,\min}(t) \le y_{k,\min}(t) < y_{k,\max}(t) \le y^*_{k,\max}(t) \tag{2.11}$$

If simulations uncertainty bands are always included in the measurements uncertainty bands, the validation procedure is then stopped for measurements uncertainty does not allow to go ahead with model defaults detection.

– If the previous condition is not satisfied, we will say that measurements are within the 99% simulations uncertainty bands when no more than 1% of measured observations fall outside them. In such a case, judgement about the validity of the model requires more sophisticate mathematical tools (see section 2.4). This first comparison between measurements and simulations only supplies information about the validity of the model at low frequencies, it does not test the model behaviour at high frequencies. The firmest conclusion we can derive on the validity of the model can be summarised as: "It seems that the model reproduces adequately the static behaviour of the system".

- If measurements are outside the 99% simulations uncertainty bands (more that 1% of measurements falling outside these bands), the model may be deficient and justifies further checking of the observed differences between measurements and simulations.

Three different techniques are generally used to estimate the model uncertainty bands. They are based respectively on Monte-Carlo methods, differential sensitivity and stochastic sensitivity analysis (cf. [10, 4]). Two of them, those that do not require modifications of the simulation codes, have been applied in the framework of the IEA Task 22:

- **Standard Monte-Carlo approach.** It assumes model parameters to be random variables whose probability density function is known. N vectors $\theta^{(s)}, s = 1, \cdots, N$ of parameters are chosen at random, based on the selected probability distribution functions (e.g. uniform distributions over $\left[\theta_{i,\min}, \theta_{i,\max}\right]$). Simulations are then performed for getting model outputs evolution associated to every parameter vector: $Y(t;\theta^{(s)})$, $s = 1, \cdots, N$. Provided there are a large number of parameters in the model, irrespective of their distributional properties, it is expected that the outputs from simulations were normally distributed (central limit theorem) with mean and standard deviation

$$m_k(t) = \frac{1}{N}\sum_{s=1}^{N} y_k(t;\theta^{(s)}) \qquad \text{and} \qquad s_k^2(t) = \frac{1}{N-1}\sum_{s=1}^{N}\left[y_k(t;\theta^{(s)}) - m_k(t)\right]^2 \tag{2.12}$$

respectively. 99% simulations uncertainty bands for the k^{th} model output are then estimated as:

$$m_k(t) \pm 2.33 s_k(t) \tag{2.13}$$

This means that the probability of observing simulations outside such bounds at time t is less than 1%. If outputs are normally distributed, the estimate of their time-dependent variance will follow a χ^2 distribution with $N-1$ degrees of freedom. Hence, the $(1-\alpha)\%$ confidence interval for the standard deviations is given by:

$$s_k(t)\sqrt{\frac{N-1}{\chi^2_{\alpha/2,N-1}}} \le \sigma_k(t) \le s_k(t)\sqrt{\frac{N-1}{\chi^2_{1-\alpha/2,N-1}}} \tag{2.14}$$

It can be proved from the equation above that the accuracy of $s_k(t)$ depends only on the number N of simulations undertaken and not on the number of free model parameters. In addition, only marginal improvements in accuracy are obtained after 100 simulations. This fact makes Monte Carlo methods a very efficient way for model outputs bounds calculation when a very high number of parameters are involved in the analysis.

- **Method founded on sensitivity analysis.** Let $\theta_o = \left\{\theta_{o,1} \quad \theta_{o,2} \quad \cdots \quad \theta_{o,p}\right\}$ be the vector of nominal values for model parameters. Parameters uncertainty is now characterised by the intervals

$$\theta_o \pm \Delta\theta = \left\{\theta_{o,1} \pm \Delta\theta_1 \quad \theta_{o,2} \pm \Delta\theta_2 \quad \cdots \quad \theta_{o,p} \pm \Delta\theta_p\right\} \tag{2.15}$$

The 99% model output bounds over this parameter set are then approximated by:

$$y_k(t;\theta_o) \pm \Delta y_k(t;\Delta\theta) \qquad (k = 1, \cdots, q) \tag{2.16}$$

with

$$\Delta y_k(t;\Delta\theta) = \sqrt{\sum_{i=1}^{p}\left(s_{k,i}(t)\Delta\theta_i\right)^2} \qquad \text{and} \qquad s_{k,i}(t) = \left(\frac{\partial\, y_k(t)}{\partial\theta_i}\right)_{\theta=\theta_o} \tag{2.17}$$

where $s_{k,i}(t)$ represents the sensitivity of the k^{th} model output to the i^{th} parameter. Methods for sensitivity calculation are presented and discussed in section 2.3.

The main advantage of this technique is its simplicity. Its application is, however, limited by the underlying hypotheses of linearity: linear relationships are assumed between any parameter change and the consequential change in the model outputs. Furthermore, the sensitivity to each parameter is supposed to be independent of the values of the other parameters. For most systems this is not strictly true. Nevertheless, for small changes in the parameters both assumptions may be reasonable (cf. [10, 15]).

Spectral domain of applicability

The validity of a model is generally in keeping with some kind of application – e.g. a model that is good enough for predicting heating load requirements could be inadequate for thermal comfort analysis. Usually, model validity depends both on the dynamic characteristics of the applied forcing functions and on the dynamic characteristics of the outputs that must be reproduced. Some pertinent advises concerning the potential field of model application can thus be supplied by checking its dynamic performances. As stated before the residuals power spectrum discloses at which frequencies the disagreements model-reality appears. However, on this basis only subjective statements are made on the goodness of the model at different frequencies.

A first attempt to check the dynamic behaviour of a model in a non sub-subjective way was the so-called "qualifying density power spectrum" (QDPS) proposed in [4]. It is a "reference" allowing us to determine in which frequencies the model performs well or badly. The performance of the model is good when the density power spectrum of the residuals is below the reference spectrum, and is performing badly in regions where the residuals spectrum is above the reference. Main drawback of this approach concern the way the QDPS is defined since there still remains some subjective judgement in the creation of QDPS. In addition, a QDPS is always associated to a binomial system-experiment, so as changing either the system or the experiment implies a new QDPS creation. A simpler and more rigorous approach is here proposed.

Let $\Gamma_{y_k}(\omega)$ and $\Gamma_{e_k}(\omega)$ be respectively the power spectrum of the measured k^{th} model output and the power spectrum of the corresponding residuals. The variance of the measurements over the frequency interval $\omega_1 \le |\omega| \le \omega_2$ is then given by

$$\mathbf{E}\left\{y_k^2(t)\right\}_{\omega_1\le|\omega|\le\omega_2} = 2\int_{\omega_1}^{\omega_2}\Gamma_{y_k}(\omega)d\omega \tag{2.18}$$

and the variance of the residuals is

$$\mathbf{E}\left\{e_k^2(t)\right\}_{\omega_1\le|\omega|\le\omega_2} = 2\int_{\omega_1}^{\omega_2}\Gamma_{e_k}(\omega)d\omega \tag{2.19}$$

The model performance over the frequency interval $\omega_1 \le |\omega| \le \omega_2$ can be defined as

$$\eta_k(\omega_1,\omega_2) = \frac{\mathbf{E}\left\{e_k^2(t)\right\}_{\omega_1\le|\omega|\le\omega_2}}{\mathbf{E}\left\{y_k^2(t)\right\}_{\omega_1\le|\omega|\le\omega_2}} \qquad k=1,\cdots,q \tag{2.20}$$

Such indices measure the significance of the residuals fluctuations compared to the fluctuations of the measured model outputs. The spectral domain of applicability of the model is then determined by all the frequency intervals $\omega_1 \le |\omega| \le \omega_2$ so as $\forall k,\ \eta_k(\omega_1,\omega_2) \le \eta_{threshold}$, where $\eta_{threshold}$ is an user-supplied threshold.

2.3. ACTIVE MODEL PARAMETERS IDENTIFICATION, CORRELATION ANALYSIS AND PRELIMINARY DIAGNOSIS

As we said before, this is a preliminary and fundamental step toward diagnosis. It aims to identify the physical phenomena and the parts of the model that can be really tested on the available experimental data. Sensitivity analysis is the main mathematical tool we are using to reach this objective. It involves:

- Calculation of the model outputs sensitivity to every model parameters. Sensitivity provides first-order estimates of the effect of parameter variations on the model response.
- Active model parameters identification. It must be noticed that all the parameters in the model can potentially affect the model behaviour, but generally only a small number of them are truly important or active. The reason is that not all the parts of the system are equally excited by the inputs, and not all the physical processes taken place have comparable effects on the quantities to be observed. The so called active model parameters are those to which model outputs are sensitive enough. They are related to the dominant parts in the model. Validation of phenomena whose mathematical representation includes any active parameter is not possible.
- Active parameters correlation analysis. Two active parameters are stated to be strongly correlated when they show similar effects on the model outputs. Identifying correlations among active parameters is a fundamental step for correlations introduce additional limitations for validation purposes. That is, no distinction can be made between two parts of the model when their corresponding active parameters are correlated among them. Correlations between parameters depends both on the model structure (the way the parameters are involved in the model), and on the model inputs behaviour. While correlations related to the model structure are usually foreseeable, correlations induced by the model inputs are generally not easy to anticipate. Different tools as statistical linear correlation and principal components techniques are here proposed to gather active model parameters into independent (or quasi-independent) groups.
- Principal components analysis and preliminary diagnosis. Principal components analysis (PCA) was introduced in statistics by Hotelling [16]. Dempster [17] gives an excellent geometric treatment of PCA as well as an overview of its history. Since 1933, applications based on PCA are growing on (image compression, model reduction, regularisation, structural instabilities analysis, etc.). As it is shown later, PCA allows de-correlating time series. In the framework of model validation we will use PCA for defining parameters signatures and for supplying some preliminary elements for diagnosis.

Sensitivity calculation methods

Sensitivity analysis studies the effect of parameter variations on the behaviour of a system. A rather complete state of the art on the techniques of sensitivity analysis is brought in [15]. One can distinguish two main families of sensitivity methods: those which follow a deterministic approach, on

the one hand, and those which adopt a statistical procedure, of another. The well-known techniques of differential sensitivity analysis are in the first group. Its characteristic is to examine the first-order derivatives of the model response with respect to its parameters.

The sensitivity of the model outputs to the parameter θ_i is defined by:

$$S_i(t) = \frac{\partial Y(t)}{\partial \theta_i} = \left\{ \frac{\partial y_1(t)}{\partial \theta_i} \quad \frac{\partial y_2(t)}{\partial \theta_i} \quad \cdots \quad \frac{\partial y_q(t)}{\partial \theta_i} \right\}^T \tag{2.21}$$

It provides first-order estimates of the effect of parameter variations on the model response. Similarly, the sensitivity of the state vector (e.g. temperature vector) to the model parameter θ_i is:

$$S_{T,i}(t) = \frac{\partial T(t)}{\partial \theta_i} = \left\{ \frac{\partial T_1(t)}{\partial \theta_i} \quad \frac{\partial T_2(t)}{\partial \theta_i} \quad \cdots \quad \frac{\partial T_n(t)}{\partial \theta_i} \right\}^T \tag{2.22}$$

According to the complexity of the problem, these derivatives either will be calculated in an approximate way (parameter-perturbation methods) or exact (sensitivity-equation methods):

Parameter-perturbation method. The sensitivity of the k^{th} model output to the i^{th} model parameter is often approached in the following way:

$$\frac{\partial y_k(t)}{\partial \theta_i} \approx \frac{y_k(t;\theta_i) - y_k(t;\theta_i \pm \Delta\theta_i)}{\Delta\theta_i} \tag{2.23}$$

where θ_i is the nominal value of the i^{th} model parameter and $\Delta\theta_i$ represents a small perturbation around its nominal value.

The parameter-perturbation method is hence based on changing the value of a single parameter at a time, running the model and comparing the new model response to the one of the nominal model.

Sensitivity-equation method. Among the exact methods (see Annex A), the so called direct or sensitivity-equation method is here considered. The equations governing the time evolution of $S_i(t)$ are obtained by simple differentiation of equations (2.2). This lead to the so-called sensitivity models ($i = 1, \cdots, p$):

$$\begin{aligned} C\frac{dS_{T,i}(t)}{dt} &= AS_{T,i}(t) + \left\{ \left(\frac{\partial E(\theta)}{\partial \theta_i} \right) U(t) + \left(\frac{\partial A(\theta)}{\partial \theta_i} \right) T(t;\theta) - \left(\frac{\partial C(\theta)}{\partial \theta_i} \right) \frac{dT(t;\theta)}{dt} \right\} \Bigg|_{\theta=\theta_o} \\ S_i(t) &= JS_{T,i}(t) + \left\{ \left(\frac{\partial G(\theta)}{\partial \theta_i} \right) U(t) + \left(\frac{\partial J(\theta)}{\partial \theta_i} \right) T(t;\theta) \right\} \Bigg|_{\theta=\theta_o} \end{aligned} \tag{2.24}$$

where C, A and J are, respectively, the matrix of thermal capacities, the state matrix and the outputs matrix of the nominal model. The terms in brackets are evaluated for $\theta = \theta_o$, where θ_o represents the vector of nominal parameters values.

Solving sensitivity problems hence involves the time integration of *p+1* state models (the nominal model and the sensitivity models) of the form:

$$C\frac{d\mathsf{X}(t)}{dt} = A\mathsf{X}(t) + \psi(t)$$
$$\mathsf{Y}(t) = J\mathsf{X}(t) + \eta(t) \tag{2.25}$$

where $\mathsf{X}(t)$ represents either $T(t)$ or $S_{T,i}(t)$, and $\mathsf{Y}(t)$ represents either $Y(t)$ or $S_i(t)$, with i = 1, 2,.., p. It must be noticed that each sensitivity model includes as many ordinary differential equations as the nominal model. Sensitivity analysis for large-scale systems including a high number of parameters (e.g. hundreds of equations and parameters) could be then computationally intensive and limited by the computer performances. A numerical approach which makes it possible to extend the application of the sensitivity-equation method to such kind of problems is proposed in Annex A. It rests on the theory of balanced realisation, which makes it possible to strongly reduce the number of differential equations in a model without introducing a significant loss of precision. An example of application shows the effectiveness of the proposed method.

Active model parameters identification and correlations analysis

Let $s_{k,i}(t)$ the sensitivity of the k^{th} model output to the i^{th} model parameter. It represents the changes in $y_k(t)$ which are brought out by a unitary change in θ_i. When the model includes more than one parameter, comparisons among sensitivities could be a tricky matter for parameters usually have different unities. So, for comparisons purposes the use of the reduced sensitivities is proposed:

$$\tilde{s}_{k,i}(t) \equiv \left(\frac{\partial\, y_k(t)}{\partial\theta_i / \theta_i} \right) = \theta_i\, s_{k,i}(t) \tag{2.26}$$

$\tilde{s}_{k,i}(t)$ represents the changes in the k^{th} output of the model caused by a relative variation in the θ_i parameter. It must be noticed that $\tilde{s}_{k,i}(t)$ and $y_k(t)$ are stated in the same unities.

The effect of the parameter θ_i on the k^{th} model output is measured by means of the following two statistics:

$$\mu_{k,i} = \frac{1}{N}\sum_{t=1}^{N} \tilde{s}_{k,i}(t) \qquad \text{and} \qquad \sigma_{k,i} = \sqrt{\frac{1}{N-1}\sum_{t=1}^{N} \left(\tilde{s}_{k,i}(t) - \mu_{k,i}\right)^2} \tag{2.27}$$

where N represents the total number of observations in the analysed time series. The first one (sensitivity mean value) measures the influence of parameters on the model static behaviour, and the second one (sensitivity standard deviation) measures their effects on the model dynamic behaviour. θ_i is said to be an active parameter with regard to the k^{th} model output when $\mu_{k,i} > \alpha$ or/and $\sigma_{k,i} > \beta$. α and β are appropriate thresholds for testing parameters significance.

Alternatively, the effect of the parameter θ_i on the k^{th} model output could be measured by means of the following distance

$$d_{k,i} = \sqrt{\mu_{k,i}^2 + \sigma_{k,i}^2} \tag{2.28}$$

θ_i is said to be an active parameter with regard to the k^{th} model output when $d_{k,i}$ is greater than a given threshold.

> The necessary condition for a physical phenomenon could be validated on the available data, is that it involves at least one active parameter in its mathematical representation. However, this is not a sufficient condition. It is also required that active parameters associated to it was not correlated with another active model parameters.

Active model parameters leading to similar effects on the model outputs must be identified for they introduce some additional limitations for validation purposes. Statistical correlations analysis can be used to identify such limitations. The degree of correlation between parameters θ_i and θ_j with regard to the k^{th} model output is measured by:

$$\rho_{ij}^{(k)} = \frac{\frac{1}{N-1}\sum_{t=1}^{N}(\widetilde{s}_{k,i}(t)-\mu_{k,i})(\widetilde{s}_{k,j}(t)-\mu_{k,j})}{\sigma_{k,i}\ \sigma_{k,j}} \tag{2.29}$$

When $\left|\rho_{ij}^{(k)}\right| > \gamma$, no significant differences can be established between the effects of these parameters on the k^{th} model output. It can be then stated that both parameters, θ_i and θ_j, belong to a same group of model parameters. A pertinent selection of γ leads to the cutting up of the active model parameters set into *g* quasi-independent groups, π_s $(s = 1, \cdots, g)$.

For optimisation purposes (see section 2.5), we will define group representatives. A group representative is the parameter in a group that show a greater effect on the model outputs. For instance, the parameter θ_m is the representative of the group $\pi_s = \left\{\theta_i \quad \theta_j \quad \theta_m\right\}$ when $d_{k,m}$ (see eq. 2.28) is greater than both $d_{k,i}$ and $d_{k,j}$. Free model parameters will be the group representatives. The number of free model parameters is hence equal to the number of quasi-independent groups.

Principal components analysis and preliminary diagnosis

Principal components analysis is a statistical tool allowing transformation of a set of correlated time series into a new set of de-correlated ones. In the framework of model validation we are using it to define parameters signatures (another way of studying parameters correlations) and to supply some preliminary elements for diagnosis.

Fundamentals of principal components analysis

Let

$$\zeta(t) = \left[\widetilde{s}_{k,1}(t) \quad \widetilde{s}_{k,2}(t) \quad \cdots \quad \widetilde{s}_{k,p}(t)\right]^T \tag{2.30}$$

be the vector including reduced sensitivity time series for the k^{th} model output. The covariance matrix

$$W = \int_{t_o}^{t_f} \zeta(t)\zeta(t)^T dt \tag{2.31}$$

is a positive definite matrix $(p \times p)$ with a set of non-negative real eigenvalues $\lambda_1 \geq \lambda_2 \geq \cdots \geq \lambda_p \geq 0$ and the corresponding mutually orthogonal eigenvectors $V = \left[\vec{v}_1 \quad \vec{v}_2 \quad \cdots \quad \vec{v}_p\right]$. Hence, it can be written as

$$W = V\Sigma V^T \tag{2.32}$$

where $\Sigma = diag\left[\lambda_1 \quad \lambda_2 \quad \cdots \quad \lambda_p\right]$ is a diagonal matrix including the so-called singular values of $\zeta(t)$.

It can be demonstrated that V defines a complete basis in $\Re^p$. Consequently, $\zeta(t)$ can be written as

$$\zeta(t) = VX(t) \tag{2.33}$$

where $X(t) = \left[x_1(t) \quad x_2(t) \quad \cdots \quad x_p(t)\right]^T$ is the vector of the decomposition coefficients of $\zeta(t)$ on V. The reduced sensitivity of the k^{th} model output to the i^{th} parameter is then written as

$$\tilde{s}_{k,i}(t) = \sum_{m=1}^{p} v_{i,m} x_m(t) \tag{2.34}$$

where $v_{i,m}$ is the (i,m) element of the matrix V. The product $v_{i,m}x_m(t)$ is the so-called « m^{th} principal component of $\tilde{s}_{k,i}(t)$ ».

Some interesting properties of principal components are:

P1. It can be proved that the components of the vector $X(t)$ are statistically uncorrelated. That is

$$W_x \equiv \int_{t_o}^{t_f} X(t)X^T(t)dt = \Sigma \qquad \text{or} \qquad \int_{t_o}^{t_f} x_i(t)x_j(t)dt = \begin{cases} \lambda_i & i = j \\ 0 & i \neq j \end{cases} \tag{2.35}$$

> ***Proof :*** *From equation 2.33, it is a simple matter to show that* $W = VW_xV^T$. *Knowing that* $VV^T = I$ *and taking into account 2.32, the previous equation becomes* $W_x = V^TWV = \Sigma$.

P2. The whole energy of $\zeta(t)$ is defined as

$$\mathsf{E} \equiv trace(W) = \sum_{i=1}^{p} \int_{t_o}^{t_f} s_{k,i}^2(t)dt \tag{2.36}$$

It can be easily demonstrated that the whole energy of $\zeta(t)$ is given by the sum of its singular values:

$$\mathsf{E} = \sum_{i=1}^{p} \lambda_i \tag{2.37}$$

Proof : *Using equation 2.32 and simple properties of matrices, it is a simple matter to show that*

$$\mathsf{E} \equiv trace(W) = trace(V\Sigma V^T) = trace(\Sigma V^T V) = trace(\Sigma) = \sum_{i=1}^{p} \lambda_i$$

PCA applications in the framework of model validation

In the framework of model validation, PCA has three main potential applications:

- It can be used to study correlations among model parameters through the analysis of the so called parameters signatures.
- It allows forming a new set of truly independent parameters for further use in optimisation (see section 2.4).
- It supplies some interesting information about diagnosis.

■ **Model parameters signatures:** From equations (2.34) and (2.35), it is easy to prove that the variance of the reduced sensitivity $\tilde{s}_{k,i}(t)$ is given by

$$\sigma^2_{k,i}(t) = \int_{t_o}^{t_f} s^2_{k,i}(t)dt = \sum_{m=1}^{p} v^2_{i,m}\lambda_m \tag{2.38}$$

Hence, $v^2_{i,m}\lambda_m$ represents the contribution of the m^{th} principal component to the variance of $\tilde{s}_{k,i}(t)$. We call signature of the i^{th} model parameter with regard to the k^{th} model output the ensemble $\left\{v^2_{i,m}\lambda_m\right\}_{m=1,\cdots,p}$. Parameters showing similar signatures are parameters leading to similar effects on the model outputs when changing their values. As correlations analysis before, model parameters signatures can be used to group parameters and to identify possible causes of ambiguity in further diagnostics.

■ **A new set of truly independent parameters:** Assuming linear relationships between model outputs and model parameters, the effect of parameters changes on the outputs can be expressed as

$$\forall k \qquad \Delta y_k(t) = \sum_{i=1}^{p} \frac{\Delta\theta_i}{\theta_{io}} \tilde{s}_{ki}(t) \tag{2.39}$$

where θ_{io} and $\Delta\theta_i$ represents respectively the nominal value and the variation of the i^{th} parameter. According to 2.34, the previous equation becomes

$$\forall k \qquad \Delta y_k(t) = \sum_{i=1}^{p} \Delta\gamma_i x_i(t) \tag{2.40}$$

with

$$\gamma_i = \sum_{j=1}^{p} \frac{\theta_j}{\theta_{jo}} v_{ji} \tag{2.41}$$

where v_{ji} is the (j,i) element of the matrix V.

The principal components analysis then suggests a new set of parameters $\{\gamma_i\}_{i=1,\cdots,p}$ that are defined as linear combinations of the physical or initial parameters. The sensitivity of the model outputs to these new parameters is determined by the projection of $\zeta(t)$ on V. That is, $x_i(t)$ represents the sensitivity of $y_k(t)$ to γ_i. As $\{x_i(t)\}_{i=1,\cdots,p}$ are statistically uncorrelated time series (see property P1), then $\{\gamma_i\}_{i=1,\cdots,p}$ is a set of truly independent parameters.

The significance of the parameter γ_i can be measured by

$$\left(\sum_{j=1}^{p} \lambda_j\right)^{-1} \lambda_i \tag{2.42}$$

which represents the contribution of $x_i(t)$ to whole energy of $\zeta(t)$ (see property P2). In the same way, the significance of the subset $\gamma_1, \gamma_2, \cdots, \gamma_m$ is measured by :

$$\left(\sum_{j=1}^{p} \lambda_j\right)^{-1} \sum_{j=1}^{m} \lambda_j \tag{2.43}$$

Knowing that $\lambda_1 \geq \lambda_2 \geq \cdots \geq \lambda_p \geq 0$, the equation before allows to determine new active/free model parameters. Parameters $\gamma_1, \gamma_2, \cdots, \gamma_m$ are stated to be active/free when

$$\left(\sum_{j=1}^{p} \lambda_j\right)^{-1} \sum_{j=1}^{m} \lambda_j > \beta \tag{2.44}$$

where β is an appropriate threshold (e.g. $\beta = 0.95$). In practice, it is often observed that only a few numbers of new parameters (mainly the first one) are really significant.

■ **Preliminary diagnosis:** When linear relationships can be assumed between model outputs and parameters, some useful information concerning diagnosis can obtained from principal components analysis. The possibilities for diagnosis are associated to two main observations:

- The significance of the first new independent parameter (see equation 2.42) is usually greater than 0.8; that is, the first component of the vector $X(t)$ explains more than 80% of the whole energy of the signals in $\zeta(t)$.

- A strong statistical correlation is generally observed between residuals and the first component of the vector $X(t)$. This mean that good enough linear relationships can be established between residuals and $x_1(t)$.

Under such conditions, it can be assumed that significant reduction of the residuals will be associated to a model output variation of the form

$$\Delta y_k(t) \approx \Delta\gamma_1 x_1(t) \tag{2.45}$$

Taking into account the functional relationship existing between $\Delta\gamma_1$ and the initial model parameters:

$$\Delta\gamma_1 = \frac{\Delta\theta_1}{\theta_{1o}} v_{11} + \frac{\Delta\theta_2}{\theta_{2o}} v_{21} + \cdots + \frac{\Delta\theta_p}{\theta_{po}} v_{p1} \tag{2.46}$$

the "minimal" modification* of model initial parameters required will be:

$$\Delta\theta_j / \theta_{jo} = v_{j1}\Delta\gamma_1 \qquad j = 1,\cdots,p \tag{2.47}$$

This equation shows that coefficients $\{v_{j1}\}_{j=1,\cdots,p}$ (the first eigenvector) supply some useful information concerning the way the initial model parameters must be modified in order to reduce the observed residuals.

2.4. FREE MODEL PARAMETERS ESTIMATION AND DIAGNOSIS

The main tool that we are proposing to guide modelling errors diagnosis is based on parameter estimation techniques. If some thing in the model is clearly wrong, it is expected to find large parameters displacements when fitting the model on the measured data. The comparison of the estimated parameters values with their nominal values, should lead to known reasons for the observed modelling errors and to suggest model improvements.

Fitting the model on the measured data usually involves:

- The definition of an objective. This can be done in very different ways. The simplest one consists on defining a scalar functional of the residuals (e.g. the residuals variance) to be minimised. More unusual objectives are those taking into account model and measurements uncertainties.

- The definition of the problem constraints if any. In the framework of model validation, constraints usually refer to the allowed values for free model parameter.

- The selection of the optimisation algorithm. Several criteria can be used for selecting the optimisation algorithm. First of all, the compatibility with the problem statement (objective and constraints). Next, the nature of the algorithm (global or local, deterministic or

* "Minimal" modification means that the maximum displacement $\Delta\theta_j / \theta_{jo}$ is the minimum of all possible maxima.

stochastic, etc.), its performances (reliability, rate of convergence, etc.), and implementation facilities.

The subject of optimisation is a fascinating blend of heuristics and rigour, of theory and experiment. It can be studied as a branch of pure mathematics, yet has applications in almost every branch of science and technology. An impressive amount of methods and optimisation algorithms have been proposed in the past. In the framework of model diagnosis, optimisation is usually a quite difficult problem because:

- Data are always associated with some uncertainty, if only because of the finite precision of the sensors used to collect them. Optimisation methods assuming errorless data, as those based on the minimisation of a scalar function of the residuals, could lead to fitted models that represents the dynamic behaviour of both the system and the measurement noise . Hence, diagnosis conclusions can be biased by data uncertainty.

- Diagnosis usually requires finding the global solution of the optimisation problem instead of a local one. The possibility of finding global minima has been largely considered in the past, but there still remain considerable difficulties. Historically, methods to solve global optimisation problems have been classified as either stochastic or deterministic. Stochastic methods evaluate the objective function at randomly sampled points from the parameter region of allowed variation. Deterministic methods, on the other hand, involve no elements of randomness.

Three different optimisation methods have been implemented and tested in the framework of this project:

- The Gauss-Newton method. This method is only generally practicable to search for local solutions rather than global solution. It has been however chosen by its simplicity and its well known efficiency for finding local minima.

- A random search global algorithm. All global optimisation algorithms can be partitioned into the two classes: reliable and unreliable. Clearly all stochastic methods, including simulated annealing, clustering, and random search, fall into the unreliable category. In fairness, however, efficiency is the strength of such methods. For now, large-scale problems may best be solved stochastically.

- A deterministic global algorithm. The class of deterministic global algorithms, including branch and bound methods, covering methods, interval methods, tunnelling, and enumerating, can be partitioned into two categories: methods which compute objective function values at sampled points (point methods); and methods which compute function bounds over compact sets (bounding methods). This division further separates reliable methods from unreliable. Point methods are inherently incapable of reliably solving the global optimisation problem. On the other hand, bounding methods, if properly implemented, can produce rigorous global optimisation solutions. A heuristic bounding method has been here proposed.

The first two methods are base on the assumption of errorless data. On the contrary, the deterministic global algorithm allows handling data uncertainty.

The three methods are briefly described below. A discussion concerning their main advantages and drawbacks is included at the end of this section.

Only single-output models have been considered. $y(t)$ and $y^*(t)$ represent respectively simulations and measurements.

Gauss-Newton method

Let

$$e(t,\theta) = y^*(t) - y(t,\theta) \tag{2.48}$$

be the residuals associated to the parameter vector θ, and let

$$J(\theta) = \sum_{t=1}^{N} e^2(t,\theta) \tag{2.49}$$

be a quadratic measure of it. The Gauss-Newton method consider the problem of finding a local minimum of the objective function $J(\theta)$. The minimising point is referred to as θ^*. Note first of all that this method is only generally practicable to search for local solutions rather than global solution.

As most of the optimisation algorithms, the Gauss-Newton one looks for the minimising point iteratively (see e.g. [18]). At iteration k, the parameters vector is modified as

$$\theta^{(k+1)} = \theta^{(k)} + p^{(k)} \tag{2.50}$$

where the direction of search $p^{(k)}$ is determined from the Hessian matrix and the gradient of the functional $J(\theta)$:

$$p^{(k)} = -\left[He^{(k)}\right]^{-1} Gr^{(k)} \tag{2.51}$$

The gradient is given by:

$$Gr^{(k)} = \frac{2}{N} \sum_{t=1}^{N} e(t,\theta^{(k)})\, \zeta^{(k)}(t) \tag{2.52}$$

with

$$\zeta^{(k)}(t) = \left[\frac{\partial y(t,\theta^{(k)})}{\partial \theta_1} \quad \frac{\partial y(t,\theta^{(k)})}{\partial \theta_2} \quad \cdots \quad \frac{\partial y(t,\theta^{(k)})}{\partial \theta_p} \right]^T \tag{2.53}$$

As for the Hessian matrix, it is approached by:

$$He^{(k)} = \frac{2}{N} \sum_{t=1}^{N} \zeta^{(k)}(t) \left(\zeta^{(k)}(t)\right)^T \tag{2.54}$$

The iteration loop is terminated when the following user-supplied convergence test become satisfied:

$$J(\theta^{(k)}) < \alpha \qquad \text{or} \qquad J(\theta^{(k)}) - J(\theta^{(k+1)}) < \beta \tag{2.55}$$

where α and β are user-supplied thresholds.

Monte Carlo approach

Monte Carlo methods consider the problem of finding the global minimum of the objective function $J(\theta)$ (eq. 2.49) over a given parameter set Θ. We remember that the parameter set is defined by the box

$$\Theta = \left[\theta_{1,\min} \quad \theta_{1,\max}\right] \times \left[\theta_{2,\min} \quad \theta_{2,\max}\right] \times \cdots \times \left[\theta_{p,\min} \quad \theta_{p,\max}\right]$$

where $\left[\theta_{i,\min} \quad \theta_{i,\max}\right]$ represents the allowed interval of variation for the i^{th} free model parameter. It defines the parameters domain where we are looking for parameters values allowing significant model residuals reduction. Such intervals have generally nothing to do with precision:

- They must be wide enough so that modelling hypothesis associated to the free model parameters could be tested.
- They must be chosen so as model outputs bounds over Θ include measurements. In this way, the parameter set hopeful includes parameter vectors leading to a good enough model behaviour.

As previously, the minimising point is referred to as $\theta^* \in \Theta$

Pure random search algorithm

Among the existing stochastic approaches (see e.g. [19]), a « pure » random search algorithm has been selected because its simplicity. It performs as follows:

a) Generates n random parameter vectors ($\theta^{(s)} \in \Theta$, $s = 1, \cdots, n$) based on uniform probability distribution functions.

b) Performs model simulations and calculates $J(\theta^{(s)})$, s=1, $\cdots$, n.

c) Estimates the minimum value of the objective function as $J^* = \min\left\{J(\theta^{(1)}), J(\theta^{(2)}), \cdots, J(\theta^{(n)})\right\}$. The solution we are looking for is then θ^* so as $J(\theta^*) = J^*$.

In order to see how close the algorithm comes to finding the global minimum, the Chevyshev inequality can be applied to the sample results. This theorem states that if the mean, m, and the standard deviation, s, of the sample of $J(\theta)$ values are obtained as estimates of the universal mean, μ, and standard deviation, σ, of the distribution of all $J(\theta)$ possible values, then for any real number, r, the probability that the observed value, x, is exceeded is given by:

$$P\left(|x - \mu| \geq \sigma\right) \leq \frac{1}{r^2}$$

In other words, the probability of a $J(\theta)$ value falling outside the interval $\left[\mu - r\sigma,\ \mu + r\sigma\right]$ is at most $1/r^2$. For instance, if the highest (or lowest) value of $J(\theta)$ is found to be 3.5s from the mean value, then it would be expected that 8.2% ($\cong 1/3.5^2$) of the expected $J(\theta)$ values would be found distributed beyond $m \pm 3.5s$. If the tails of the $J(\theta)$ distribution are found to be similar, then an upper bound for the probability of $J(\theta)$ values exceeding the highest (or lowest) observed value would be 0.041.

Multi-step random search algorithm

The previous algorithm allow us to find the global minimum of the objective function $J(\theta)$ over a user-supplied parameters set Θ. Choosing it is a non trivial task and the quality of diagnosis could be biased by the selection of Θ. Hence, an iterative procedure has been proposed to get the optimisation solution we are looking for (see figure 2.2):

(a) First of all, a prior parameter set Θ is selected.

(b) Random search is then carried out and model outputs bounds over Θ are calculated.

(c) Next, the parameter set consistency with data is tested. One said that Θ is consistent with data when the corresponding model outputs bounds include measurements. In other words, measurements and model simulations are in good agreement.

(d) If Θ is stated to be consistent with data, the procedure is stopped; otherwise, the parameter set is re-defined and we come back to b).

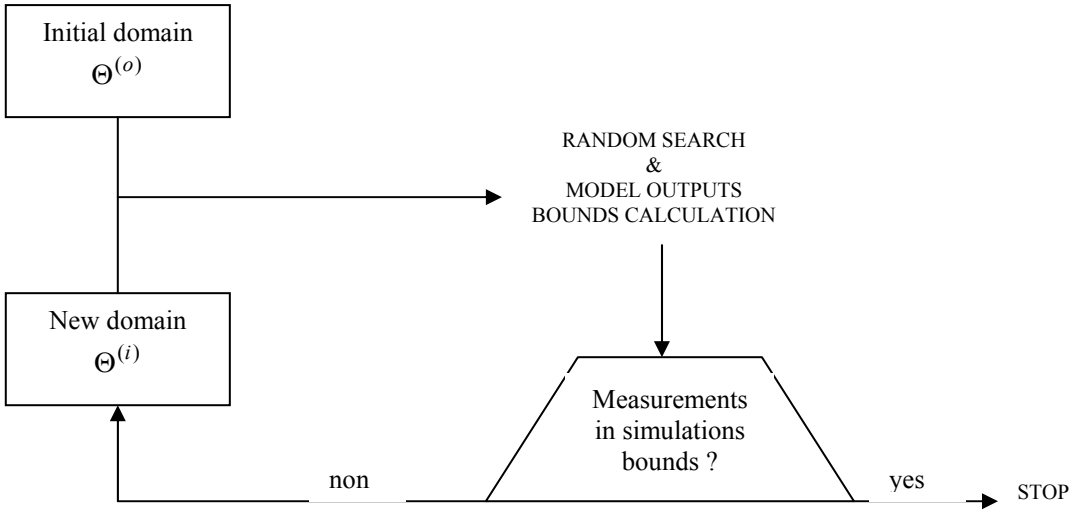

Figure 2.2. *Multi-step random search algorithm loop.*

Heuristic bounding method

The development of techniques for estimating model parameters from uncertain data is in full expansion (see [20] for a quite complete survey). Deterministic global algorithms are among them a very promising way to tackle such kind of estimation problems, especially algorithms that compute the objective function over compact sets (bounding methods) instead of at sample points. A heuristic bounding algorithm (HBA) has been proposed in the framework of the IEA Task 22.

Contrary to the algorithms presented previously, the HBA takes into account data uncertainty. The problem is no longer stated as: "looking for $\theta^* \in \Theta$ that minimizes an objective function measuring the simulation error". Instead of that, we are looking for a parameter set Θ providing simulation uncertainty bands including measurements. Two main statements of the problem have been considered:

First statement. Look for Θ of minimum width so that:

$$\forall t \quad y^*(t) \in \left[y_{\min}(t) \quad y_{\max}(t) \right] \tag{2.56}$$

where $y_{\min}(t)$ and $y_{\max}(t)$ are respectively the model output lower and upper bounds over Θ (see section 2.1 for definition).

Second statement. Look for Θ so that:

$$\forall t \quad \left[y_{\min}(t) \quad y_{\max}(t)\right] \subset \left[y^*_{\min}(t) \quad y^*_{\max}(t)\right] \tag{2.57}$$

where $y^*_{\min}(t)$ and $y^*_{\max}(t)$ are respectively the measurements lower and upper bounds.

The HBA algorithm performs iteratively as follows:

a) Performs model simulations using the parameter vector $\theta = \left[\theta_1 \quad \theta_2 \quad \cdots \quad \theta_p\right]$. Results are noted $y(t)$.

b) Calculate model output sensitivity to every parameter around the trajectory $y(t)$ (see section 2.3; "sensitivity calculation methods"):

$$\zeta(t) = \left[\widetilde{s}_1(t) \quad \widetilde{s}_2(t) \quad \cdots \quad \widetilde{s}_p(t)\right]^T$$

c) Performs principal components analysis on $\zeta(t)$ (see section 2.3 ; "principal components analysis "):

- calculate the singular values of $\zeta(t)$ ($\lambda_1 \geq \lambda_2 \geq \cdots \geq \lambda_p \geq 0$) and the corresponding eigenvectors ($V = \left[\vec{v}_1 \quad \vec{v}_2 \quad \cdots \quad \vec{v}_p\right]$);
- project of $\zeta(t)$ onto the eigen-basis V, $X(t) = V^T \zeta(t)$; and
- identify significant components of $X(t)$ using the energy criterion given by equation (2.44): $x_1(t) \quad x_2(t) \quad \cdots \quad x_d(t)$, with $d \leq p$. Frequently, only a few numbers of the $X(t)$ components (mainly the first one) are really significant.

d) Estimate the parameter set Θ that verify (2.56) or (2.57) assuming linear relationships between the model output and the model parameters (see equation 2.39):

For the first statement

- calculate $\Delta y(t)$ so as $\forall t, y^*(t) = y(t) + \Delta y(t)$;
- calculate $\Delta\gamma_i(\mathrm{t})$ with $(i = 1, \cdots, d)$ so that $\forall t$ the equation $\Delta y(t) = \Delta\gamma_1 x_1(t) + \cdots + \Delta\gamma_{\mathrm{d}} x_d(t)$ is verified;
- select times $t_{\min}$ and $t_{\max}$ where $\Delta y(t)$ takes respectively its maximum and minimum values, and define the vectors $\Delta\gamma_{\min} = \left\{\Delta\gamma_i(\mathrm{t}_{\min})\right\}_{i=1,\cdots,d}$ and $\Delta\gamma_{\max} = \left\{\Delta\gamma_i(\mathrm{t}_{\max})\right\}_{i=1,\cdots,d}$;

For the second statement

- calculate $\Delta y_{\min}(t) = y^*_{\min}(t) - y(t)$ and $\Delta y_{\max}(t) = y^*_{\max}(t) - y(t)$;
- calculate $\Delta\gamma_{\min} = \left\{\Delta\gamma_{i,\min}\right\}_{i=1,\cdots,d}$ so that the variance of $r(t) = \Delta y_{\min}(t) - \left(\Delta\gamma_{1,\min} x_1(t) + \cdots + \Delta\gamma_{\mathrm{d},\min} x_d(t)\right)$ is minimised (linear least squared method);

– calculate $\Delta\gamma_{\max} = \{\Delta\gamma_{i,\max}\}_{i=1,\cdots,d}$ so that the variance of $r(t) = \Delta y_{\max}(t) - (\Delta\gamma_{1,\max} x_1(t) + \cdots + \Delta\gamma_{d,\max} x_d(t))$ is minimised (linear least squared method);

For both statements

– estimate the parameter set Θ solving the equations

$$\Delta\gamma_{\min(\max)} = V_d^T \Delta\hat{\theta}_{\min(\max)} \tag{2.58}$$

where V_d is the matrix ($p \times d$) including the eigenvectors $\vec{v}_1$ to $\vec{v}_d$. Taking into account that $V_d V_d^T = I$ (orthonormal eigen-basis), the solution of the equation before is:

$$\Delta\hat{\theta}_{\min(\max)} = V_d \Delta\gamma_{\min(\max)}$$

where

$$\Delta\hat{\theta}_{\min(\max)} = \left[\frac{\Delta\theta_{1,\min(\max)}}{\theta_{1,o}} \quad \frac{\Delta\theta_{2,\min(\max)}}{\theta_{2,o}} \quad \cdots \quad \frac{\Delta\theta_{p,\min(\max)}}{\theta_{p,o}} \right]^T$$

It must be noticed that if $d < p$ the solution of (2.57) is not unique, the number of unknowns is greater than the number of equations available. In such case, the solution Θ proposed by the algorithm is the one leading to smaller parameter displacements ("minimal" changes).

e) Define a new vector of parameters θ_{new} as the geometrical centre of Θ and calculate the difference $|\theta - \theta_{new}|$. If $|\theta - \theta_{new}| < \varepsilon$, the estimation procedure is stopped ; otherwise, make $\theta = \theta_{new}$ and return to a).

Main hypothesis underlying the HBA is linearity. That is, linear relationships are assumed between any parameter change and the consequential change in the model output. For most systems this is not strictly true. Nevertheless, for small changes in the parameters such an assumption is valid. The hypothesis of linearity, and thus the quality of the solution Θ proposed, can be verified by comparing model output bounds over Θ calculated by Monte Carlo techniques with those coming form sensitivity analyses.

Discussion

Main advantages and drawbacks of the three optimisation methods described in this section are here summarised.

The Gauss-Newton method is only generally practicable to search for local solutions rather than global ones. In addition, the method is associated to a problem statement that assumes errorless data. It is however a simple and quite efficient method when practicable.

The random search algorithm belongs to the non-reliable category of stochastic global methods. As the previous method, errorless data are assumed in the problem statement. Main drawback of this approach is related to its non-reliability: the closeness of the solution to the global optimum can only be evaluated *a posteriori* and in terms of probability. Additionally, there is no way to decide *a priori* the number of trials to be carried out. In fairness, however, efficiency is the strength of such method. For now, large-scale problems may best be solved stochastically.

The heuristic bounding method has been developed in the framework of the IEA Task 22. It seems to us a promising way for modelling diagnostic purposes. Main reason is that HBA allows to incorporate data uncertainty (see problem statement) and it is conceived for reliable global solution searching. In addition, HBA computer implementation is quite easy and it does not require any simulation code modification. Main limitation is associated to the assumption of linear relationships between model outputs and parameters. As we said before, for most systems this is not strictly true. Nevertheless, for small changes in the parameters (small parameter set solution width) such an assumption is valid.

2.5. A ILLUSTRATIVE EXAMPLE

To illustrate the principles and methods we are proposing, a simple model validation exercise is here proposed. The object under analysis is a multi-layer vertical wall that separates two rooms in an actual building (see Fig. 2.3). The wall exchanges heat by convection with the air in the rooms, and it absorbs solar radiation by its right facade.

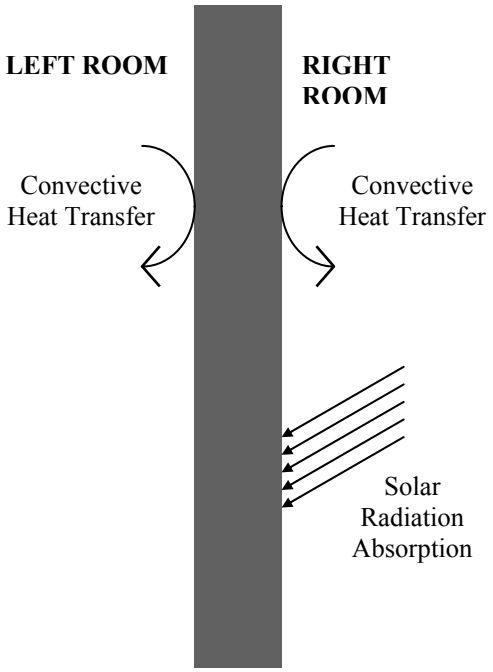

LAYER	(m)
Paper	0.001
Plasterboard	0.010
Polyestyrene	0.080
Air	0.010
Hollow blocks	0.200
Facing	0.020

Figure 2.3. *Wall sketch and composition (from the right to the left side).*

The model and the experimental data

A one-dimensional conduction model is adopted for each one of the wall layers $(k = 1,\cdots,6)$:

$$\rho^{(k)} c_p^{(k)} \frac{\partial T(x,t)}{\partial t} = \lambda^{(k)} \frac{\partial^2 T(x,t)}{\partial x^2} \qquad x_o^{(k)} < x < x_l^{(k)} \tag{2.57}$$

where $x_o^{(k)}$ and $x_l^{(k)}$ are the left and right coordinates of the k^{th} layer. $\rho^{(k)}$, $c_p^{(k)}$ and $\lambda^{(k)}$ are, respectively, the density, the specific heat and the thermal conductivity of the layer. Boundary conditions at $x = x_o^{(k)}$ (resp. $x = x_l^{(k)}$), when in contact with another capacitive layer j, are:

$$\begin{aligned} &T(x_o^{(k)},t) = T(x_l^{(j)},t) \\ &-\lambda^{(k)} \frac{\partial T(x,t)}{\partial x}\bigg|_{x=x_o^{(k)}} + \lambda^{(j)} \frac{\partial T(x,t)}{\partial x}\bigg|_{x=x_l^{(j)}} = 0 \end{aligned} \tag{2.58}$$

Boundary conditions at $x = 0$ and at $x = L$ (L = wall thickness) are:

$$-\lambda^{(1)} \frac{\partial T(x,t)}{\partial x}\bigg|_{x=0} = -h_{left}(T(0,t) - T_{left}(t)) \tag{2.59}$$

and

$$-\lambda^{(6)}\left.\frac{\partial T(x,t)}{\partial x}\right|_{x=L} = -h_{right}(T(L,t)-T_{right}(t))+\eta\varphi(t) \tag{2.60}$$

where $T_{left}(t)$ and $T_{right}(t)$ are respectively the air temperature in the left and right rooms, and $\varphi(t)$ represents the solar irradiance on a south oriented vertical surface. h_{left} and h_{right} are constant convective coefficients for wall-air heat exchanges representation, and η is the solar efficiency of the wall referred to the solar irradiance on a south oriented vertical surface. The model involves 18 parameters whose nominal values are given in Table 2.1.

	Thickness (m)	$\rho c_p \times 10^{-3}$ $(J.m^{-3}.K^{-1})$	λ $(W.m^{-1}.K^{-1})$	h $(W.m^{-2})$	η $(-)$
Plasterboard	0.010	680	0.350	4.0	0.008
Polystyrene	0.080	18	0.043		
Air	0.010	1.29	0.071		
Hollow blocks	0.200	1140	1.052		
Facing	0.020	1657	1.150	4.0	

Table 2.1. *Nominal values for model parameters:* ρ, *density;* c_p, *specific heat;* λ, *thermal conductivity;* h, *convective coefficients;* η, *optical efficiency.*

Spatial discretisation of equations (2.57) to (2.60) leads to a state model of the form (2.1), which includes 36 ordinary differential equations. The input signals to the model are the air temperature in the left and the right rooms (see Fig. 2.4, right), and the global solar irradiance on an outdoor south vertical surface (see Fig. 2.4, left). Concerning outputs, we will focus our attention on the wall right surface temperature, whose measured behaviour is represented in figure Fig. 2.5 (left).

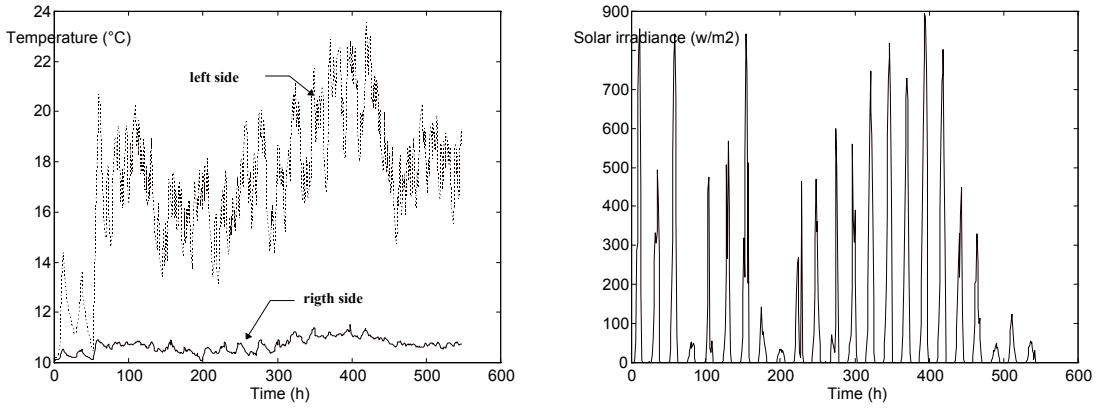

Figure 2.4. *Left: Air temperature in the left and right rooms; Right: Solar irradiance.*

The differences observed between measurements and model simulations (residuals) are shown in Fig. 2.5 (right). It seems to be clear that the model does not reproduce adequately the static behaviour of the system, it overestimates the wall temperature (residuals mean value = $-0.88°C$). Concerning its dynamical performances, no much better results are observed: residuals show low frequency trends and peaks, and its standard deviation value is $0.4°C$. Figure 2.5b includes the residuals density power spectrum. It shows that problems in the model mainly appear at low frequencies. Conclusions from simulations-measurements consistency analysis doest not differ from the previous ones. 100% of measurements fall outside the simulation uncertainty bands. Last ones have been calculated assuming ±10% of uncertainty for all model parameters. The model or the inputs to the model are wrong.

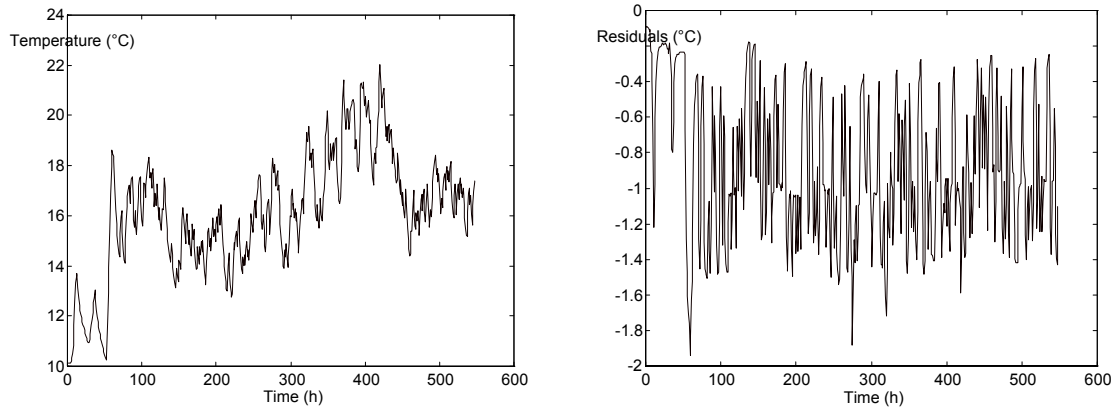

Figure 2.5. *Left: Wall surface temperature; Right: Residuals.*

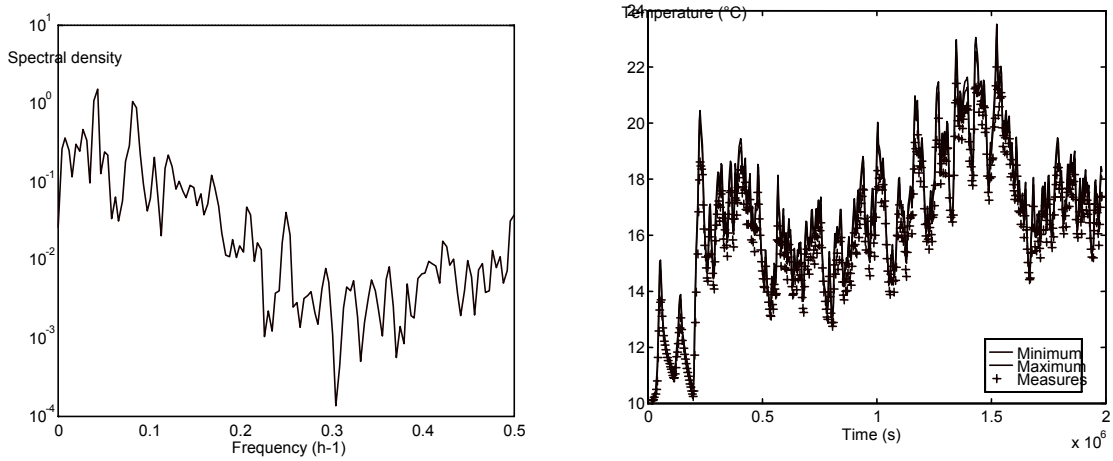

Figure 2.5b. *Left: Residual spectral density; Right: Simulations uncertainty bands (continuous lines) and measurements (crosses).*

Sensitivity analysis

The sensitivity of the model output (wall surface temperature, right side) to the model parameters variations has been calculated by time integration of the corresponding sensitivity models (sensitivity-equation method).

Active model parameters

Table 2.2 includes the mean and the standard deviation values of the reduced sensitivities.

		Mean (°C)	Standard Deviation (°C)
Conductivity	Plasterboard	-0.0065	0.0094
	Polystyrene	-0.4243	0.1790
	Air	-0.0315	0.0132
	Hollow blocks	-0.0404	0.0148
	Facing	-0.0034	0.0017
Capacity	Plasterboard	-0.0060	0.2501
	Polystyrene	-0.0006	0.0185
	Air	0. 0000	0.0000

	Hollow blocks	-0.0068	0.0184
	Facing	0.0006	0.0039
Thickness	Plasterboard	0.0001	0.2449
	Polystyrene	0.3861	0.1619
	Air	0.0298	0.0125
	Hollow blocks	0.0304	0.0254
	Facing	0.0037	0.0035
Others	h_{left}	-0.0502	0.0228
	h_{right}	0.3892	0.3568
	η	0.1815	0.3353

Table 2.2. *Results from sensitivity time series statistical analysis.*

Active model parameters are assumed to be those leading to mean and standard deviation values greater than 0.05°C :

1 Plasterboard - Heat Capacity
2 Polystyrene - Thermal Conductivity
3 Left side Convective coefficient
4 Right side Convective coefficient
5 Solar efficiency
6 Polystyrene - Thickness
7 Plasterboard - Thickness

Figures 2.6 and 2.7 show the time evolution of the reduced sensitivities corresponding to the active model parameters. It can be seen that the effect of parameters 1 and 7 (plasterboard heat capacity and thickness) on the wall temperature merge. Parameters 2 and 6 (polystyrene thermal conductivity and thickness) produce opposite but similar effects on the wall temperature. No similarities are found among the sensitivity behaviour from the other parameters.

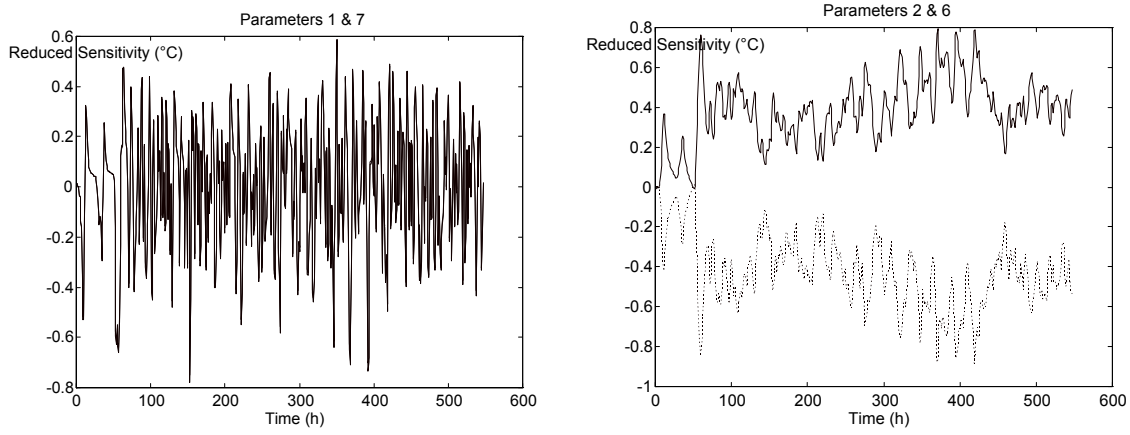

Figure 2.6. *Time evolution of reduced model output sensitivities to parameters 1 and 7 (left) and to parameters 2 and 6 (right).*

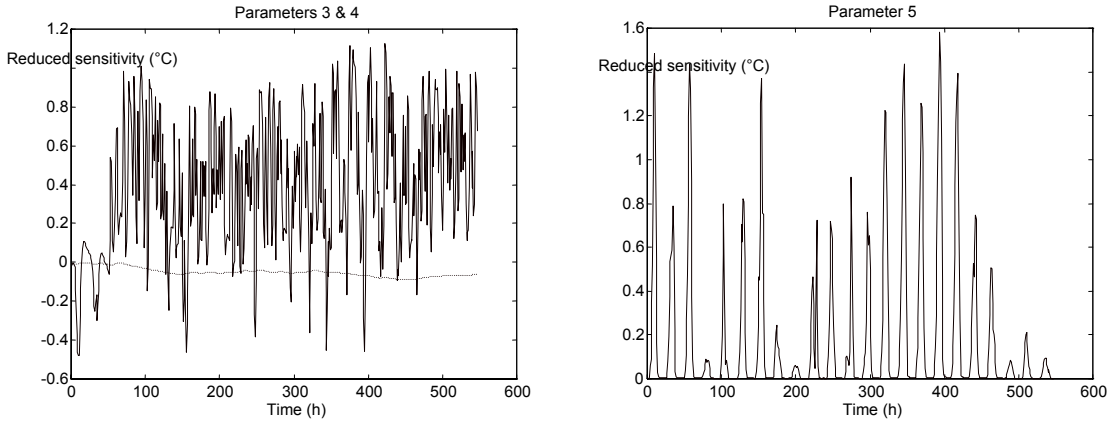

Figure 2.7. *Time evolution of reduced model output sensitivities to parameters 3 and 4 (left) and to parameter 5 (right).*

Correlations analysis

Table 2.3 includes correlation values among parameters sensitivity time series.

	1	**2**	**3**	**4**	**5**	**6**	**7**
1	1.0000	0.0821	-0.4148	-0.0303	-0.4066	0.0306	0.9996
2	0.0821	1.0000	-0.3884	0.3667	-0.3110	-0.9935	0.0777
3	-0.4148	-0.3884	1.0000	-0.2522	-0.4589	0.3461	-0.4092
4	-0.0303	0.3667	-0.2522	1.0000	0.0020	-0.3750	-0.0345
5	-0.4066	-0.3110	-0.4589	0.0020	1.0000	0.2630	-0.4085
6	0.0306	-0.9935	0.3461	-0.3750	0.2630	1.0000	0.0353
7	0.9996	0.0777	-0.4092	-0.0345	-0.4085	0.0353	1.0000

Table 2.3. *Results from active model parameters correlation analysis.*

As previously, it can be seen that the parameters 1 and 7 (plasterboard heat capacity and thickness) and the parameters 2 and 6 (polystyrene thermal conductivity and thickness) are strongly correlated. Small changes of their values lead to similar effects on the model output. Active parameters are then grouped as:

	Parameters in the group	**Group representative**
1	Plasterboard Heat Capacity Plasterboard Thickness	Plasterboard Heat Capacity
2	Polystyrene Thermal Conductivity Polystyrene Thickness	Polystyrene Thermal Conductivity
3	Left side Convective coefficient	Left side Convective coefficient
4	Right side Convective coefficient	Right side Convective coefficient
5	Solar efficiency	Solar efficiency

Table 2.4. *Active model parameters groups and groups representatives..*

The phenomena in the model that can be tested using the available data are : heat conduction in the plasterboard and the polystyrene layers, heat convection at the wall surfaces and the solar processor.

Principal components analysis

The principal component analysis has been performed on the sensitivity time series corresponding to the 7 active model parameters:

$$\zeta(t) = \left[\tilde{s}_1(t) \quad \tilde{s}_2(t) \quad \cdots \quad \tilde{s}_7(t)\right]^T$$

The spectral decomposition of the $\zeta(t)$ - covariance matrix leads to

$$W = \int_{t_o}^{t_f} \zeta(t)\zeta(t)^T dt = V\Sigma V^T$$

with the following eigenvectors

$$V = \begin{bmatrix} 0.0695 & -0.2035 & 0.6106 & -0.1020 & 0.0264 & -0.7410 & 0.1442 \\ 0.5680 & -0.0859 & -0.2498 & -0.2489 & -0.3725 & 0.0161 & 0.6376 \\ -0.5902 & -0.5004 & -0.3589 & -0.2331 & -0.4220 & -0.1995 & -0.0147 \\ 0.0617 & 0.0012 & -0.0286 & 0.8667 & -0.4696 & -0.1538 & 0.0019 \\ -0.2329 & 0.8104 & 0.0332 & -0.2516 & -0.4293 & -0.2004 & -0.0144 \\ -0.5123 & 0.0618 & 0.2716 & 0.1781 & 0.1559 & 0.2808 & 0.7246 \\ 0.0605 & -0.2007 & 0.6003 & -0.1646 & -0.5033 & 0.5178 & -0.2171 \end{bmatrix}$$

and the eigenvalues bellow

$$\Sigma = diag\left[342.29 \quad 92.44 \quad 76.98 \quad 0.38 \quad 0.0445 \quad 0.0061 \quad 0.0000\right]$$

The vector $\zeta(t)$ then can be written as $\zeta(t) = VX(t)$, where $X(t) = \left[x_1(t) \quad x_2(t) \quad \cdots \quad x_7(t)\right]^T$ is the vector of decomposition coefficients resulting from projection of $\zeta(t)$ onto the eigen-basis V. The time evolution of the first five components of $X(t)$ is represented in figure 2.8. It can be seen that only the first three components of $X(t)$ show significant fluctuations.

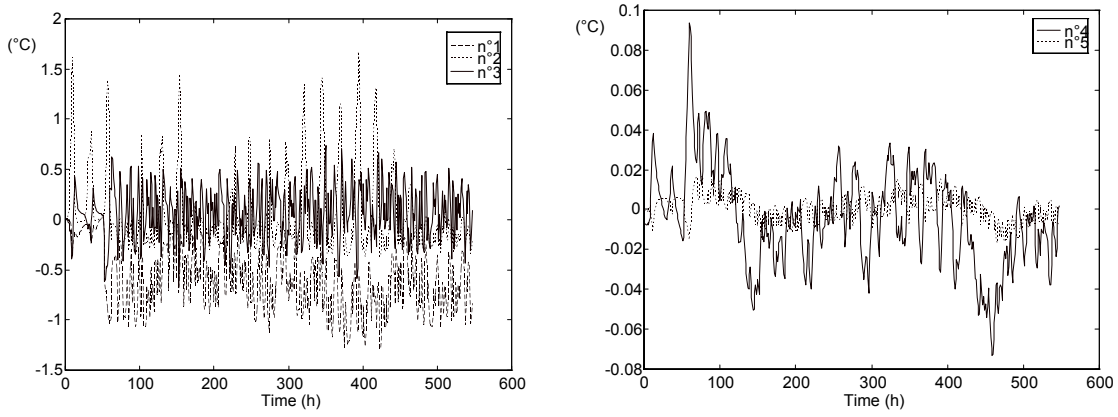

Figure 2.8. *Time evolution of the $X(t)$ vector components.*

The resulting model parameters signatures (see eq. 2.38) are given in Table 2.5. They are defined as the contribution of the principal components to the variance of the sensitivity time series. Table 2.5 shows that only the first three principal components significantly contribute to explain the variance of the sensitivity time series associated to the active model parameters. In addition, it can be seen that parameters 1 and 7 (plasterboard heat capacity and thickness), as well as parameters 2 and 6 (polystyrene thermal conductivity and thickness), exhibit similar signatures. This leads us to propose the same parameter grouping than the one coming from correlations analysis (see Table 2.4).

	Contribution to the variance of the principal component number						
	1	**2**	**3**	**4**	**5**	**6**	**7**
1	0.0484	0.1119	0.8395	0.0001	0.0000	0.0001	0.0000
2	0.9524	0.0059	0.0414	0.0002	0.0001	0.0000	0.0000
3	0.7828	0.1520	0.0651	0.0001	0.0001	0.0000	0.0000
4	0.7846	0.0001	0.0378	0.1716	0.0059	0.0001	0.0000
5	0.2338	0.7647	0.0011	0.0003	0.0001	0.0000	0.0000
6	0.9369	0.0037	0.0592	0.0001	0.0000	0.0000	0.0000
7	0.0382	0.1138	0.8473	0.0003	0.0003	0.0000	0.0000

Table 2.5. *Active model parameters signatures.*

As it was discussed in section 2.3, principal components analysis allows us to propose a new set of truly independent parameters. Such parameters are defined as simple functions of the initial ones:

$$\Delta\gamma_i = \sum_{j=1}^{7} \frac{\Delta\theta_j}{\theta_{jo}} v_{ji} \qquad i = 1,\cdots,7$$

where v_{ji} is the (j,i) element of the matrix V. The sensitivity of the model output to these new parameters is given by:

$$\frac{\partial y(t)}{\partial \gamma_i} = x_i(t) \qquad i = 1,\cdots,7$$

Hence, γ_i parameters significance can be studied by means of:

- the mean time and the standard deviation values of $x_i(t)$;
- the contribution of $x_i(t)$ to the whole energy in $\zeta(t)$ (see eq. 2.42); and
- the statistical correlation existing between the residuals and $x_i(t)$.

	Sensitivity mean value	Sensitivity standard deviation	Contribution to the $\zeta(t)$ energy	Correlation with residuals
γ_1	**-0.7143**	**0.3402**	**0.6683**	**-0.9327**
γ_2	0.0138	0.4113	0.1805	0.2318
γ_3	0.0751	0.3679	0.1503	0.0599
γ_4	-0.0049	0.0259	0.0007	-0.0013
γ_5	-0.0006	0.0090	0.0001	0.0956
γ_6	-0.0002	0.0033	0.0000	-0.0022
γ_7	0.0000	0.0002	0.0000	-0.0723

Table 2.6. *Results from the analysis of the γ_i parameters significance.*

Table 2.6 shows that only the first three new parameters are really significant. Indeed, the first one explains more than 65% of the whole energy in $\zeta(t)$. In addition, it is the only parameter showing a significant effect on the model static behaviour (remember that the main problem in the model concern the static regime) as well as a high degree of correlation with residuals.

Consequently, a preliminary diagnosis of the model could be intended from first eigenvector (first column of the matrix V). It has been represented if figure 2.9, where we can see that physical parameters showing a greater contribution to γ_1 value are: the polystyrene layer thermal conductivity and thickness (parameters 2 and 6), the left side convective coefficient (parameter 3) and the solar efficiency (parameter 5). Improving the model performances likely involves significant changes in the values of these parameters. This probably means that the thermal conduction modelling, the heat convective flux at the wall-air interface representation and the solar processor must be reviewed. Such preliminary conclusions must be however confirmed by optimisation techniques.

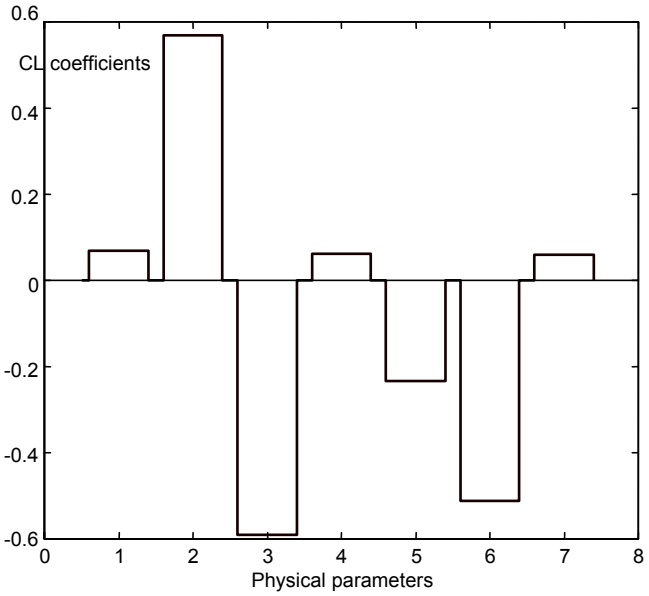

Figure 2.9. *First eigenvector representation*.

Optimisation and diagnosis

The model has been fitted on the available data to estimate the group representatives in table 2.7 (free model parameters). We have applied both the Gauss-Newton method (GNM) and the HBA developed by us. The results achieved are presented in Table 2.7. First of all, we can see that no fundamental differences concerning diagnosis are observed between Gauss-Newton and HBA methods. The parameter set proposed by the HBA includes the parameter vector estimated by the Gauss-Newton algorithm.

Concerning residuals, the solution proposed by GNM significantly improves the model behaviour. The residuals mean value is -0.04°C and standard deviation is 0.2°C. Simulations uncertainty bands over the parameter set proposed by HBA are represented in figure 2.10. We can see that ≈100% of measurements fall into these bands.

	Nominal value	Gauss-Newton estimations	Bounding method estimations
Plasterboard Heat Capacity	680.0	635.8	[646.0, 650.3]
Polystyrene Conductivity	0.043	0.063	[0.059, 0.078]
Left side Convective coefficient	4.0	2.47	[1.93, 3.43]
Right side Convective coefficient	4.0	3.99	[4.46, 4.81]
Solar efficiency	0.008	0.0034	[0.0025, 0.0026]

Table 2.7. *Active model parameters nominal values and estimations*.

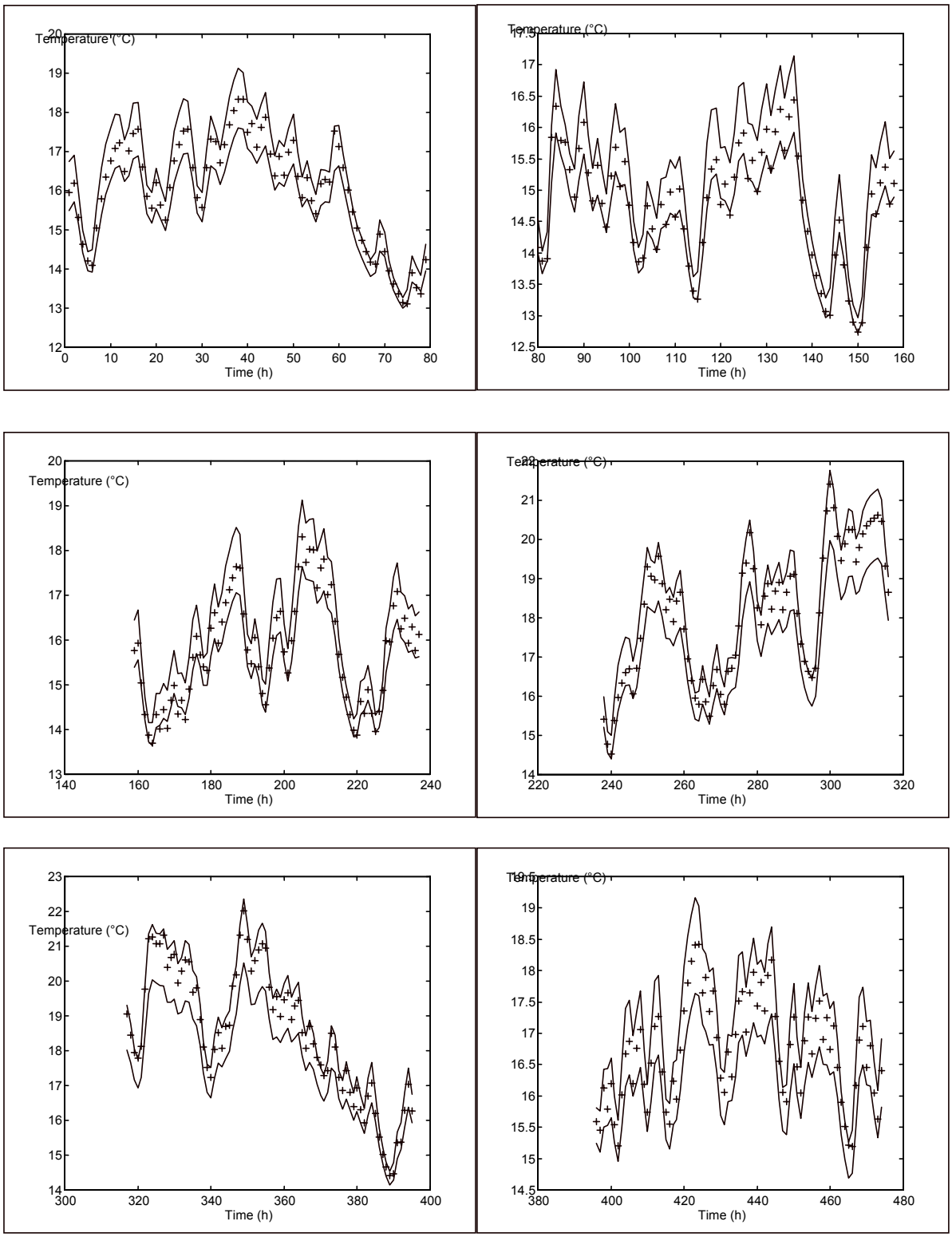

Figure 2.10. *Simulation uncertainty bands over the parameter set solution and measurements.*

From Table 2.7, we can conclude that improving the model behaviour implies strongly modifications of the thermal conductivity of the polystyrene layer, the heat convective coefficient at the wall left side, and the solar efficiency. Values for the first one must be increased, and values for the second and third one have to be decreased. Hence, modelling heat transfer conduction must be reviewed (the augmentation of the conductivity suggest the existence of thermal bridges or nominal material properties not fully matching the final as-constructed conditions of the test cell), the solar

processor have to be improved, and the heat convection representation at the wall-air interfaces must be reviewed too.

2.6. COMPUTER IMPLEMENTATION

Two main tools for validation purposes have been developed within IEA's Task 22: MED (Modelling Errors Diagnosis Tool) and MEDLab (Matlab Modelling Errors Diagnosis Tool). There are briefly described in this section. Please, contact the authors for getting the corresponding β-versions and the user manuals [21, 22].

MED

MED is an ensemble of Fortran codes and Unix procedures that does not include any modelling-simulation environment. Fortran codes contain validation methods and algorithms, and Unix procedures serve for MED codes and simulation environment management.

The link between MED and a modelling-simulation environment is made by means of some "bridges" files. The modelling-simulation environments that have been already connected to MED are:

- M2m [23], developed by the Groupe Informatique et Systèmes Energétiques of the Ecole Nationale des Ponts et Chaussées (GISE-ENPC).
- Clim2000 [24], developed at Electricité de France (EDF). The Clim2000 solver is ESACAP [25].
- CA-SIS [26], an EDF's modelling-simulation environment based on TRNSYS [27].

MED has been tested both on SUN and HP Unix workstations. The MED graphical interface is based on Gnuplot [28].

MED allows:

- Checking model validity as described in section 2.2 (residuals main characteristic analysis, comparisons between model outputs uncertainty bands and measurements, and calculation of the spectral domain of application of the model).
- Model diagnosis using spectral residuals analysis techniques. PAMTIS [29, 30], the software package for residuals analysis developed in PASSYS, has been included in MED.
- Modelling errors diagnosis by model parameters space analysis techniques as described in section 2.3 (sensitivity analysis and optimisation).

The ensemble of methods included in MED is summarized in Table 2.8:

SPECTRAL ANALYSIS	Power spectra calculations Spectral test for model applicability Multiple squared coherence function Test for zero multiple coherence Partial squared coherence functions
PARAMETERS SENSITIVTY ANALYSIS	Parameter-perturbation method Screening based on mean and variance values Parameters correlation matrix calculations
MODEL OUTPUTS BOUNDS	Standard Monte Carlo methods PSV interacting approximation [21]

OPTIMISATION	Pure random search algorithm Multi-start random algorithm [21] Branch and bound algorithm [21]

Table 2.8. *Methods and algorithms in MED*.

MEDLab

MEDLab has been developed under Matlab. Contrary to MED, it only addresses linear models. It is then more restrictive than MED but implemented methods are more efficient. As MED, it does not include any modelling environment. It has been already linked to M2m [23] and to Clim2000 [24].

MEDLab allows:

- Checking model validity as described in section 2.2 (residuals main characteristic analysis, comparisons between model outputs uncertainty bands and measurements, and calculation of the spectral domain of application of the model).
- Modelling errors diagnosis by model parameters space analysis techniques as described in sections 2.3 and 2.4 (sensitivity analysis and optimisation).

The ensemble of methods included in MEDLab is summarised in Table 2.9:

RESIDUALS ANALYSIS	Trends, means and standard deviations Power spectra calculations
MODEL OUTPUTS BOUNDS	Standard Monte Carlo method Sensitivity based method
SENSITIVITY ANALYSIS	Sensitivity-equation method Screening based on mean and variance values Parameters correlation matrix calculations Principal components analysis
OPTIMISATION	Gauss-Newton method Random search algorithm Heuristic bounding algorithm

Table 2.9. *Methods and algorithms in MEDLab*.

2.7. SUMMARY AND CONCLUSION

The IEA empirical model validation approach has been presented in this chapter. Two main steps can be distinguished in this approach:

Checking model validity. The objective is to test the model performances by identification of significant disagreements between measurements and simulations. It involves residuals analysis, simulations-measurements consistency analysis, and the estimation of the model spectral domain of application. Standard mathematical tools have been proposed for reaching such an objective.

Model diagnosis. Main objective of this step is to explain the differences observed between measurements and simulations and to propose model improvements. This means going up from the observed disagreements to the faulty modelling hypothesis. A new approach based on the model parameters space analysis has been developed. It involves:

- Sensitivity analysis. The principal aim of this part if to identify the parts of the model as well as physical phenomena that can be really tested on the available data. Sensitivity calculations, correlation analysis and principal components analysis are the main tools proposed to reach

this objective. Some preliminary elements for diagnosis are already supplied by PCA at this stage.

- Optimisation. Parameters estimation techniques are the main mathematical tool we are proposing to guide model diagnosis. Free model parameters values allowing significant residuals reduction are here identified by fitting the model on the available data. Diagnosis mainly involves comparisons between estimated and nominal model parameters values. Three different algorithms for optimisation have been proposed and discussed.
- Diagnosis. The possible causes of discrepancies between measurements and simulations are finally elucidated using:
  - Some knowledge about the model. The main information required concerns the phenomena considered in the model and the parameters involved in their representation.
  - Modelling hypothesis analysis. Foreseeable model parameter values for each one of the hypothesis in the model, as well as for their negative statement, are desired but difficult to obtain. Instead, some knowledge about what kind of model parameter displacements are expected when inadequate modelling hypothesis, can be used. For instance, un-modelled thermal bridges (when significant) will lead to systematic increasing of thermal conductivity values when fitting the model to the data.
  - Parameter changes analysis. It involves comparisons between estimated and nominal model parameters values. Large differences are expected for parameters involved in phenomena which are not correctly represented in the model.

  The combination of these three elements of judgement should lead to know reasons for the observed model errors, and to suggest model improvements.

Chapter 3

APPLICATION TO THE VALIDATION OF THE THERMAL MODEL OF AN ACTUAL BUILDING

The methodology and the methods described in the previous chapter are here applied for testing modelling hypothesis in the framework of the thermal analysis of an actual building. The experimental device (ETNA building) is described in section 3.1. Next section includes experimental design matters and a qualitative analysis of the recorded data. The adopted modelling hypothesis and the resulting model are presented in section 3.3. Model validation and diagnosis results are contained in next sections. Two French modelling-simulation environments have been used: CLIM2000 and CA-SIS. Results for the first one are included in this chapter. On the contrary, CA-SIS results are presented in Annex B.

3.1. THE EXPERIMENTAL DEVICE

ETNA is an experimental building that has been specifically designed by EDF for empirical model validation purposes (see Fig. 3.1). It is 30° south oriented and it is located near Paris. It is formed by two identical and symmetrical testing rooms (41.3 m3), surrounded all over, the south facade excepted, with guard zones where the air temperature can be controlled (see Fig. 3.2). The testing room with an almost 100% convective heating device (*test cell* in the following), is here considered. The air in the room can be stirred in order to ensure a homogeneous air temperature distribution. The construction of the building is deemed to be known with good confidence (see [31] for a detailed description). The building has been designed to minimise both thermal bridges effects and infiltrations. The permeability measurements carried out allows considering that thermal losses generated by infiltrations are negligible.

Figure 3.1. *Photograph of the ETNA building.*

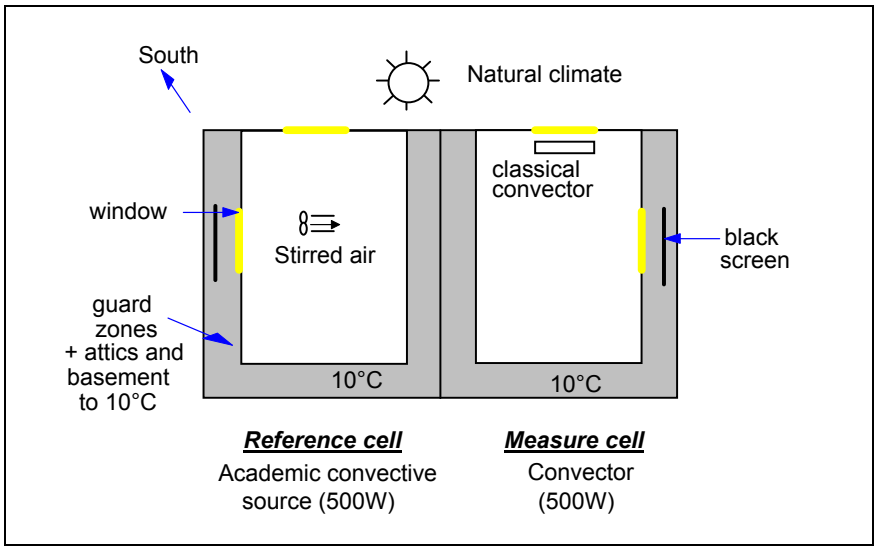

Figure 3.2. *ETNA building sketch (horizontal cutting)*

The test cell components and the walls composition are presented in Tables 3.1. and 3.2 respectively. The floor and the ceiling are described in figures 3.3 and 3.4 respectively.

Component	Surface (m^2)	Slop (°)	Orientation (°S)	Controlled Environnement
South wall	7.25	90	30	-
West wall	11.81	90	120	Computer room
North wall	7.00	90	210	Cell bis
East wall	10.17	90	290	Air-lock
Ceiling	16.28	0	-	Attics
Floor	16.28	180	-	Basement
South glazing	0.967	90	30	-
South framework	0.665	90	30	-
East glazing	0.967	90	290	Air-lock
East framework	0.665	90	290	Air-lock
Door	1.89	90	210	Cell bis

Table 3.1. *Test cell components.*

North wall	7.0 m²	**East wall**	10.17 m²	**Glazing**	0.967 m²
Plasterboard	0.013 m	Plasterboard	0.01 m	Glass	0.04 m
Honeycomb	0.046 m	Polystyrencl:2	0.08 m	Air3	0.007 m
Plasterboard	0.013 m	Air4	0.01 m	Glass	0.04 m
Styrodur	0.06 m	HollowBlocks	0.2 m		
		Air4	0.01 m		
		Polystyrencl:2	0.08 m		
		Plasterboard	0.01 m		
South wall	7.25 m²	**West wall**	10.17 m²	**Frameworks**	0.665 m²
Plasterboard	0.01 m	Plasterboard	0.01 m	ColonialTimber	0.06 m
Polystyrencl:2	0.08 m	Polystyrencl:2	0.08 m		
Air1	0.01 m	Air1	0.01 m	**Door**	1.89 m²
Hollowblocks	0.2 m	Hollowblocks	0.2 m	HollowDoor	0.044 m
Facing	0.02 m	Facing	0.02 m		

Table 3.2. *Walls composition description from an outward direction.*

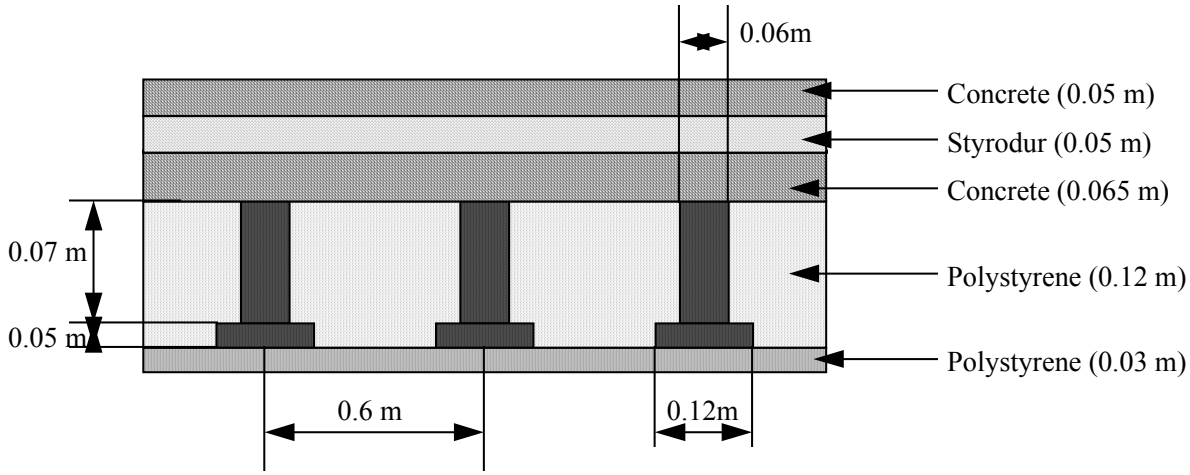

Figure 3.3. *Floor composition.*

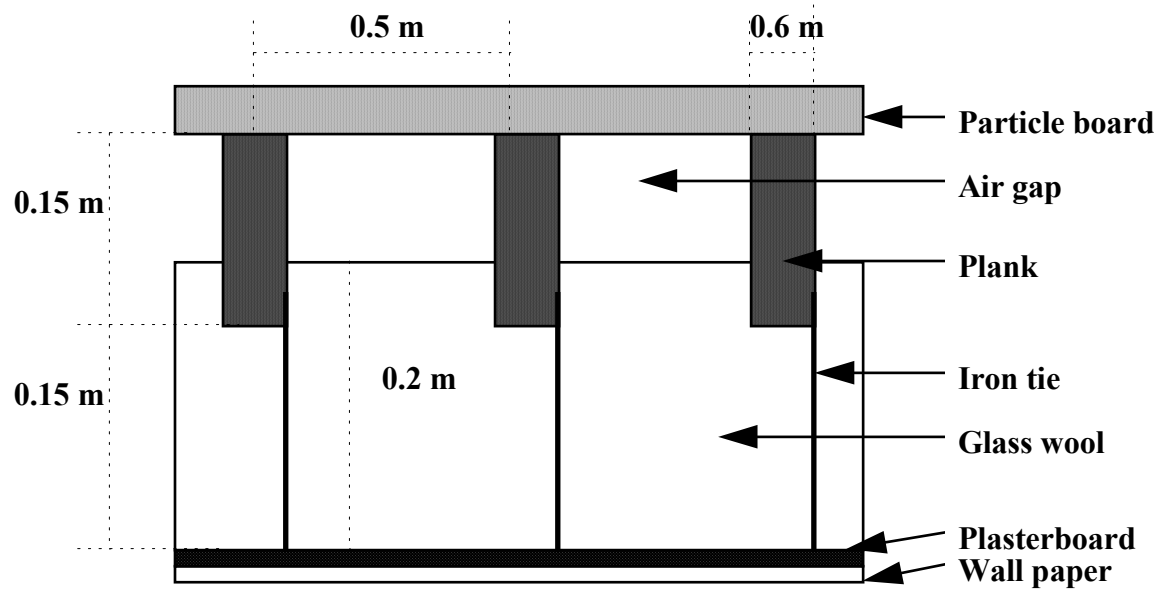

Figure 3.4. *Ceiling composition.*

The thermophysical properties of the test cell materials are included in Table 3.3. The optical properties of the windows glazing are given in Table 3.4.

Material	λ (w.m^{-1}.K^{-1})	ρc_p(kJ.m^{-3}.K^{-1})	**Material**	λ (w.m^{-1}.K^{-1})	ρc_p(kJ.m^{-3}.K^{-1})
Air1	0.071	1.24	HollowBlocks	1.052	1140.0
Air2	0.762	62.5664	HollowDoor	0.090	275.0
Air3	0.063	1.24	Honeycomb	0.287	34.974
Beams1	0.382	522.56	Particleboards	0.170	840.0
Beams2	0.211	277.535	Plasterboard	0.350	680.0
ColonialTimber	0.250	1680.0	Polyamide	0.300	1200.0
Concrete	1.750	2090.0	Polystyrenecl:2	0.043	18.0
Concrete*	1.390	1957.0	Polystyrenecl:3	0.040	21.6
Facing	1.150	1657.5	Styrodur	0.032	21.6
Glass	1.150	2025.0	Styrodur2505	0.029	42.0

GlassWool	0.042	8.8	

Table 3.3. *Thermophysical properties of the materials.*

(°)	0	10	20	30	40	50	60	70	80	90
α	0.104	0.104	0.107	0.110	0.114	0.119	0.123	0.127	0.121	0.000
τ	0.683	0.680	0.672	0.656	0.633	0.597	0.540	0.442	0.220	0.000

Table 3.4. *Glazing optical laws (a = solar absorptance; t = solar transmittance).*

3.2. THE EXPERIMENTAL DESIGN AND THE DATA

Test cell configuration and recorded data

The experiment carried out in the test cell from 25/02/95 to 19/03/95 (23 days) is here analysed. The test cell configuration during the experiment was as follows:

- Guard temperatures were controlled at approximately 10°C.
- Internal heating was conducted by an electrical heat source. A binary pseudo random sequence was used to drive heater operation (on/off). The smallest heating period was 5 minutes, and the nominal value was 500W (see Fig. 3.7).
- The air inside the test cell was stirred using a fan to warrant temperature homogeneity. The fan is on when the heating power is on, and it is off otherwise.

All data were measured at a 5 minutes time step, except solar radiation which was measured at 1 minute time step. The data were then averaged and under-sampled at 1 hour time step.

The following meteorological variables were actually measured:

- Global solar radiation on the south vertical wall - 30°W oriented wall (see Fig. 3.6).
- Outdoor dry bulb temperature and guard temperatures (see Fig. 3.5).

The variables recorded inside the test cell are:

- Heating power (see Fig. 3.7).
- Indoor air temperature, that was taken as a space average of several shielded dry-bulb temperature sensors (see Fig. 3.8).
- The mean radiant temperature, which was taken as the average of three black globe temperature sensors (see Fig. 3.8).
- The wall indoor surface temperatures, which were taken as the average of several surface temperature sensors (see Fig. 3.9).

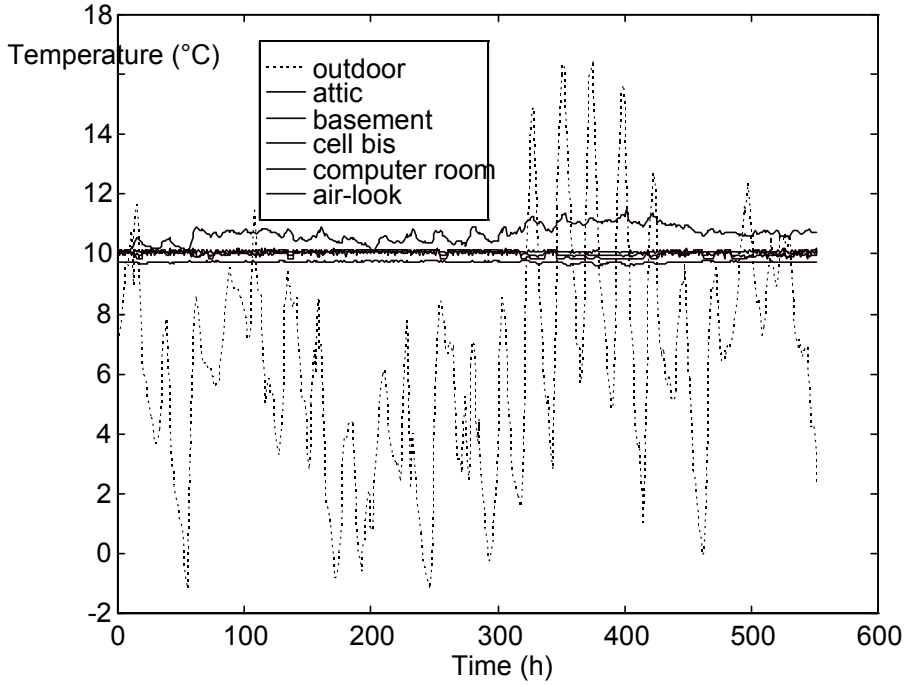

Figure 3.5. *Outdoor temperature measurements (dashed line) and air temperature in the test cell surrounding spaces (continuous lines).*

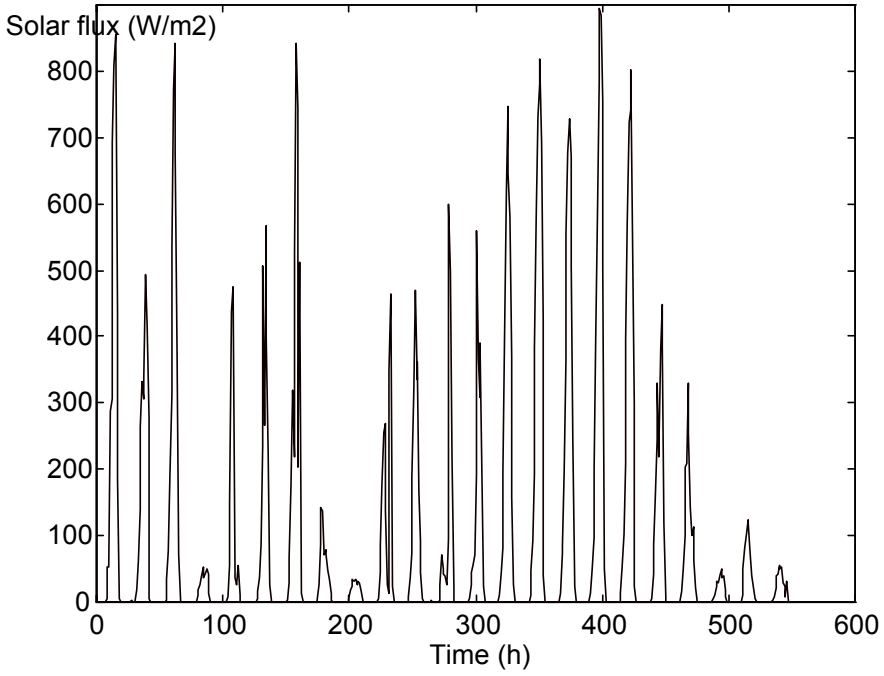

Figure 3.6. *Solar irradiance on the south vertical wall.*

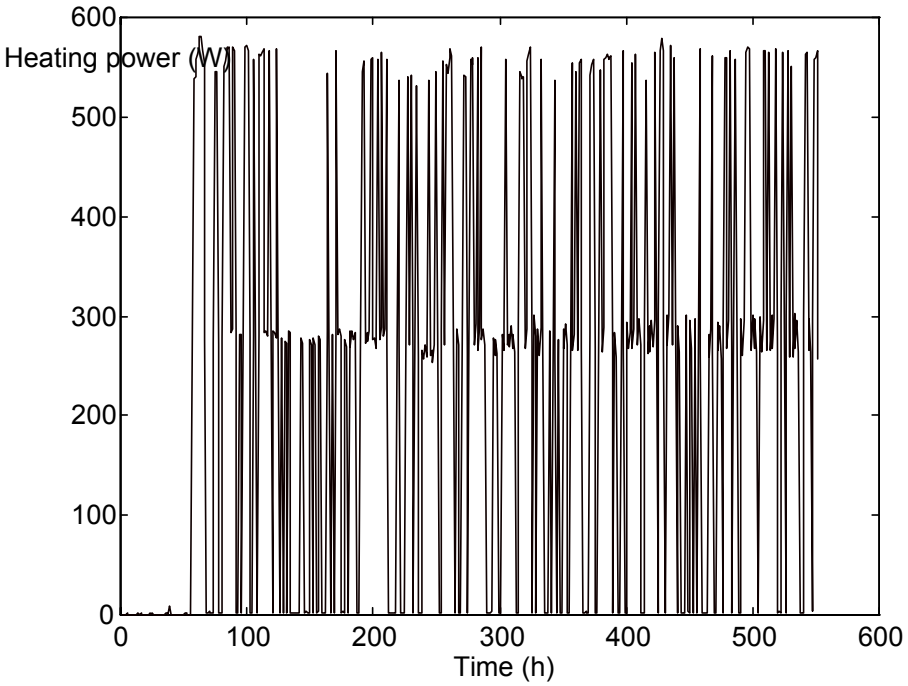

Figure 3.7. *Heating power measurements.*

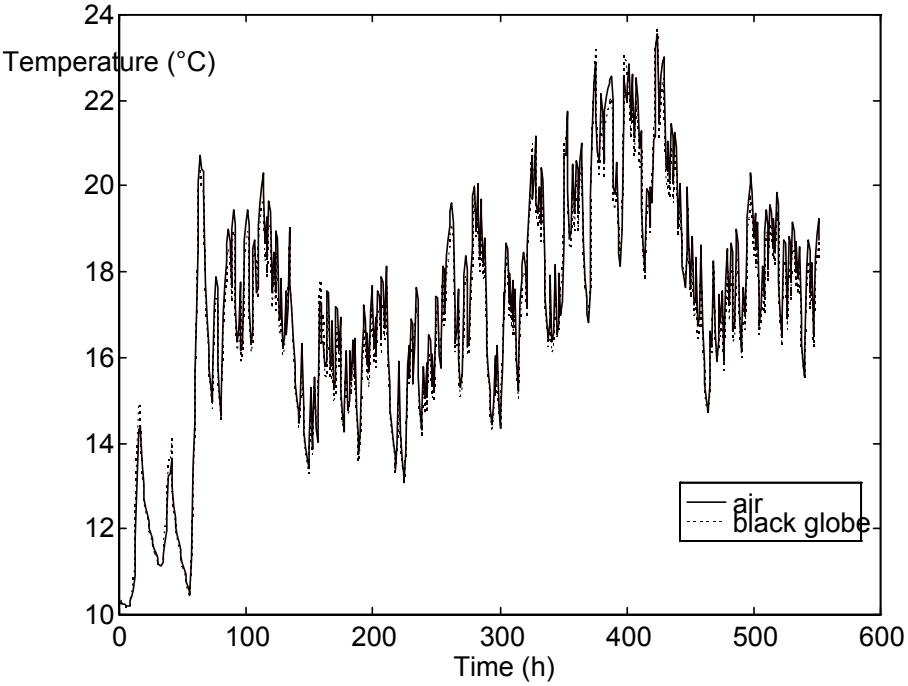

Figure 3.8. *Indoor air temperature (continuous line) and mean radiant temperature measurements (dashed line).*

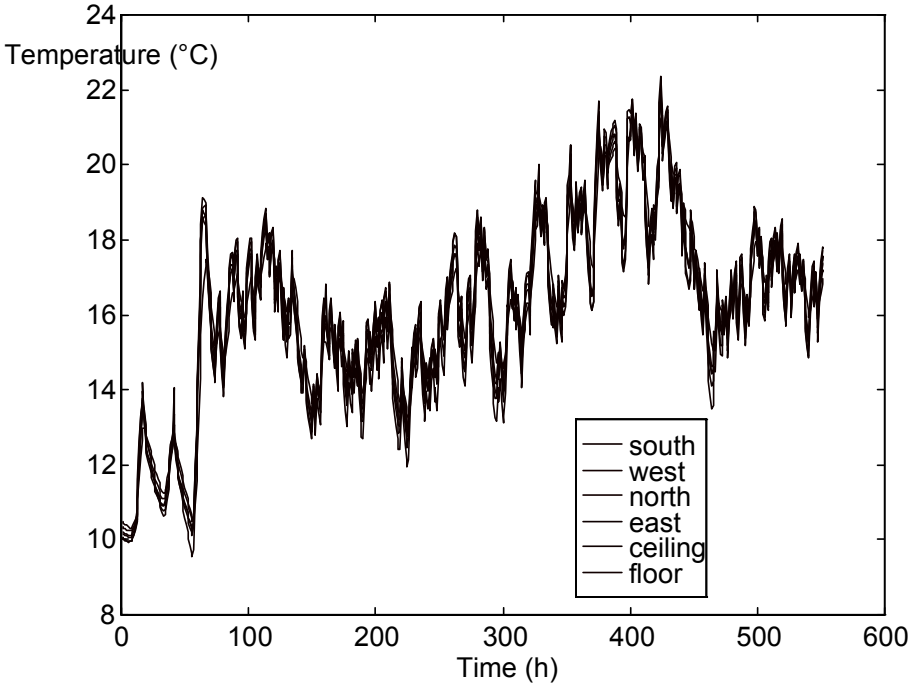

Figure 3.9. *Indoor wall surfaces temperatures.*

Qualitative data analysis

In Fig. 3.10 are represented black globe temperature data against indoor air temperatures. The differences observed between them are always less than 1°C, the black globe temperature being most of the time colder than the air temperature. So small differences are a little bit surprising because greater ones are observed between the air and the indoor test cell surfaces. To understand this behaviour, it must be noticed that:

- The measured black globe temperature does not represent the mean radiant temperature. The last one can be certainly estimated from the globe temperature, the air temperature and the indoor air velocity data, but it cannot be directly taken as the spatial average of the globe temperatures as supposed before. The temperature of the globe thermometer is the result of both the radiative exchanges between the globe and the wall surfaces, and the convective exchanges between the globe and the indoor air.

- The indoor air temperature is measured using non-ventilated shielded (solar radiation protection) temperature sensors. Consequently, the recovered air temperature data could be corrupted (underestimated) by the wall surfaces temperatures, which are most of the time colder than the air temperature.

Probably both, the black globe temperature and the air temperature date are close to the so called « resultant temperature », which take values in between the actual mean radiant and indoor air temperatures.

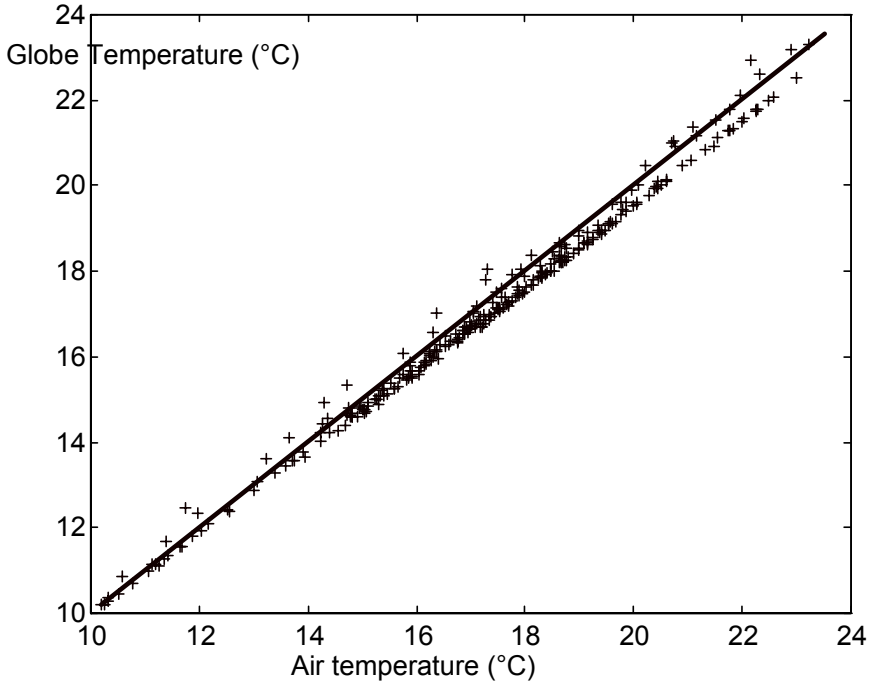

Figure 3.10. *Air temperature data vs. Black globe temperature data.*

The wall surface temperatures (indoor side) are represented against the measured indoor air temperatures in figures 3.11 (south, west, north, west and ceiling) and 3.12 (floor). It can be seen that most of the time the temperature of the wall surfaces is smaller than the air temperatures. This is a reasonable behaviour because:

- one of the main inputs to the test cell is the heating power;
- the heating system can be assumed to be a pure convective heater (the air inside the cell was stirred);
- the outdoor wall surfaces are in contact with an air mass at approximately 10°C (thermal guards), or lower (south wall).

Due to a higher inertia, the thermal behaviour of the floor surface is slightly different from the one of the others wall surfaces. The proportion of time during which the floor surface temperature is higher than the air temperature increases, and the difference between both quantities can be greater than 2-3°C.

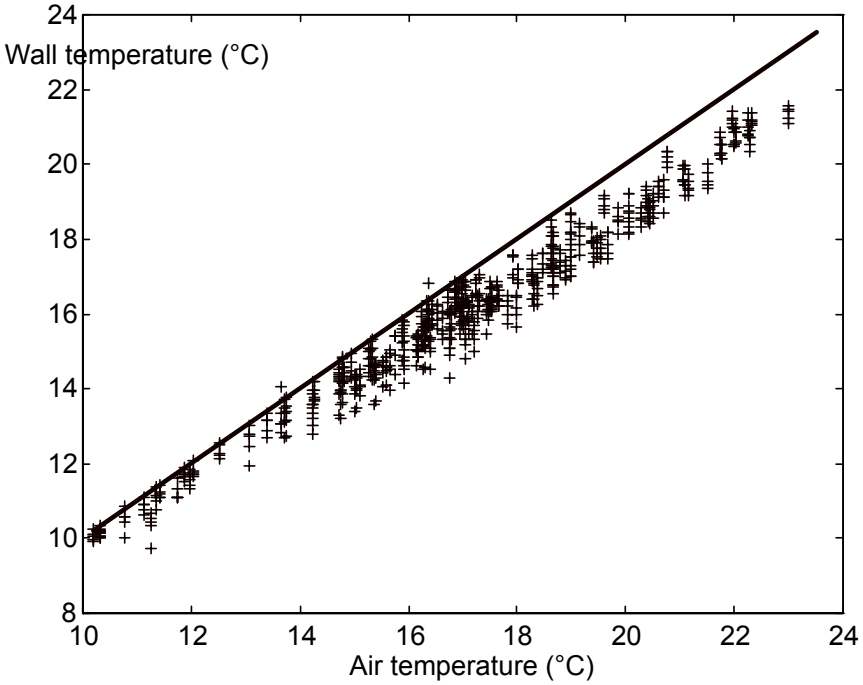

Figure 3.11. *Air temperature data vs. Wall surfaces temperature data.*

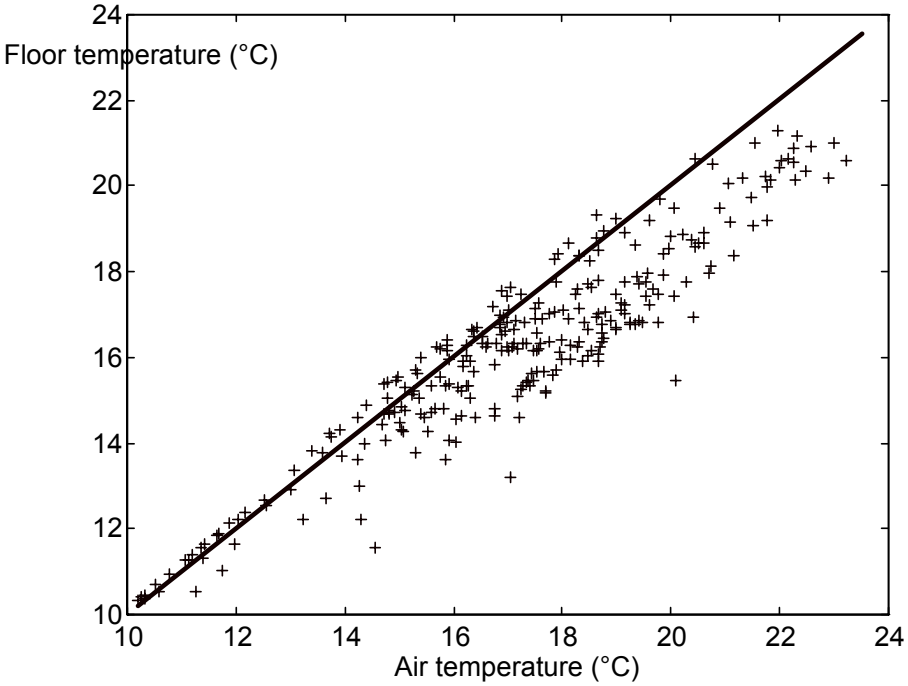

Figure 3.12. *Air temperature data vs. Floor surface temperature data.*

Spectral analysis of the data

The analysis of the model inputs spectra allow to identify the frequency ranges over which the building and hence the model are mainly excited. It is within these ranges that one should expect exhibit any modelling error. Figure 3.13 shows the estimated density power spectra for the three main building inputs: the outdoor air temperature, the solar radiation flux (global, horizontal), and the heating power. In figure 3.14, their respective normalized cumulative spectra are shown. The analysis of such statistics leads to the following conclusions:

- Outdoor temperature. More than 97% of the variance is concentrated over the frequency range [0, 1/10 h^{-1}] (see Fig. 3.14). It exhibits a clear 24 h periodicity, as well as spectral peaks (variance concentration) at 1/12 h^{-1} and 1/6 h^{-1} frequencies (see Fig. 3.13).
- Solar radiation. More than 95% of the variance is concentrated over the frequency range [0, 1/7 h^{-1}] (see Fig. 3.14). As in the previous case, it exhibit a clear 24 h periodicity and a spectral peak at 1/12 h^{-1} .
- Heating power. It is an input with significant spectral power over the whole frequency range. 95% of its variance is concentrated over the frequency interval [0, 1/3 h^{-1}]. Up to frequency 1/10 h^{-1}, no more than 50% of the signal variance is found.

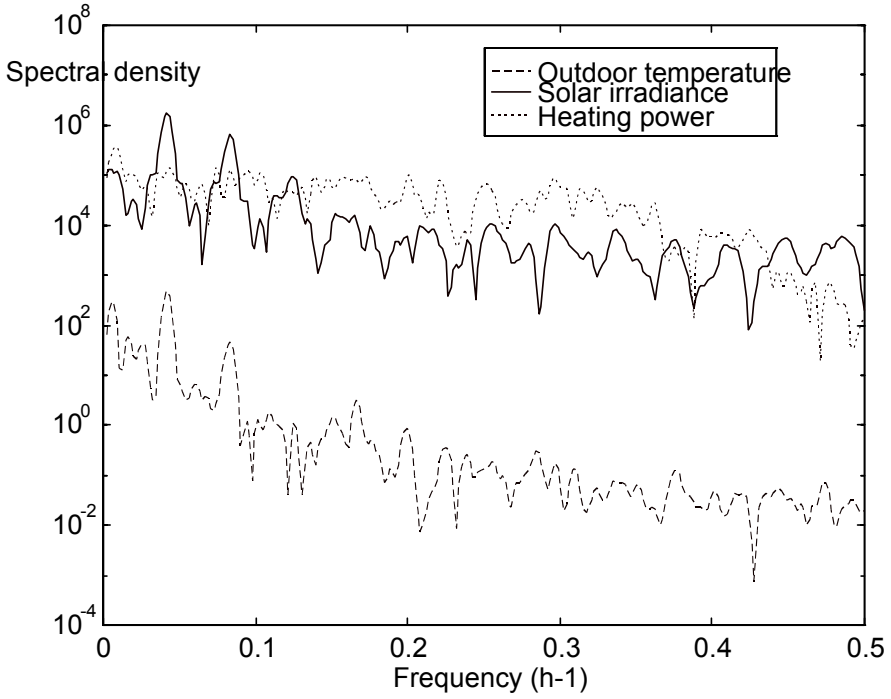

Figure 3.13. *Inputs data spectral density.*

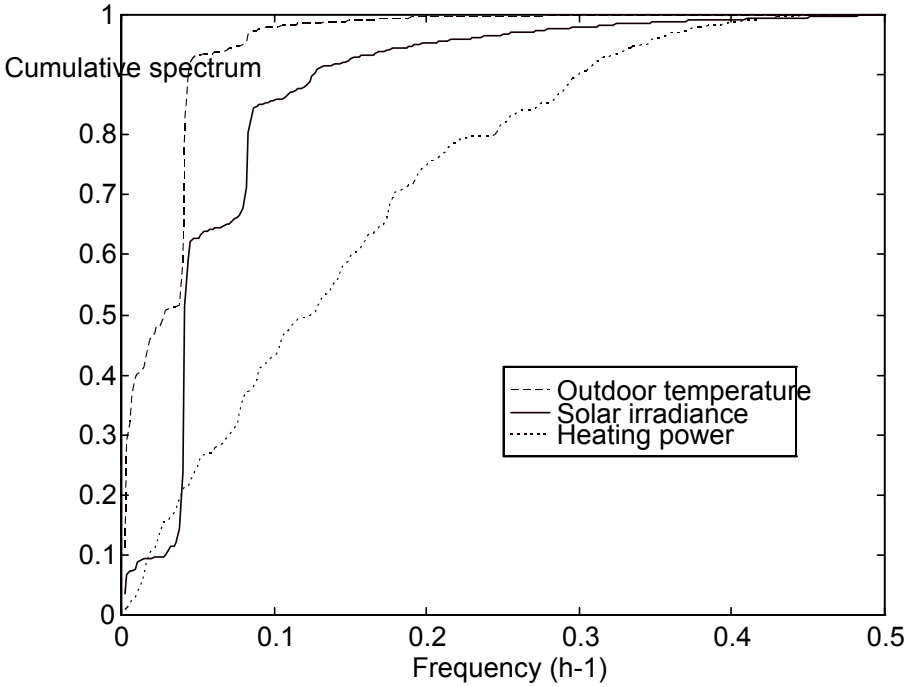

Figure 3.14. *Inputs data cumulative spectra.*

The spectra of the temperature time series describing the building response (air temperature, black globe temperature and wall indoor surface temperatures) are represented in figures 3.15 (density power spectra) and 3.16 (normalized cumulative spectra). From their analysis, it can be concluded that:

- The building acts as a low-pass filter. 95% of the variance of the wall surface temperatures is distributed over the [0, 1/20 h^{-1}] frequency range (see Fig. 3.16). The variance of both, the air and the black globe temperatures, is mainly concentrated over the range [0, 1/10 h^{-1}].
- All the observed temperature time series are 24 h and 12 h harmonic (see Fig. 3.15).

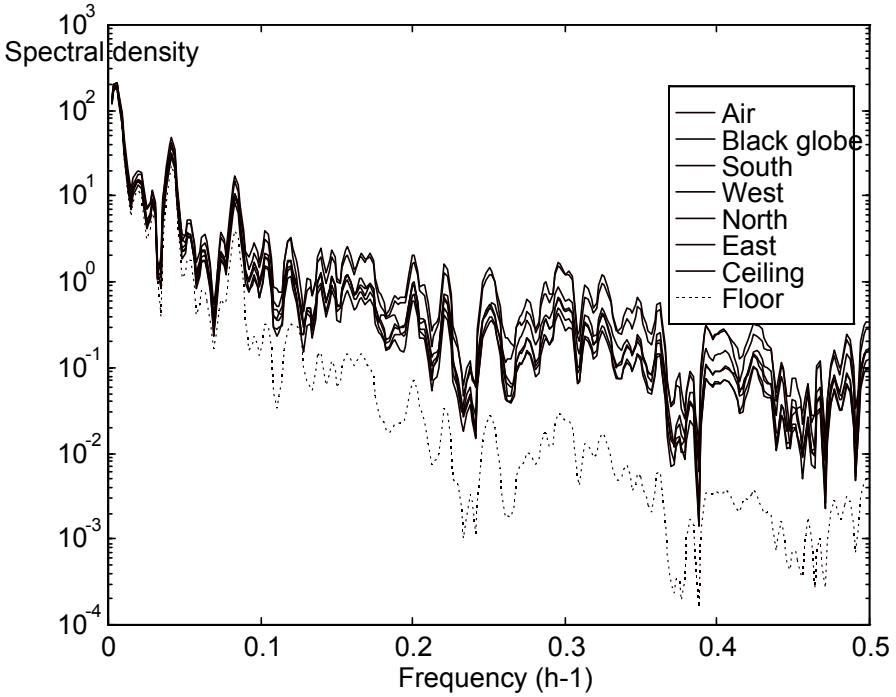

Figure 3.15. *Outputs data spectral density.*

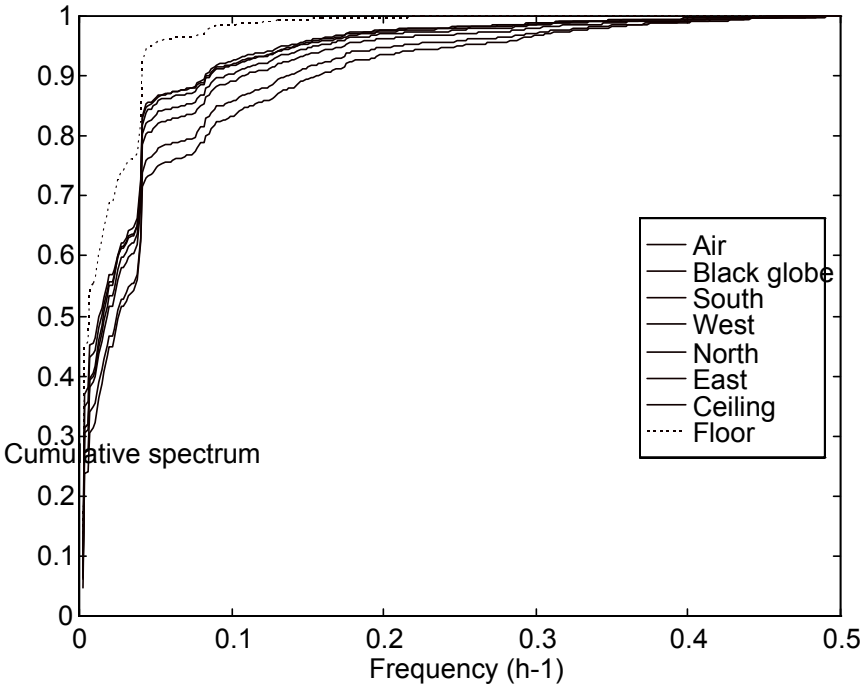

Figure 3.16. *Output data cumulative spectra.*

3.3. THE NOMINAL TEST-CELL MODEL

Clim2000 [24] is a modelling-simulation environment developed by EDF for thermal buildings analysis purposes. It is based on electrical analogy and models are supplied as electrical networks.

Modelling hypothesis

The main modelling hypotheses are classified by physical phenomena as follows:

- *Heat conduction phenomena*: a) Heat conduction is considered as a one dimensional process, thermal bridges are not modelled. An equivalent homogeneous-multilayer wall is used for representing both the floor and the ceiling (see Table 3.4). b) Constant thermophysical properties are assumed for all the materials in the test cell (see Table 2 for nominal values). c) Perfect contact between layers is supposed.
- *Long-wave radiative exchanges and heat convective flux at the wall-air interfaces*: The global convective-radiative flux at any solid-air interface is estimated as: $\phi = h\left(T_{surface} - T_{air}\right)$ where h is a constant exchange parameter taking into account both radiative and convective exchanges. Standard values for coefficients h are adopted.
- *Indoor air and heating power treatment*: a) The indoor air temperature is supposed to be homogeneous. Hence, the air is represented by a single node in the model. b) Air infiltrations are assumed to be zero. c) The output from the heater is assumed 100% convective. The electrical heating power is entirely transmitted to the indoor air node. d) The heater inertia is neglected.
- *Solar radiation processor*: a) The solar irradiance on the vertical south facade is calculated from the available horizontal global and diffuse irradiance data. Diffuse solar radiation is assumed to be isotropic, and the soil reflectivity is supposed to be 0.2. b) The assumed glazing optical properties are given in Table 3.4. c) Incoming solar radiation is supposed to be completely absorbed by the floor.

Floor	16.28 m^2	**Ceiling**	16.28 m^2
Concrete*	0.05 m	Plasterboard	0.013 m
Styrodur2505	0.05 m	GlassWool	0.20 m
Polyamide	0.002 m	Air2	0.10 m
Concrete	0.065 m	Particleboard	0.021 m
Beams2	0.07 m		
Beams1	0.05 m		
Polystyrencl:3	0.03 m		

Table 3.4. *Walls composition description from an outward direction.*

The model

The electrical network created by Clim2000 has been transformed in a state-space model of the form:

$$C\frac{dT(t)}{dt} = AT(t) + EU(t)$$
$$y(t) = HT(t)$$

where $T(t)$ is the vector of temperatures at the nodes of the discretisation mesh, $U(t)$ is the vector of the model input variables, and $y(t)$ represents the model output. C is a diagonal matrix including thermal capacities at the discretisation nodes, A is a squared symmetric matrix including parameters

describing thermal exchanges among nodes, and E is a matrix that contains system-environment coupling parameters . Matrix H is formed by zeros and ones, it serves to select model outputs.

The model output is the indoor air temperature. Model input variables are :

- the solar irradiance on the test cell vertical south façade ;
- the heating power ;
- the outdoor air temperature; and
- the air temperature in every guard zone (5 zones).

The model includes 170 modifiable parameters:

	Parameters			
Component	**Geometry**	**Thermophysical**	**Optical**	**Total**
Floor	8	16	1	25
North wall	5	10	1	16
West wall	6	12	1	19
South wall	6	12	2	20
East wall	8	16	1	25
Ceiling	5	10	1	16
South window	6	12	4	22
West window	6	12	2	20
Door	2	4	1	7
				170

Table 3.5. *Number of parameters in the model.*

Blind model validation

Model simulations have been carried out using hourly data in figures 3.5 to 3.7 as input variables. The differences between indoor air temperature measurements and simulations are represented in figure 3.17. The model underestimates the indoor air temperature during the first four days, afterward it globally overestimates it. Temperature underestimations and temperature overestimations are respectively associated to the free-floating and to the heating periods.

The mean value of the residuals is –0.22°C and its standard deviation is 0.72°C. The model is unable to correctly reproduce both the static and the dynamic thermal behaviour of the test cell. Figure 3.18 includes the power spectral density of the residuals. It shows that residuals variance is mainly concentrated at low frequencies.

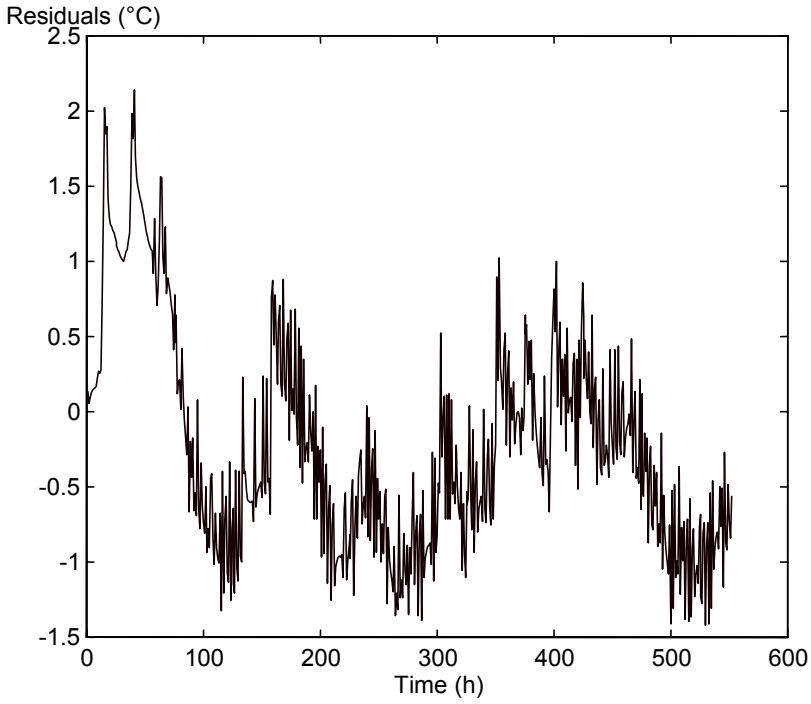

Figure 3.17. *Residuals time evolution*

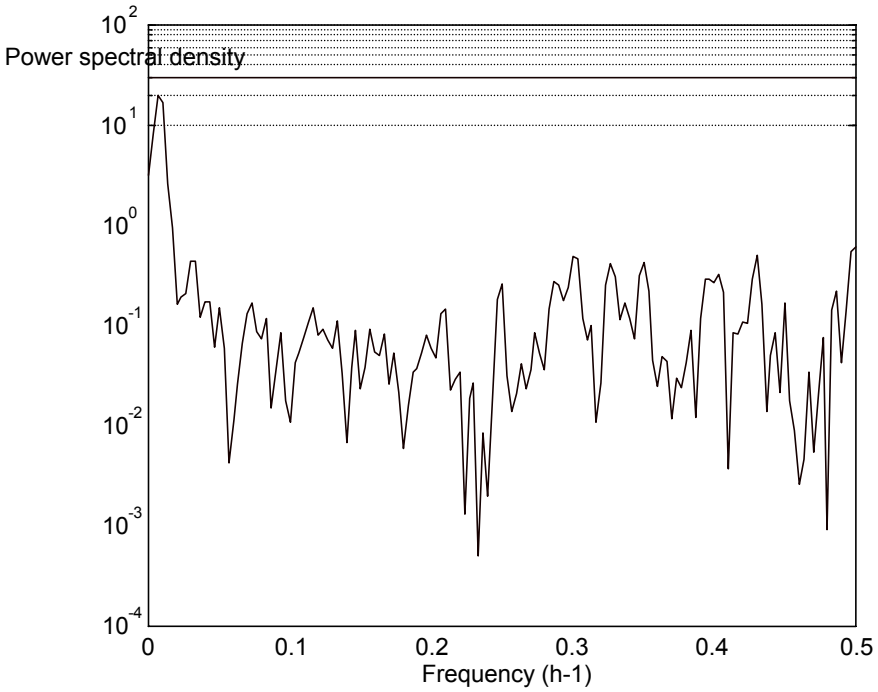

Figure 3.18. *Residuals power spectral density*

For checking model validity purposes, parameters uncertainty is assumed to be:

$$\theta_i \in \left[0.9\theta_{io} \quad 1.1\theta_{io}\right] \qquad i = 1,\cdots,170$$

where θ_{io} represents the nominal value of the i^{th} parameter.

Model output bounds over the parameter set above are calculated by the standard Monte Carlo method described in section 2.2. Figure 3.19 includes the time evolution of the upper and lower model output bounds (continuous lines) as well as measurements. It can be seen that measurements are most of the time (59%) outside the model uncertainty bands. The nominal model is unable to represents the thermal behaviour of the test cell.

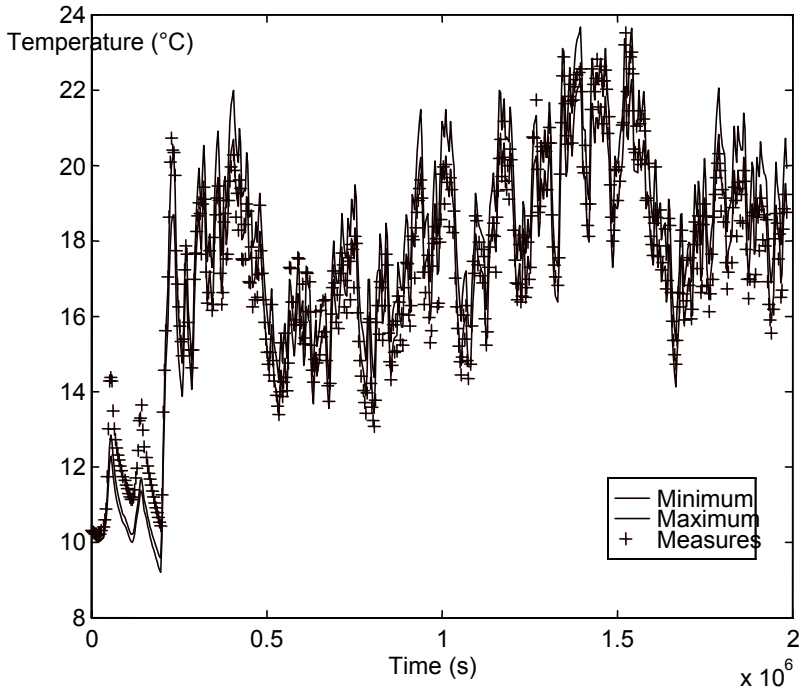

Figure 3.19. *Results from checking model validity: Model output uncertainty bands (continuous lines) and measurements (crosses) comparison.*

3.4. PARAMETERS SENSITIVITY ANALYSIS

Indoor air temperature sensitivity to every model parameter has been calculated by the sensitivity-equation method (see section 2.3 and Annex A).

Test cell components

Tables 3.6 to 3.14 present sensitivity analysis results for the different test cell components: the floor, the north wall, the west wall, the south wall, the east wall, the ceiling, the south window and the west window. They include active model parameters related to each one to the test cell components:

Column	Contents
1	Parameters Group
2	Parameters in the group
3	Mean time value of the indoor air temperature sensitivity to the parameter (see equation X)
4	Standard deviation of the indoor air temperature sensitivity to the parameter (see equation X)
5	Distance (see equation X)

The following criteria have been applied to choose active parameters and to form groups:

– A parameter θ_i is assumed to be active when

$$d_i = \sqrt{\mu_i^2 + \sigma_i^2} \geq 0.1$$

μ_i and σ_i are respectively the mean time value and the standard deviation of the indoor air temperature sensitivity to the i^{th} parameter.

– Parameters in a same group $\pi_s = \{\theta_i \quad \theta_j \quad \cdots \quad \theta_m\}$ show correlation degrees greater that 0.8. That is, they verify

$$\forall i, j \qquad \left|\rho_{ij}\right| \geq 0.8$$

where ρ_{ij} is the linear correlation (see equation 2.29) between the sensitivity time series associated to parameters θ_i and θ_j.

Main conclusions from results in tables 3.6 to 3.14 are:

- **FLOOR**. Three groups of active parameters concerning thermal conduction have been identified (F1, F2 and F3), as well as a group concerning convection at the floor-indoor air interface (F4) and a group related to solar absorption (F5). This is one of the test cell components offering *a priori* greater possibilities for validation.

- **NORTH WALL**. Three groups of active parameters have been identified. The first one includes parameters related to the heat conduction through the wall (N1), the second one concerns heat convection exchanges between the wall and the indoor air (N2), and the third one is the wall surface (N3).

- **WEST WALL.** All the active parameters related to the west wall modelling are strongly correlated among them; they are merged in a same group (W1). This component does not offer many possibilities for validation.

- **SOUTH WALL.** Active parameters related to heat conduction through the wall form a unique group (S1). In the second group (S2) are merged the outdoor convective coefficient and the optical efficiency of the wall surface. The third group (S3) contains the heat convective coefficient at the wall-indoor air interface

- **EAST WALL.** Four groups of active parameters have been identified. The first and the second one include parameters associate to the heat conduction modelling through the wall (E1 and E2). Next groups (E3 and E4) contain parameters related respectively to the heat convection at the wall-indoor air interface and to the solar radiation absorption.

- **CEILING.** Heat conduction is represented by three groups of parameters (C1, C2 and C4), and the third group includes the wall surface optical efficiency.

- **SOUTH WINDOW.** Active parameters of this component form three groups. The first one (SW1) represents heat conduction, the second one (SW2) concern solar absorption and the third one (SW3) is related to the heat convection between the glazing and the indoor air.

- **WEST WINDOW.** Active parameters related to heat conduction are merged with outdoor convective parameters in a same group (WW1). The wall-indoor air convective coefficient defines the second group (WW2).

- **DOOR.** All its active parameters are in the same group (D1). This component does not offer many possibilities for validation.

Group	Parameters	Mean	STD	Distance
F1	*Concrete* - Thermal capacity*	-0.1560	0.6379	0.6567
	Concrete - Thickness*	-0.1426	0.6281	0.6440
	Surface	-1.3044	0.8734	1.5699
F2	Styrodur - Thermal conductivity	-0.6931	0.1813	0.7164
	Styrodur - Thickness	0.6285	0.1627	0.6492
F3	*Beams2 - Thermal conductivity*	-0.1032	0.0352	0.1091
	Polystyrene - Thermal conductivity	-0.2219	0.0890	0.2391
	Polystyrene - Thickness	0.2042	0.0797	0.2192
F4	Indoor h- coefficient	-0.0586	0.4687	0.4724
F5	Optical efficiency	0.1251	0.0718	0.1442

Table 3.6. *FLOOR. Active model parameters and groups.*

Group	Parameters	Mean	STD	Distance
N1	Styrodur - Thermal conductivity	-0.5850	0.1197	0.5971
	Styrodur - Thickness	0.5322	0.1090	0.5432
N2	Indoor h- coefficient	-0.8620	0.1673	0.8781
N3	Surface	-0.6836	0.1631	0.7028

Table 3.7. *NORTH WALL. Active model parameters and groups.*

Group	Parameters	Mean	STD	Distance
W1	*Polystyrene - Thermal conductivity*	-0.8826	0.1803	0.9009
	Polystyrene - Thickness	0.8550	0.1649	0.8217
	Surface	-1.0121	0.2091	1.0334
W2	Indoor h- coefficient	-0.8620	0.1673	0.8781

Table 3.8. *WEST WALL. Active model parameters and groups.*

Group	Parameters	Mean	STD	Distance
S1	*Polystyrene - Thermal conductivity*	-0.8131	0.1840	0.8337
	Polystyrene - Thickness	0.7418	0.1695	0.7609
	Surface	-0.9265	0.2446	0.9583
S2	Outdoor h-coefficient	-0.2036	0.1096	0.2312
	Optical efficiency	0.1767	0.1189	0.2130
S3	Indoor h-coefficient	-0.8620	0.1673	0.8781

Table 3.9. *SOUTH WALL. Active model parameters and groups.*

Group	Parameters	Mean	STD	Distance
E1	Polystyrene *- Thermal conductivity	-0.2700	0.0637	0.2775
	*Polystyrene *- Thickness*	0.2454	0.0558	0.2517
E2	Polystyrene - Thermal conductivity	-0.2573	0.0587	0.2639
	Polystyrene - Thickness	0.2346	0.0539	0.2407
	Surface	-0.5335	0.1472	0.5534
E3	Indoor h- coefficient	-0.8620	0.1673	0.8781
E4	Optical efficiency	0.0921	0.0630	0.1116

Table 3.10. *EAST WALL. Active model parameters and groups.*

Group	Parameters	Mean	STD	Distance
C1	Plasterboard - Thermal capacity	-0.0128	0.1464	0.1469
	Plasterboard - Thickness	-0.0077	0.1450	0.1452
C2	GlassWool - Thermal conductivity	-0.6898	0.1438	0.7047
	GlassWool - Thickness	0.6272	0.1316	0.6409
C3	Optical efficiency	0.1280	0.0884	0.1555
C4	Surface	-0.6428	0.1989	0.6729

Table 3.11. *CEILING. Active model parameters and groups.*

Group	Parameters	Mean	STD	Distance
SW1	*Air - Thermal conductivity*	-0.2326	0.0825	0.2468
	Air - Thickness	0.2120	0.0753	0.2250
	ColonialTimber - Thermal conductivity	-0.1804	0.0734	0.1947
	ColonialTimber - Thickness	0.1631	0.1107	0.1972
	Glass surface	-0.7230	0.2605	0.7685
	Frame surface	-0.3492	0.1298	0.3725
SW2	*Glass optical efficiency*	0.2700	0.1865	0.3282
	Frame optical efficiency	0.1525	0.0969	0.1807
	Outdoor h-coefficient	-0.7638	0.1838	0.7857
SW3	Indoor h-coefficient	-0.8620	0.1673	0.8781

Table 3.12. *SOUTH WINDOW. Active model parameters and groups.*

Group	Parameters	Mean	STD	Distance
WW1	*Air - Thermal conductivity*	-0.2314	0.0472	0.2362
	Air - Thickness	0.2110	0.0431	0.2153
	Outdoor h-coefficient	-0.3130	0.0641	0.3195
	Glass surface	-0.6983	0.1414	0.7125
	Frame surface	-0.3498	0.0715	0.3570
	ColonialTimber - Thermal conductivity	-0.1843	0.0376	0.1881
	ColonialTimber - Thickness	0.1660	0.0359	0.1698
WW2	Indoor h-coefficient	-0.8620	0.1673	0.8781

Table 3.13. *WEST WINDOW. Active model parameters and groups.*

Group	Parameters	Mean	STD	Distance
D1	*HollowDoor - Thermal conductivity*	-0.4464	0.0900	0.4554
	HollowDoor - Thickness	0.4052	0.0825	0.4135
	Outdoor h-coefficient	-0.1003	0.0202	0.1023
	Surface	-0.6327	0.1258	0.6451
D2	Indoor h-coefficient	-0.8620	0.1673	0.8781

Table 3.14. *DOOR. Active model parameters and groups.*

Whole test cell

Sensitivities correlation analysis has also been carried out on the whole set of active parameters. Results achieved are included in Table 3.15. Ten "quasi-independent" groups of active model parameters have been identified (meta-groups in the table, MG below):

- **MG1, MG2 and MG3**. These three independent meta-groups contain only parameters related to the heat conduction though the floor.

- **MG4**. The only parameter in this meta-group is the heat convective coefficient between indoor vertical walls and the indoor air.

- **MG5.** This meta-group merges the coefficient describing heat convection between the floor and the indoor air with two parameters concerning heat conduction through the ceiling.

- **MG6.** Active model parameters related to the heat conduction through the south wall as well as those concerning heat conduction through the south window are included in this meta-group.

- **MG7**. Optical properties of the floor, the south wall, the east wall and the ceiling appear in this meta-group. It also includes the heat convective coefficient associated to the south wall – outdoor air interface.

- **MG8**. This meta-group merges a high number of active parameters related to heat conduction. Those of the door, the west wall and the west window as well as part of parameters involved in the heat conduction modelling through the west wall, the east wall and the ceiling.

- **MG9**. The surface of the north wall, the surface of the ceiling and the thermal conductivity of the polystyrene layer in the east wall are this group. It must be noticed that some statistical correlation remains among parameters in this meta-group and those in the previous one.

	Test-cell components groups	**Chosen representative**
Meta Group n°1	**F1**	Floor surface area
Meta Group n°2	**F2**	Floor styrodur layer conductivity
Meta Group n°3	**F3**	Floor polystyrene layer conductivity
Meta Group n°4	**N2**	Indoor vertical walls convective coefficient
Meta Group n°5	**F4** **C1**	Indoor floor/air convective coefficient
Meta Group n°6	**S1** **SW1**	South wall surface area
Meta Group n°7	**F5** **S2** **E4** **C3**	Solar efficiency of the south wall (outdoor surface)
Meta Group n°8	**N1** **E1** **C2** **WW1** **W1** **D1**	Ceiling Glass Wool layer conductivity
Meta Group n°9	**N3** **E2** **C4**	North wall surface area

Table 3.15. *TEST CELL. Active model parameters groups and group representatives.*

Model validation possibilities on the available data are quite limited. At most, modelling of the following parts and phenomena could be tested:

- Heat conduction through the floor.
- Heat convection between vertical walls and the indoor air.

- Heat conduction through the south façade without making distinction between the wall and the window.
- Heat conduction through the west, east, north and ceiling test cell envelope.
- Part of the solar processor.

Preliminary diagnosis

For preliminary diagnostic purposes, only one parameter by meta-group is taken into account. Principal components analysis is thus carried out on the sensitivity time series associated to the parameters in the third column of Table 3.15*:

$$\zeta(t) = \left[\widetilde{s}_{MG1}(t) \quad \widetilde{s}_{MG2}(t) \quad \cdots \quad \widetilde{s}_{MG9}(t)\right]^T$$

The spectral decomposition of the $\zeta(t)$ - covariance matrix leads to

$$W = \int_{t_o}^{t_f} \zeta(t)\zeta(t)^T \, dt = V \Sigma V^T$$

where Σ is a (9×9) diagonal matrix including the singular values of $\zeta(t)$, and V is a (9×9) squared matrix including the corresponding eigenvectors placed by columns.

The vector $\zeta(t)$ then can be written as $\zeta(t) = VX(t)$, where $X(t) = \left[x_1(t) \quad x_2(t) \quad \cdots \quad x_9(t)\right]^T$ is the vector of decomposition coefficients resulting from projection of $\zeta(t)$ onto the eigen-basis V. The time evolution of the components of $X(t)$ is represented in figure 3.20. It can be seen that only the first two components show significant fluctuations.

* Remember that a meta-group parameter representative represents the effect of the whole set of parameters in the meta-group. We note them MG1 to MG9 in the following.

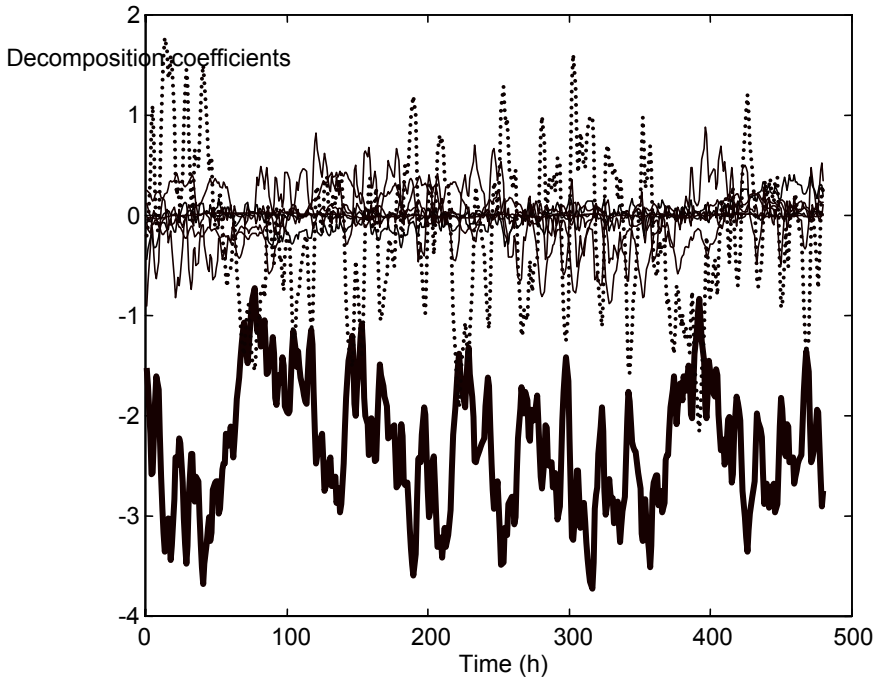

Figure 3.20. *Time evolution of the decomposition coefficients resulting from the projection of* $\zeta(t)$ *onto the eigen-basis* V *(Thick line: First coefficient; Discontinuous line: Second coefficient).*

Table 3.16 includes some statistical analysis on the $X(t)$ components: the time mean value, the standard deviation, the contribution to the whole energy in $\zeta(t)$ (see equation 2.42) and the linear correlation between residuals and the $X(t)$ components. It can be seen that the first component explains more than 87% of the whole energy in $\zeta(t)$. In addition, it shows a significant effect on the model static behaviour (remember that the main problem in the model concern the static regime) as well as a high degree of correlation with residuals.

	Mean value	**Standard Deviation**	**Contribution to the whole variance of** $\zeta(t)$	**Linear correlation with residuals**
$x_1(t)$	**-2.3091**	**0.6293**	**0.8740**	**-0.6010**
$x_2(t)$	-0.1751	0.7445	0.0891	-0.1786
$x_3(t)$	0.0098	0.3526	0.0189	0.0085
$x_4(t)$	-0.0054	0.2817	0.0121	0.4942
$x_5(t)$	-0.0078	0.1505	0.0035	0.1849
$x_6(t)$	-0.0019	0.1020	0.0016	0.0167
$x_7(t)$	0.0007	0.0667	0.0007	0.2088
$x_8(t)$	0.0002	0.0224	0.0001	0.1386
$x_9(t)$	0.0002	0.0141	0.0000	-0.0688

Table 3.16. *Statistical analysis on the* $X(t)$ *components.*

Model output changes due to small variations in active model parameters can be thus approached by (see section 2.3):

$$\Delta y(t) \approx \Delta\gamma_1 x_1(t) \qquad \text{with} \qquad \Delta\gamma_1 = \frac{\Delta\theta_1}{\theta_{1o}} v_{11} + \frac{\Delta\theta_2}{\theta_{2o}} v_{21} + \cdots + \frac{\Delta\theta_9}{\theta_{9o}} v_{91}$$

where θ_{io} and $\Delta\theta_i$ represent respectively the nominal value and the variation of the i^{th} model parameter. The previous equation shows that the effect of parameters on the model output are weighted by the elements $\{v_{i1}\}_{i=1,\cdots,9}$ of the first eigenvector of the basis V.

In Figure 3.21, the first eigenvector $\{v_{i1}\}_{i=1,\cdots,9}$ has been represented. It can be seen that:

- The first meta-group of parameters is the one showing a greater contribution to the model output variations. It includes active model parameters related to heat conduction through the first layer of the floor.
- Meta-groups 6 and 4 have also a significant effect on the model output. The first one represents heat conduction through the south facade (wall and window included), and the second one is the convective coefficient at the indoor air–vertical walls interfaces.
- Next meta-groups in order of significance are meta-groups 2, 8 and 9. Meta-group 2 includes parameters related to heat conduction through the floor, and meta-groups 8 and 9 represent heat conduction through the north, east, west and ceiling test cell envelope.

Improving the model performances likely involves significant changes in the values of these parameters. This probably means that modelling of thermal conduction as well as heat convection at the wall-air interfaces have to be reviewed. Such preliminary conclusions must be however confirmed by optimisation techniques.

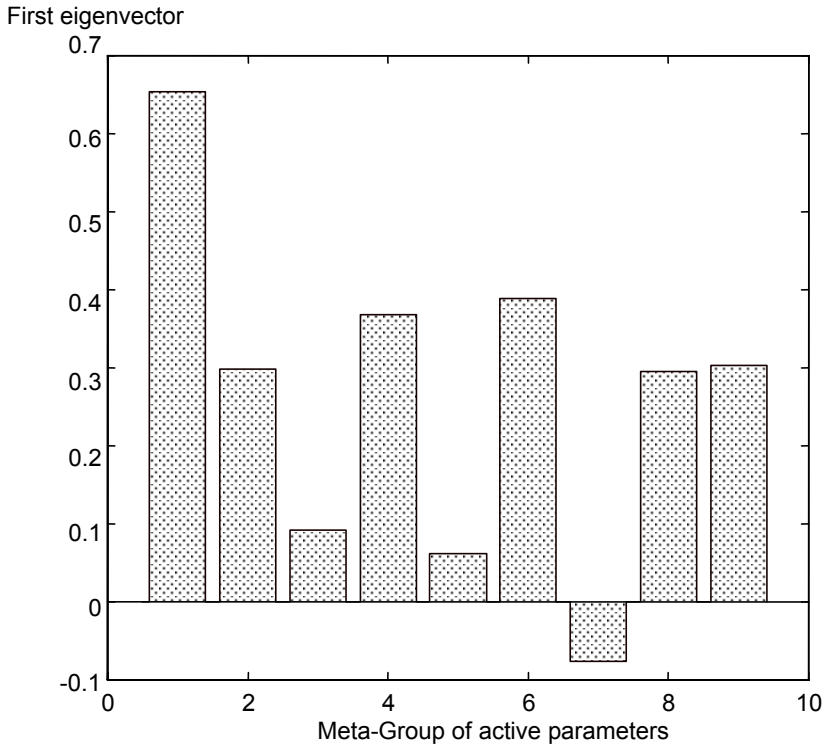

Figure 3.21. *First eigenvector of the basis V . The meta-groups MG1 to MG9 are represented by the model parameters in the third column of Table 3.15.*

3.5. FREE MODEL PARAMETERS ESTIMATION AND DIAGNOSIS

Fitting the model on the available data has been performed by the following three methods:

- The heuristic bounding methods (HBM) described in section 2.4. It allows finding the parameters domain leading to model output uncertainty bands showing a significant overlapping with measurements uncertainty intervals.

- The random search algorithm (SRA) described in section 2.4. It is a stochastic algorithm for searching the global minimum of the residuals variance on a given parameters set. The parameter set we are using is the one proposed by the HBM.

- The Gauss-Newton method (GNM) described in section 2.4. It considers the problem of finding a local minimum of the residuals variance from an initial parameter vector. The initial parameter vector we are using is the one of nominal values.

In all the cases, free model parameters considered for optimisation are the meta-groups representatives in Table 3.15. The solutions proposed by the different methods are summarised in Table 3.17. Looking at the results from the HBM, we can conclude that improving the model mainly means:

- Reviewing the floor model. The HBM estimations indicate that the thermal conductivity of some floor layers as well as its area must be significantly increased (see results for meta-groups MG1 and MG3).

- Reviewing heat convection modelling between the test cell walls and the indoor air. It seems that values for convective coefficients at the indoor vertical walls have to be significantly reduced (see results for meta-group MG4).

- Reviewing heat conduction modelling through the test cell envelope (ceiling and south, east, west and north facades). The HBM estimations (see results for meta-groups MG6, MG8 and MG9) indicate that heat conduction through the envelope is clearly underestimated by the nominal model.

- Reviewing the solar processor or the heat convection between the south wall and the outdoor environment (see results for the meta-group MG7).

Meta-Group	Representative	Nominal value	HBM	SRA	GNM
MG1	Floor surface area	16.28 m^2	[19.45, 20.22]	20.05	19.96
MG2	Floor styrodur layer conductivity	0.029 $W.m^{-1}.K^{-1}$	[0.0234, 0.0305]	0.026	0.0313
MG3	Floor polystyrene layer conductivity	0.040 $W.m^{-1}.K^{-1}$	[0.0801 , 0.0753]	0.08	0.0968
MG4	Indoor vertical walls convective coefficient	9.1 $W.m^{-2}$	[3.9059 , 3.6326]	3.56	1.666
MG5	Floor-indoor air convective coefficient	5.88 $W.m^{-2}$	[4.6327 , 4.4079]	4.49	4.68
MG6	South wall area	7.25 m^2	[10.58, 16.34]	14.01	15.87
MG7	South wall solar	0.30	[1.0137, 0.6581]	0.822	1.357

	absorptivity (outdoor side)				
MG8	Ceiling glass wool layer conductivity	0.042 $W.m^{-1}.K^{-1}$	[0.0623, 0.0674]	0.066	0.1015
MG9	North wall area	7.0 m^2	[12.06, 12.48]	12.53	10.75

Table 3.17. *Results from optimisation. HBM = Heuristic Bounding Method; SRA = Search Random Algorithm; GNM = Gauss-Newton Method.*

In figure 3.22, we have represented model output uncertainty bands corresponding to the HBM solution as well as measurements uncertainty intervals (±0.5°C). A good enough overlapping is observed between simulations and measurements uncertainty bands.

Concerning diagnosis, results from the SRA and the GNM methods lead to identical conclusions than HBM even thought GNM propose a slightly different solution. Both RSA and GNM solutions lead to simulations showing residuals with zero mean and 0.39°C standard deviation value.

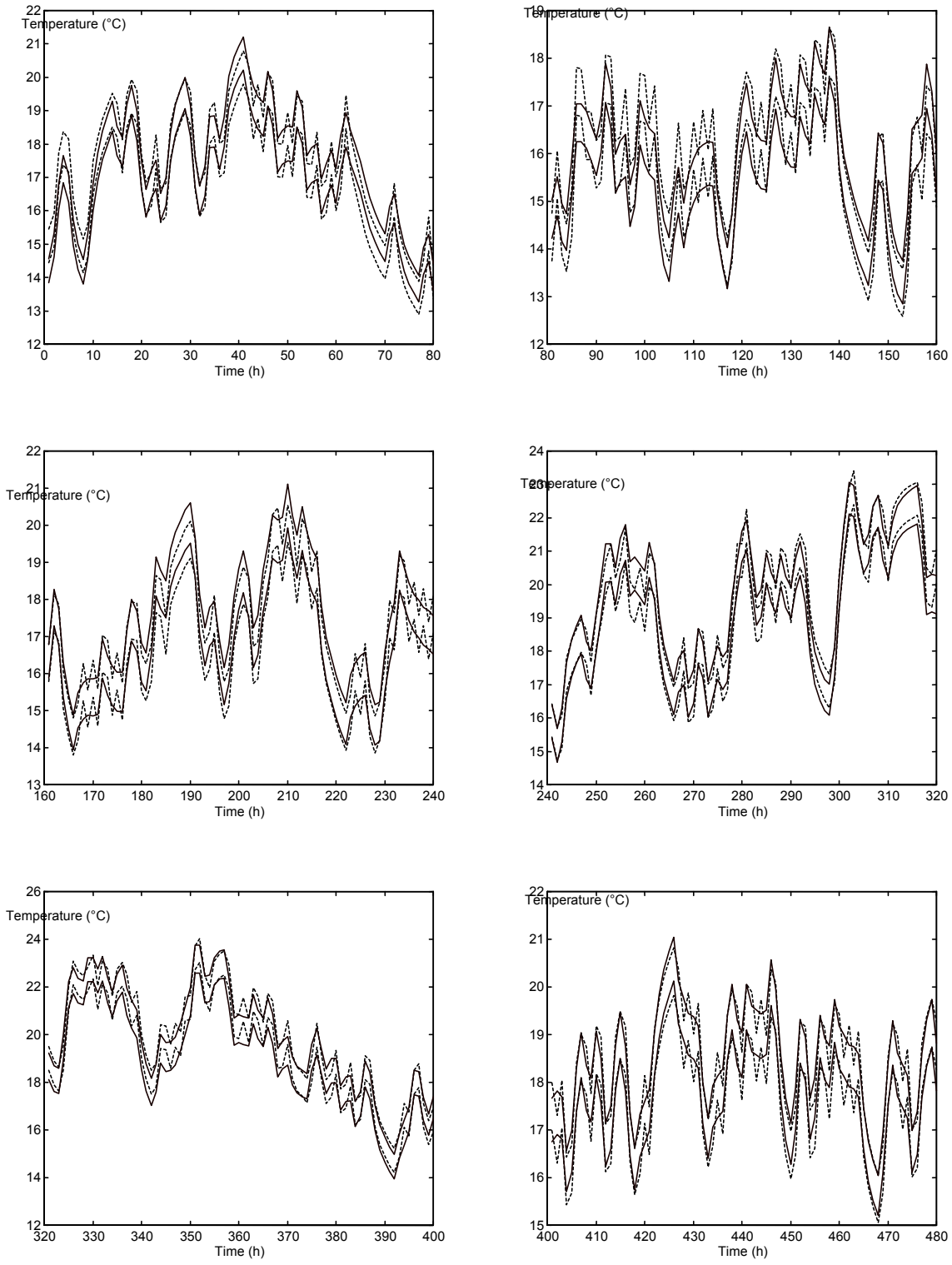

Figure 3.22. *Comparison between measurements uncertainty intervals (dotted lines) and model output bounds over the HBM parameter set (continuous line).*

3.6. CONCLUSION

The methodology as well as the methods described in chapter 2 has been used here for empirical validation of the ETNA test cell model created by CLIM2000. Main conclusions from this validation exercise are:

- **The data quality**. The spectral analysis of the available data show that most of the information contained in the experiment concerns the low-frequency behaviour (daily) of the test cell. High dynamics parts (hourly) of the test cell model cannot be checked from this experiment.

- **The nominal model performances**. It has been created using the ETNA test cell specifications supplied in [31]. Usual modelling hypothesis have been adopted. Residuals analysis show than the nominal model is able to reproduce neither the static nor the dynamic behaviour of the test cell. Main disagreements between measurements and simulations are observed at the low-frequency range.

- **The parts of the model that could be tested on the available data**. Sensitivity analysis indicates that model validation possibilities on the available data are quite limited. At most, modelling of the following parts and phenomena could be tested:

  - Heat conduction through the floor.
  - Heat convection between vertical walls and the indoor air.
  - Heat conduction through the south façade without making distinction between the wall and the window.
  - Heat conduction through the west, east, north and ceiling test cell envelope.
  - Part of the solar processor.

- **Preliminary diagnosis based on PCA**. Principal components analysis provides some useful information for diagnosis. It indicates that model performances improvement likely involves modifications of the heat conduction modelling through the test cell envelope as well as of the representation of the heat convection at the walls – indoor air interfaces.

- **Diagnosis from optimisation**. Comparisons between nominal and estimated values for model parameters point out heat conduction through the test cell envelope as being the main problem in the model. Thermal conductivities values and/or wall surfaces have to bee significantly increased to improve the model response. Such parameters displacements could be explained by nominal test cell material properties not fully matching the final as-constructed conditions of the test cell. They could also be explained by un-modelled thermal bridges if nominal values for material properties supplied in [31] are right. In addition, it seems that indoor convective coefficient values must to be reviewed.

This example of application, show how model parameters space analysis is a useful and powerful tool for empirical validation. In particular, diagnosis possibilities are largely increased in comparison with residual analysis techniques.

SUMMARY AND CONCLUSIONS

The methodology for empirical model validation developed in the framework of the IEA Task 22 involves two main steps: checking model validity and diagnosis.

First step aims to test the model performances by identification of significant disagreements between measurements and simulations. It rest both on residuals analysis techniques and on comparisons between model outputs uncertainty bands and measurements uncertainty intervals. The pertinence of the mathematical tools underlying this step is today well recognised.

Second step intends to explain the differences observed between model simulations and measurements. This is a difficult task that has been overlooked (or performed in a very subjective way) for a long time. First attempts to establish methods for rigorous model diagnosis are relatively new. They mainly concerns the so-called "residuals analysis techniques (RAT)" whose aim is to identify model input variables strongly correlated with residuals. Results from RAT could help the modellers to sort the model inputs and to target those responsible of the major part of the error over a given frequency area. This approach to diagnosis has been largely used in the 90's. However, it presents two severe limitations: firstly, it cannot be applied to non-linear models; secondly, going up from inputs-residuals correlations to modelling hypothesis is frequently impossible. A new approach for models diagnosis has been thus proposed here. It rests on the analysis of the model parameters space. The main objective is to identify the changes in parameters values that are required for a significant model behaviour improvement. Diagnosis is then provided by comparison of such results with the knowledge we have about both the actual system and the model itself.

The IEA diagnostic approach involves three main parts:

- Sensitivity analysis. The principal aim of this part if to identify the parts of the model as well as physical phenomena that can be really tested on the available data. Sensitivity calculations, correlation analysis and principal components analysis are the main tools proposed to reach this objective. Some preliminary elements for diagnosis are already supplied by principal components analysis at this stage.
- Optimisation. Parameters estimation techniques are the main mathematical tool we are proposing to guide model diagnosis. Free model parameters values allowing significant residuals reduction are here identified by fitting the model on the available data. Diagnosis mainly involves comparisons between estimated and nominal model parameters values. Three different algorithms for optimisation have been proposed and discussed.
- Diagnosis. The possible causes of discrepancies between measurements and simulations are finally elucidated using:
  - Some knowledge about the model. The main information required concerns the phenomena considered in the model and the parameters involved in their representation.
  - Modelling hypothesis analysis. Foreseeable model parameter values for each one of the hypothesis in the model, as well as for their negative statement, are desired but difficult to

obtain. Instead, some knowledge about what kind of model parameter displacements are expected when inadequate modelling hypothesis can be used. For instance, un-modelled thermal bridges (when significant) will lead to systematic increasing of thermal conductivity values when fitting the model to the data.

- Parameter changes analysis. It involves comparisons between estimated and nominal model parameters values. Large differences are expected for parameters involved in phenomena which are not correctly represented in the model.

The combination of these three elements of judgement should lead to know reasons for the observed model errors, and to suggest model improvements.

Concerning the mathematical methods underlying the IEA empirical model validation methodology, some new contributions can be pointed out:

- An efficient computational method has been developed for differential sensitivity analysis involving large scale systems of differential equations with a large number of parameters. It is based on both the well known sensitivity-equation method and the theory of balanced realisations.

- Principal components analysis has been introduce as a simple and useful tool for active model parameters identification and grouping. In addition, it has been proven that it can supply some preliminary elements for diagnosis.

- A new algorithm for fitting models on the data has been proposed: the heuristic bounding method (HBM). It seems to us a promising way for modelling diagnostic purposes. Main reason is that HBM allows incorporation of data uncertainty and it is conceived for reliable global solution searching. In addition, HBM computer implementation is quite easy and it does not require any simulation code modification.

Two main computer tools have been developed within the IEA Task 22 for empirical model validation purposes: MED and MEDLab. Please, contact the authors for obtaining the corresponding β-versions and the user manuals.

The IEA Task 22 methodology has been applied for model checking and diagnosis in the framework of the thermal analysis of the ETNA test cells. Two different modelling-simulation environments have been used: CLIM2000 and CA-SIS. Such examples of application show how model parameters space analysis is a useful and powerful tool for empirical validation. In particular, diagnosis possibilities are largely increased in comparison with residual analysis techniques. In both cases, comparisons between nominal and estimated parameters values pointed out heat conduction through the test cell envelope as being the main problem in the models. Thermal conductivities values and/or wall surfaces areas have to be significantly increased to improve the models response. Such parameters displacements could be explained by nominal test cell material properties not fully matching the final as-constructed conditions of the test cell. They could also be explained by un-modelled thermal bridges if assumed nominal values for material properties are right.

Even though we are convinced that our proposal is a step forward in empirical model validation, it is not immune to criticism. Main limitations of the proposed methodology are related to the data and the experiment quality as well as to the diagnosis required expertise. In practice, it is frequently noticed that the information contained in the available experiments is quite limited for model validation purposes. Usually only a few parts and phenomena in the model can be really tested on the available data. Concerning diagnosis, going up from the model parameters displacements to the modelling hypothesis to be changed requires a real expert knowledge on both the studied system and the model.

REFERENCES

[1] R. JUDKOFF et al., Methodology for validating building energy analysis simulations, Report TR-254-1508, Solar Energy Research Institute (1983).

[2] D. BLOMFIELD et al., An investigation into analytical and empirical validation techniques for dynamic thermal models of building, In Final Grant Report, Science and Engineering Research Council, Polaris House, England (1988).

[3] S. O. JENSEN, The PASSYS Project Phase I, Subgroup Model Validation and Development, In Final Report 1986-1989, Commission of the European Communities DGXII (1989).

[4] S. O. JENSEN, Model Validation and Development, In Research Final Report, PASSYS: Part II, Commission of the European Communities DGXII (1993).

[5] E. PALOMO, J. MARCO and H. MADSEN, Methods to compare measurements ans simulations, In Building Simulation'91, IBPSA Conference, Nice, France (1991).

[6] E. PALOMO and J. MARCO, The pertinence and limitations of different statistical tools for empirical validation purposes, In 3er European Conference on Architecture, Florence, Italy (1993).

[7] A. M. DUBOIS at al., The model coupling problem: Methods used in some building analysis tools and ALMETH propositions, In Building Simulation'91, IBPSA Conference, Nice, France (1991).

[8] N. FENTON and G. HILL, *Systems Construction and Analysis: A Mathematical and Logical Framework*, International Series in Software Engineering, McGraw-Hill (1993).

[9] M. M. IZQUIERDO et al., A statistical methodology for model validation in ALLAN simulation environment, In Building Simulation'95, IBPSA Conference, Madison, USA (1995).

[10] K. J. LOMAS and H. EPPEL, Sensitivity analysis techniques for building thermal simulation programs, *Energy and Building*, 19, 21-44 (1992).

[11] Y. CANDAU and G. PIAR, An application of spectral decomposition to model validation in thermal building analysis, *Int. J. of Heat and Mass Transfer*, 3, 645-650 (1993).

[12] N. RAMDANI, Validation expérimentale et analyse des signaux: Développement d'une méthodologie de comparaison modèle/mesures en thermique du bâtiment, PH. D. thesis, Université Paris 12 (1994).

[13] N. RAMDANI et al., How to improve building thermal simulation programs by use of spectral analysis, *Energy and Building* (1997).

[14] C. J. MARTIN and D. M. J. WATSON, Empirical validation of the model SERI-RES using data from test rooms, *Building and Environment*, 2, 175-187 (1993).

[15] N. RAHNI, Validation de modèles et variabilité des paramètres: Analyse de sensibilité et d'incertitude – Procédures d'optimisation. Application à des modèles thermiques du bâtiment, Ph. D. thesis, Université Paris 12, Paris (1998).

[16] H. HOTELLING, Analysis of a complex statistical variables into principal components, *J. Educ. Psych.*, 24, 417-441 & 498-520 (1933).

[17] A. P. DEMPSTER, *Elements of continuous multivariate analysis*, Reading, M.A: Addison-Wesley (1969).

[18] R. FLETCHER, *Practical methods of optimisation. Volume 1: Unconstrained optimisation*, John Wiley & Sons, Chichester (1986).

[19] R. Y. RUBINSTEIN, *System, models, simulations and Monte Carlo methods*, John Wiley & Sons, New York (1981).

[20] E. WALTER and H. PIET-LAHANIER, Estimation of parameters bounds from bounded-error data: a survey, *Mathematics and Computer in Simulations*, 32, 449-468 (1990).

[21] E. PALOMO and G. GUYON, Using parameters estimation techniques to model errors diagnostic in building thermal analysis: Theory, applications and computer implementation, Electricité de France, Internal Report (1999).

[22] E. PALOMO, MEDLab (v1.0). Un outil pour le diagnostic des erreurs de modélisation en thermiques des bâtiments, Electricité de France, Internal Report (1999).

[23] G. LEFEBVRE, Modal-based simulation of the thermal behaviour of a building : the M2m software, *Energy&Buildings* (1996).

[24] D. BONNEAU and al., CLIM2000: Modular software for energy simulations in buildings, in Proc. IBPSA'93, Adelaide (1993).

[25] P. STANGERUP, ESACAP User's Manual, StamSim, Denmark (1994).

[26] EDF, CA-SIS: Conditionnement d'Air – Simulation de Systèmes, Electricité de France (1990).

[27] S. A. KLEIN and W. A. BECKMANN, TRNSYS v14.2 : TRaNsient SYstems Simulation program, SEL, University of Wisconsin, Madison (1986).

[28] T. WILLIAMS and C. KELLEY, GNUPLOT: An iteractive plotting program (1996).

[29] E. PALOMO and F. TELLEZ, PAMTIS: Package to Analyse Multivariate TIme Series. Installation and Userguide, PASSYS Ref.: 194-91-PASSYS-MVD-WD-216 (1991).

[30] E. PALOMO and F. TELLEZ, Mathematical and numerical methods in PAMTIS, PASSYS Ref.: 194-91-PASSYS-MVD-WD-214 (1991).

[31] P. GIRAULT and S. DELILLES, Description of ETNA cells. Physical and geometrical configuration, Electricité de France, Internal Report (1995).

ANNEXES

ANNEX A. **An efficient computational method for solving large-scale differential sensitivity problems**

ANNEX B. **Validation of two French building energy programs : Part 2 - Parameter Estimation Method Applied to Empirical Validation.**

Annex A

AN EFFICIENT COMPUTATIONAL METHOD FOR SOLVING LARGE-SCALE DIFFERENTIAL SENSITIVITY PROBLEMS

Elena PALOMO DEL BARRIO
LEPT-ENSAM UMR 8508
Esplanade des Arts et Métiers, 33405 Talence Cedex FRANCE
e-mail: palomo@lept-ensam.u-bordeaux.fr

(To be published in "Numerical Heat Transfer – Part B Fundamentals")

Abstract

An efficient computational method has been developed for differential sensitivity analysis involving large systems of differential equations with a large number of parameters. It is based on both the sensitivity-equation method and the theory of balanced realisations. The sensitivity-equation method is first used to generate the whole set of sensitivity models (one state-variable model per parameter). A sensitivity model, as well as its corresponding balanced realisation, is characterised by three matrices of the same dimension than those in the nominal model: the state matrix, the command matrix and the output matrix. However, such matrices remain unchanged regardless of the parameter under consideration. Consequently, a single calculation suffices to obtain the balanced realisation of all the sensitivity models. Such representation allows ranking the state variables according to their degree of controllability/observability. A low-dimension balanced realisation is then obtained by only keeping the more controllable/observable state variables. The sensitivity problem solution is finally obtained by time integration of the low-dimension sensitivity models instead of the corresponding full-dimension ones.

NOMENCLATURE

A	Matrix [$n \times n$] of heat exchanges among the nodes of the discretisation mesh
B	Command matrix [$n \times n$]
C	Matrix [$n \times n$] of heat capacities
$c(M)$	Heat capacity, J/m^{3}K
F	State matrix [$n \times n$]
$k(M)$	Thermal conductivity, W/mK
O	Output matrix [$q \times n$]
P	Transformation matrix [$n \times n$]
$r(M, M')$	Distribution of radiative coefficients of exchange
$T(M,t)$	Temperature field at point M and time t , K
$T(t)$	Vector [$n \times 1$] of temperatures at the nodes of the mesh of discretisation, K
$U(t)$	Vector [$p \times 1$] of forcing functions or input variables
$\vec{v}(M)$	Fluid velocity field, m/s

W_c	Gramian of controllability, matrix [$n \times n$]
W_o	Gramian of observability, matrix [$n \times n$]
$X(t)$	Vector [$n \times 1$] of state variables
$Y(t)$	Vector [$p \times 1$] of output variables
$y_l(t)$	Output variable
λ_i	i^{th} Hankel singular value
$\vec{\theta}$	Vector [$m \times 1$] of model parameters ($\vec{\theta}_o$, nominal values)
θ_k	k^{th} model parameter
$\Theta_k(M,t)$	Sensitivity of $T(M,t)$ to the parameter θ_k
$\Theta_k(t)$	Sensitivity of the vector $T(t)$ to the parameter θ_k
$\sigma(M,t)$	Heat sources (W/m^3 for $M \in \Omega$; W/m^2 for $M \in \partial\Omega$)
$\sigma_{l,k}(t)$	Sensitivity of $y_l(t)$ to the parameter θ_k
$\sigma_k(t)$	Sensitivity of the vector $Y(t)$ to the parameter θ_k
Ω	System domain $\Omega = \Omega_o \cup \partial\Omega$
$\partial\Omega$	System frontier ($\partial\Omega = \partial\Omega_1 \cup \partial\Omega_2$)
$\partial\Omega_1$	Part of the frontier with Dirichlet boundary conditions
$\psi(M,t)$	Solicitations field (W/m^3 for $M \in \Omega_o$; W/m^2 for $M \in \partial\Omega$)

Special symbols

L	Heat operator for coupled thermal transfers
B	Boundary conditions operator

Superscripts

$\sim$	Approximation
^{T}	Transposed matrix
$\dot{}$	Time derivative

1. INTRODUCTION

Sensitivity analysis studies the effect of parameter variations on the behaviour of a dynamic system. It is recognised as an important step for getting an enhanced understanding of the systems performance, and for providing guidance for optimal design purposes. Therefore it proved its effectiveness in uncertainty propagation studies, as well as in models validation and models calibration. A rather complete state of the art on the techniques of sensitivity analysis is brought in [1]. One can distinguish two main families of sensitivity methods: those that follow a deterministic approach, on the one hand, and those that adopt a statistical procedure, of another. The well-known techniques of differential sensitivity analysis are in the first group. Its characteristic is to examine the first-order derivatives of the model response with respect to its parameters. According to the complexity of the problem, the derivatives either will be calculated in an approximate way (parameter-perturbation methods) or exact. One is interested here in the exact methods, among which one distinguishes the so called direct and adjoint methods.

The direct method (sensitivity-equation method) involves differentiation of the model equations with respect to the parameters. This leads to a model of sensitivity per studied parameter. The resolution of the sensitivity problem then involves the integration of as many systems of differential equations than there are parameters. One sensitivity model integration leads to the time evolution of all dependent variables of the model with respect to a single parameter.

The theoretical bases of the adjoint method are established in [2], where a general formulation, applicable to all kinds of models (linear, non-linear, dynamic, static), is brought. This method starts by defining the model response as a functional of the dependent variables of the model. A system of adjoint equations (adjoint model) is then built from a differentiated form of the original model. In contrast to the direct model, a single integration of the adjoint model leads to the sensitivity of the model response to all the parameters. However, the adjoint model depends on the model response and it must be solved anew for each model dependent variable.

In practice, for about de same amount of computation, the adjoint method gives de sensitivity of a functional of the model variables to all the parameters, while the direct method gives the sensitivity of all variables to a single parameter. The direct method is computationally efficient only when effects of few parameters on a large number of variables are being evaluated, while the adjoint method adapts better to the contrary case. These two techniques become ineffective when the analysis of sensitivity involves both a large number of dependent variables and a great number of parameters, the problem being all the more significant as the dimension of the original model is large. Common thermal modelling problems often involve large systems of differential equation with a large number of uncertain parameters. A numerical approach that makes it possible to extend the application of the sensitivity-equation method to such kind of problems is here proposed.

The second section presents the mathematical formulation of the problem of sensitivity. The most typical parameters are initial conditions, time-invariant coefficients, time-variant coefficients, forcing functions, sampling intervals, round-off errors, etc. In this paper, the attention is focused on time-invariant coefficients. Furthermore, one addresses to linear thermal systems. Despite such a limitation, however, there still exists a vast class of problems of practical importance that can be studied assuming linearity. The third section describes the fundamentals of the computational method that is proposed for solving large-scale sensitivity problems. It rests on the theory of balanced realisation, which makes it possible to strongly reduce the number of differential equations in a model without introducing a significant loss of precision. It must be noticed that the number of sensitivity models to integrate remains equal to the number of parameters concerned with the analysis. However, their dimension is strongly reduced and the computing time hence decreases significantly. The method is all the more effective as the dimension of the original model and the number of studied parameters is large. The last section includes an example of application that shows the effectiveness of the suggested method.

2. MATHEMATICAL FORMULATION OF THE PROBLEM

Let Ω be a geometrically bounded thermal system in $\Re^3$, and let $\partial\Omega$ be its frontier. It is assumed that the system domain Ω can be split-up in a finite number of solid or/and fluid subdomains with invariant geometry. Each one of the subdomains is formed by a continuous and monophasic medium whose thermophysical properties (thermal conductivity, density, specific heat, transfer coefficients, etc.) are space continuous functions. Furthermore, such properties are assumed to be time invariant and independent of the temperature. Incompressible and low viscosity fluids are supposed. In addition, the velocity field is assumed to be time invariant and known.

Energy transfer in Ω can take place by the following mechanisms: heat conduction, convection and radiation. It is assumed that a linear model linking-up radiative flux to the thermal field can be used for thermal radiation exchanges representation.

2.1. The nominal model

In the framework of the previous hypothesis, the only knowledge of the evolution of the temperature field is enough to define the thermodynamic state of the system in any point and at any moment. One presents below the most general possible equations within the limits of the allowed assumptions. All the other forms of the equations of evolution are particular cases. The energy conservation equation is then written in the operational form:

$$\left.\begin{array}{ll} M \in \Omega_o & \mathsf{L}\left[T(M,t)\right] + \Psi(M,t) = c(M)\dfrac{\partial T(M,t)}{\partial t} \\ M \in \partial\Omega & \mathsf{B}\left[T(M,t)\right] + \Psi(M,t) = 0 \end{array}\right\} \quad (1)$$

L is the heat operator for coupled thermal transfers. It is given by [3]:

$$\mathsf{L}\left[T(M,t)\right] = \vec{\nabla}\left[k(M)\vec{\nabla}T(M,t)\right] - \vec{u}(M)\vec{\nabla}T(M,t) + \int_{\Omega} r(M,M')T(M',t)dM' \quad (2)$$

where one can recognise the heat transferred by conduction (first term), by mass transfer (second term) and by thermal radiation (last term). $k(M)$ is thermal conductivity at the point M. $\vec{u}(M)$ represents the product of the heat capacity $c(M)$ by the speed vector $\vec{v}(M)$. $r(M,M')$ is a distribution of radiative coefficients of exchange. It takes into account the geometric configuration factors between the differential elements dM and dM', their optical properties and those of the optical way which separates them [3, 4].

B is the operator of the boundary conditions. At points $M \in \partial\Omega_1 \subset \partial\Omega$ verifying Dirichlet boundary conditions, B is the identity operator. Otherwise ($M \in \partial\Omega_2 \subset \partial\Omega$), B is given by [3]:

$$\mathsf{B}\left[T(M,t)\right] = -\left[k(M)\vec{\nabla}T(M,t)\right]\vec{n}(M) + \int_{\Omega} r(M,M')T(M',t)dM' \quad (3)$$

$\Psi(M,t)$ represents the so-called solicitations field. For any point $M \in \Omega_o$ inside the system, it generally includes two terms:

$$\Psi(M,t) = \sigma(M,t) + \int_{\Omega'} r(M,M')T(M',t)dM' \quad (4)$$

The first one represents the sources or sinks of heat, and the second one is the radiative flux coming from the system environment Ω'. For any point $M \in \partial\Omega_2$, $\Psi(M,t)$ is given by:

$$\Psi(M,t) = \sigma(M,t) + \int_{\Omega'} r(M,M')T(M',t)dM' + \left[k(M)\vec{\nabla}T(M,t) - \vec{u}(M)T(M,t)\right]\vec{n}(M) \quad (5)$$

where one recognises equation (4) increased of a heat conduction flux and a term due to the transport of mass. Such a term is zero everywhere except at the fluid inlets and outlets. Finally, at any point $M \in \partial\Omega_1$, $\Psi(M,t)$ is equal to the prescribed temperature.

In practice, the objective for modelling could be focus on some intensive or extensive quantities at some points in Ω instead of the complete temperature field. Such quantities are called observation variables or outputs. The time evolution of the observation variable $y_l(t)$ can be written as:

$$y_l(t) = J_l(T(M,t)) + G_l(\psi(M,t)) \quad (6)$$

where J_l and G_l are linear and real functionals.

2.2. The sensitivity models

One notes $\vec{\theta} = \{\theta_1 \quad \theta_2 \quad \cdots \quad \theta_m\}$ the vector of the model parameters. Among the parameters one finds those that define the system geometry, those that determine its thermal or optical properties,

the velocity field, etc. The sensitivity of $T(M,t)$ and $y_l(t)$ to the parameter θ_k are respectively defined by:

$$\Theta_k(M,t) \equiv \frac{\partial T(M,t)}{\partial \theta_k} \qquad \text{and} \qquad \sigma_{l,k}(t) \equiv \frac{\partial y_l(t)}{\partial \theta_k} \tag{7}$$

They are first-order estimations of the effect of a weak variation of the parameter θ_k on $T(M,t)$ and $y_l(t)$, the other parameters being maintained constant. The equation that describes the time evolution of $\Theta_k(M,t)$ is obtained by simple differentiation of the equations (1) to (5). One get:

$$\left.\begin{array}{ll} M \in \Omega_o & \mathsf{L}\left[\Theta_k(M,t)\right] + \Psi_k(M,t) = c(M)\dfrac{\partial \Theta_k(M,t)}{\partial t} \\ M \in \partial\Omega & \mathsf{B}\left[\Theta_k(M,t)\right] + \Psi_k(M,t) = 0 \end{array}\right\} \tag{8}$$

with:

$$\left.\begin{array}{ll} M \in \Omega_o & \Psi_k(M,t) = \mathsf{L}_k\left[T(M,t)\right] + \dfrac{\partial \psi(M,t)}{\partial \theta_k} - \dfrac{\partial c(M)}{\partial \theta_k}\dfrac{\partial T(M,t)}{\partial t} \\ M \in \partial\Omega & \Psi_k(M,t) = \mathsf{B}_k\left[T(M,t)\right] + \dfrac{\partial \Psi(M,t)}{\partial \theta_k} \end{array}\right\} \tag{9}$$

According to (2) and (3), L_k and B_k are given by:

$$\begin{aligned} \mathsf{L}_k\left[T(M,t)\right] &= \vec{\nabla}\left[\frac{\partial k(M)}{\partial \theta_k}\vec{\nabla}T(M,t)\right] - \frac{\partial \vec{u}(M)}{\partial \theta_k}\vec{\nabla}T(M,t) + \int_\Omega \frac{\partial r(M,M')}{\partial \theta_k}T(M',t)dM' \\ \mathsf{B}_k\left[T(M,t)\right] &= -\left[\frac{\partial k(M)}{\partial \theta_k}\vec{\nabla}T(M,t)\right]\vec{n}(M) + \int_\Omega \frac{\partial r(M,M')}{\partial \theta_k}T(M',t)dM' \end{aligned} \tag{10}$$

It must be noticed that the different terms in equations (9) and (10) are evaluated at the point $\vec{\theta}_o$ of the space of the parameters (vector of the nominal values). Therefore $T(M,t)$ represents the solution of (1) for $\vec{\theta} = \vec{\theta}_o$.

In the same way, the equation describing the time evolution of $\sigma_{l,k}(t)$ is obtained by simple differentiation of (6):

$$\sigma_{l,k}(t) = J_l(\Theta_k(M,t)) + \eta_{l,k}(M,t) \tag{11}$$

with:

$$\eta_{l,k}(t) = \frac{\partial J_l}{\partial \theta_k}(T(M,t)) + \frac{\partial G_l(\psi(M,t))}{\partial \theta_k} \tag{12}$$

2.3. The finite dimension formulation

Since no general theory is currently available for the analytic solution of partial differential equations, approximate methods and numerical solutions are the only practical alternative that scientist and engineers usually resort to solve this type of equations. Spatial discretisation of equations (1) or (8) leads to a system of ordinary differential equations (state-space model) of the form:

$$C\dot{\mathsf{Z}}(t) = A\mathsf{Z}(t) + \psi_k(t)$$
$$\mathsf{Y}(t) = J\mathsf{Z}(t) + \eta_k(t) \tag{13}$$

where C is the matrix $[n \times n]$ of heat capacities at the nodes of the discretisation mesh, A is the matrix $[n \times n]$ of heat exchanges between nodes (numerical approach of L) and J is a matrix of dimension $[q \times n]$. These three matrices (calculated for $\vec{\theta} = \vec{\theta}_o$) remain unchanged regardless of the parameter under consideration. Consequently, a single calculation suffices to obtain the nominal model and all the sensitivity models.

In the nominal model $\mathsf{Z}(t) = T(t)$ and $\mathsf{Y}(t) = Y(t)$, where $T(t)$ is the vector $[n \times 1]$ of temperatures at the nodes of the discretisation mesh and $Y(t)$ is the vector $[q \times 1]$ of the output variables. $\psi_0(t)$ $[n \times 1]$ and $\eta_0(t)$ $[q \times 1]$ represent the effect of the solicitations on the mesh nodes and on the output variables respectively. They usually take the following form:

$$\psi_0(t) = EU(t) \qquad \eta_0(t) = GU(t) \tag{14}$$

where $U(t)$ $[p \times 1]$ is the forcing functions or inputs vector. E and G are matrices of dimension $[n \times p]$ and $[q \times p]$ respectively.

In the $k^{ème}$ sensitivity model ($k = 1, \cdots, m$), $\mathsf{Z}(t)$ and $\mathsf{Y}(t)$ are given by:

$$\mathsf{Z}(t) = \Theta_k(t) = \frac{dT(t)}{d\theta_k} \qquad \mathsf{Y}(t) = \sigma_k(t) = \frac{dY(t)}{d\theta_k} \tag{15}$$

As for $\psi_k(t)$ and $\eta_k(t)$, they are given by

$$\psi_k(t) = \left(\frac{\partial A}{\partial \theta_k}\right) T(t) + \left(\frac{\partial E}{\partial \theta_k}\right) U(t) - \left(\frac{\partial C}{\partial \theta_k}\right) \frac{dT(t)}{dt} \tag{16}$$

and

$$\eta_k(t) = \left(\frac{\partial J}{\partial \theta_k}\right) T(t) + \left(\frac{\partial G}{\partial \theta_k}\right) U(t) \tag{17}$$

where all the derivatives are evaluated for $\vec{\theta} = \vec{\theta}_o$.

3. NOMINAL AND SENSITIVITY MODELS REDUCTION

The resolution of the problem of sensitivity involves the time integration of $1 + m$ state-variable (Eq. 13), the nominal model and the sensitivity models, which include as many ordinary differential equations than there are capacitive nodes in the discretisation mesh. Consequently, their size increases with the complexity and the dimension of the system geometry, as well as with the accuracy we are looking for. Sensitivity analysis could then be computationally intensive and limited by computer performance. In order to handle such kind of problems, an approximation based on model size reduction techniques is here proposed.

The objective of model size reduction techniques is to replace the state model (13) by a low-dimension one without introducing a significant loss of precision. A satisfactory representation of the full-dimension model behaviour is then get with a limited number of calculations. Model reduction has been the subject of many investigations and a great number of reduction techniques have been proposed in the past. A rather complete state of the art is brought in [5]. The most efficient methods are the so-called truncation methods. They consist in representing the state variables of the problem as a linear combination of the eigenfunctions of a particular basis (e.g. modal basis [6, 7, 8], balanced realisation [9] and singular basis [10, 11]). If the projection basis allows highlighting a small number

of significant directions, the solution can then be approached using a reduced number of eigenelements. A reduced r-order model is get by the following procedure:

– Separation of the pseudo-steady and dynamic terms of the state variables: $\mathsf{Z}(t) = \mathsf{Z}_g(t) + \mathsf{Z}_d(t)$. The pseudo-steady term represents the state variables behaviour when the thermal capacity of the system is assumed to be zero. It follows that: $\mathsf{Z}_g(t) = -A^{-1}\psi_k(t)$. So, the dynamic term and the outputs verify:

$$\begin{aligned} \dot{\mathsf{Z}}_d(t) &= C^{-1}A\mathsf{Z}_d(t) + A^{-1}\dot{\psi}_k(t) \\ \mathsf{Y}(t) &= J\mathsf{Z}_d(t) + (\eta_k(t) - JA^{-1}\psi_k(t)) \end{aligned} \tag{19}$$

Using the formulation (19) instead of equations (13) presents some clear advantages for model reduction purposes. Practice indicates that to yield accurate results for small values of r it is often necessary starting reduction from (19). Otherwise, the convergence rate with r will be much lower (cf. [5]).

– Calculation of a pertinent equivalent full-order model. Let P be a non-singular matrix of dimension $[n \times n]$ containing, column wise placed, the vectors p_1, p_2, ⋯, p_n of a given basis. Let us consider the transformation $\mathsf{Z}_d(t) = PX(t)$, where $X(t)$ is the vector $[n \times 1]$ of the decomposition coefficients of $\mathsf{Z}_d(t)$ on the chosen basis. From equation (13), it follows the equivalent state model:

$$\begin{aligned} \dot{X}(t) &= FX(t) + B\dot{\psi}_k(t) \\ \mathsf{Y}(t) &= OX(t) + (\eta_k(t) - JA^{-1}\psi_k(t)) \end{aligned} \tag{20}$$

with $F = P^{-1}C^{-1}AP$ (state matrix), $B = P^{-1}A^{-1}$ (command matrix) and $O = JP$ (output matrix).

– Full-order model truncation. Assuming vectors p_1, p_2, ⋯, p_n have been ordered in a convenient way, a reduced-order model of dimension r is then obtained as

$$\begin{aligned} \dot{\widetilde{X}}(t) &= \widetilde{F}\widetilde{X}(t) + \widetilde{B}\dot{\psi}_k(t) \\ \widetilde{\mathsf{Y}}(t) &= \widetilde{O}\widetilde{X}(t) + (\eta_k(t) - JA^{-1}\psi_k(t)) \end{aligned} \tag{21}$$

where the state matrix $\widetilde{F}$ $[r \times r]$ is formed by the r first columns and rows of F, the command matrix $\widetilde{B}$ $[r \times n]$ includes the r first rows of B, and the output matrix $\widetilde{O}$ $[q \times r]$ is formed by the r first columns of O.

It should be noticed that obtaining the whole set of reduced models is not more expensive in time than obtaining only one them, the matrices $\widetilde{F}$, $\widetilde{B}$ and $\widetilde{O}$ being the same ones for all the models of the set.

Practice indicated that the selection of the transformation matrix P has a significant influence on the quality of the resulting low-dimension model, the balanced realisation [9] being one of the best choices. It is based on the central notions of controllability and observability. Assuming eigenvalues of matrix $C^{-1}A$ to be strictly in the left half-plane, then we can define the controllability gramian and the observability gramian of (19) as:

$$W_c \equiv \int_0^\infty e^{(C^{-1}A)t}(A^{-1})(A^{-1})^T e^{(C^{-1}A)^T t}dt \qquad \text{and} \qquad W_o \equiv \int_0^\infty e^{(C^{-1}A)^T t} J^T J e^{(C^{-1}A)t}dt$$

respectively. By considering the corresponding matrix differential equations it is easily verified that W_c and W_o satisfy the following Lyapunov equations [12]:

$$\begin{aligned}(C^{-1}A)W_c + W_c(C^{-1}A)^T + (A^{-1})(A^{-1})^T &= 0\\ (C^{-1}A)^T W_o + W_o(C^{-1}A) + J^T J &= 0\end{aligned} \tag{22}$$

Both W_c and W_o are definite positive matrices of dimension $[n \times n]$. It is easily demonstrated that they depend on the state-space co-ordinates. If it is changed to $Z_d(t) = PX(t)$ for some non-singular P, the controllability and observability gramians become:

$$W_{c(x)} = P^{-1}W_c(P^{-1})^T \qquad \text{and} \qquad W_{o(x)} = P^T W_c P \tag{23}$$

A balanced realisation is obtained for a matrix P which verifies the following equation:

$$W_{c(x)} = W_{o(x)} = \Sigma \tag{24}$$

where $\Sigma = diag\left[\lambda_1 \quad \lambda_2 \quad \cdots \quad \lambda_n\right]$ is a diagonal matrix containing the Hankel singular values, which are fundamental invariants of the system. Such transformation may be obtained in different ways [9, 13, 14]. The method proposed by Laub [14] is one of the most efficient ones. The matrix W_c is first decomposed as (Cholesky factorisation method):

$$W_c = RR^T \qquad (R = \text{low triangular matrix}) \tag{25}$$

The product $R^T W_o R$ is then a definite positive matrix. It can be transformed in a diagonal matrix by solving the following symmetric eigenvalues problem:

$$R^T W_o R = U\Sigma^2 U^T \qquad \text{with} \qquad UU^T = I \tag{26}$$

The matrix P we are looking for is given by (see [14] for demonstrations):

$$P = RU\Sigma^{-1/2} \tag{27}$$

The components of $X(t)$ (the state vector of the balanced realisation) are arranged so as the elements of the matrix Σ appear in the decreasing order $\lambda_1 \geq \lambda_2 \geq \cdots \geq \lambda_n > 0$. The balanced realisation is then truncated keeping the more controllable and observable state variables; those associated to the greatest r Hankel singular values. The controllability/observability gramian Σ brings a way for measuring both the sensitivity of the state variables to the forcing signals and the sensitivity of the model outputs to the state variables. Hence, elimination of the state variables showing a weak degree of controllability/observability should be a good way for model size reduction.

It has been proved in [15] that the L_∞-norm of the error introduced by truncation of the balanced realisation can be bounded by « twice the sum of the tail » of the Hankel singular values spectrum:

$$\left\| G(j\omega) - G_r(j\omega) \right\|_{L_\infty} \leq 2\left(\lambda_{r+1} + \lambda_{r+2} + \cdots + \lambda_n\right) \tag{28}$$

where $G(j\omega)$ and $G_r(j\omega)$ are, respectively, the transfer functions matrix of the full-order and the r-order models. This error bound gives strong theoretical support to the observation that truncated balanced realisations so as $\lambda_{r+1} >> \lambda_r$ give very good results in practice.

4. STEP BY STEP SOLVING PROCEDURE

The proposed procedure for solving large-scale sensitivity problems is briefly summarised here.

Step 1. Spatial discretisation of equation (1): calculate the matrices C, A and J.

Step 2. Calculation of the balanced realisation:
- Calculate the gramians W_c and W_o by solving the Lyapunov equations (22).
- Calculate of the transformation matrix P using the procedure described by equations (25) to (27).
- Calculate of the matrices $F = P^{-1}C^{-1}AP$, $B = P^{-1}A^{-1}$ and $O = JP$.

Step 3. Truncation of the balanced realisation:
- Choose the reduction order r so as $\lambda_{r+1} >> \lambda_r$.
- Calculate the low-dimension matrices $\widetilde{F}$, $\widetilde{B}$ and $\widetilde{O}$.

Step 4. Time integration of the low-dimension nominal model:

$$\dot{\widetilde{X}}(t) = \widetilde{F}\widetilde{X}(t) + \widetilde{B}\dot{\psi}_o(t)$$
$$\widetilde{\Upsilon}(t) = \widetilde{O}\widetilde{X}(t) + (\eta_o(t) - JA^{-1}\psi_o(t))$$

with $\psi_0(t) = EU(t)$ and $\eta_0(t) = GU(t)$. Estimate $T(t)$ and its time derivative:

$$\widetilde{T}(t) = \widetilde{P}\widetilde{X}(t) - A^{-1}\psi_o(t)$$

where $\widetilde{P}$ is formed by the first r columns of P.

Step 5. Time integration of the low-dimension sensitivity models ($k = 1, \cdots, m$):

$$\dot{\widetilde{X}}(t) = \widetilde{F}\widetilde{X}(t) + \widetilde{B}\dot{\psi}_k(t)$$
$$\widetilde{\Upsilon}(t) = \widetilde{O}\widetilde{X}(t) + (\eta_k(t) - JA^{-1}\psi_k(t))$$

where $\psi_k(t)$ and $\eta_k(t)$ are given by equations (16) and (17) respectively.

5. EXAMPLE

Thermal building analysis usually leads to large-scale models including a large number of parameters. Hence, the sensitivity of the thermal behaviour of a simple building to the thermophisical and optical properties of its components, as well as to the parameters defining its geometry, has been chosen to illustrate the advantages of the proposed computational method.

ETNA is an EDF's experimental building that has been specifically designed for empirical model validation purposes (see Fig. 1). It is formed by two identical and symmetrical testing rooms (41.3 m3). Only one of them is here considered (test cell in the following). Its southern facade is in contact with the outdoor environment, while the other ones (west, north, east, floor and ceiling) are

surrounded with thermal guards at controlled ambient temperature. One can refer to [16] for a detailed description of the test cell (geometry, walls compositions, materials properties, etc.).

A test cell model of the form (13) was generated using the building simulation environment M2m [17]. The main physical phenomena considered are: heat conduction in walls, heat convective exchanges at the wall-air interfaces, long wave radiative exchanges among building surfaces, short-wave radiative exchanges with the environment (solar radiation effects), and air infiltration. The model is formed by 421 linear ordinary differential equations. It includes 8 inputs variables (the outdoor air temperature, the air temperature in the guards zones, the solar flux density on the south facade, and the heating power which is supplied to the indoor air by means of a 100% convective heater) and 421 output variables (the temperatures at the nodes of the discretisation grid). The total number of model parameters is 207, among which one finds the surface of the different walls and windows, the thickness of the layers of the walls, the thermophysical properties of the materials (conductivity and heat capacity), the optical properties of the different surfaces, the walls-air heat convective coefficients, etc.

The hourly data from the experiment carried out from the 25/02/95 to 19/03/95 (23 days) are here used for simulation purposes. Figure 2 includes the time evolution of the outdoor air temperature, as well as the air temperature in the thermal guards (controlled at 10°C). Figure 3 represents the solar flux density on the south facade. The heating power was provided by an electric source whose operation was controlled by a pseudo-random binary sequence (see Fig. 4). Furthermore, Figure 5 shows the time evolution of the test cell indoor air temperature (simulations from the nominal model).

Results achieved for one of the model outputs are here presented. The reduced sensitivity of the indoor air temperature to the variations of the parameter θ_k is defined by:

$$\sigma_k^*(t) = \frac{\partial y(t)}{(1/\theta_k)\partial\theta_k}$$

The units are identical to those of the output variable (°C). When the goal of the analysis is to establish a hierarchy among the parameters of the model according to their influence on the output, the comparisons in term of reduced sensitivity are more interesting than those in terms of sensitivity. One notes $\widetilde{\sigma}_k^*(t)$ the reduced sensitivity estimated starting from a 6-order reduced model.

The average values and the standard deviations of the reduced sensitivities make it possible to analyse the influence of the parameter on the static and dynamic behaviour of the cell test respectively. One notes m_k and $\widetilde{m}_k$ the average values of $\sigma_k^*(t)$ and $\widetilde{\sigma}_k^*(t)$, respectively. Similarly, s_k and $\widetilde{s}_k$ represent the standard deviations of $\sigma_k^*(t)$ and $\widetilde{\sigma}_k^*(t)$. The relative errors:

$$\frac{m_k - \widetilde{m}_k}{m_k} \qquad \text{and} \qquad \frac{s_k - \widetilde{s}_k}{s_k}$$

can be used as a first measure of the quality of the proposed approach.

Figure 6 represents the relative errors on the average values versus the corresponding average values m_k ($k = 1,\cdots,207$), and Figure 7 includes the relative errors on the standard deviations versus the standard deviations s_k ($k = 1,\cdots,207$). In both cases, the most significant errors are associated to the least influential parameters. The maximum relative error on the average is lower than 0.06%; it corresponds to a parameter with a weak influence on the static behaviour of the cell test. Similarly, the maximum relative error on the standard deviation (1.2%) is associated to a parameter showing a negligible effect on the dynamic behaviour.

The results in figures 8 and 9 are representative of the most unfavourable conditions (worst results). That is, they are associated to a not very significant parameter ($m_k = 0.01°C$ and $s_k = 0.035°C$). The relative errors on the average and on the standard deviation are -0.0147% and 1.16% respectively. Figure 8 represents the time evolution of the reduced sensitivity, while Figure 9 shows the time evolution of the differences observed between the reduced sensitivity calculated

starting from the full-order model and that which is obtained with the 6-order balanced realisation. It can be seen that errors due to the model size reduction are less than $\pm 2 \times 10^{-3} \circ C$.

Figures 10 and 11 are representative of the best results achieved. The relative errors on the average and the standard deviation are -0.001% and 0.0001% respectively. The error due to the replacement of the complete model by the reduced model is lower than $\pm 3 \times 10^{-6} \circ C$.

Results of intermediate quality are provided in figures 12 and 13. The relative errors on the average and the standard deviation are 0.013% and 0.41% respectively. The differences between the simulations coming from the full-order model and those from the 6-order one are lower than $\pm 3 \times 10^{-4} \circ C$.

Whatever may be the parameter, the errors introduced by the truncation of the balanced realisation remain negligible. The problem which consists in integrating 207 state models including each one 421 of ordinary differential equations (ode) can then be replaced by the integration of 207 low-dimension models (6 ode by model) without introducing a significant loss of precision. This implies a strong reduction (98% approximately) of the calculating time required.

6. CONCLUSIONS AND PERSPECTIVES

An efficient numerical method for solving large-scale differential sensitivity problems has been proposed. The sensitivity-equation method is first applied to generate the whole set of sensitivity models (one state-variable model per parameter). A sensitivity model, as well as its balanced realisation, is characterised by three matrices of the same dimension than those in the original model: the state matrix, the command matrix and the output matrix. However, these matrices remain unchanged regardless of the parameter under consideration. Consequently, a single calculation suffices to obtain the balanced realisation of all the sensitivity models. Such representation allows ranking the state variable according to their degree of controllability and observability. A low-dimension balanced realisation is then obtained by keeping the more controllable and observable state variables. The sensitivity problem is finally solved by time integration of as many low-dimension sensitivity models than there are parameters instead of the corresponding full-order models.

The interest of the method increases significantly with the dimension of the nominal model and with the number of parameters. An example has been used to illustrate its effectiveness. The nominal model includes 421 ordinary differential equations and 207 physical parameters. So, the sensitivity problem involves 87147 differential equations (207 systems of 421 ordinary differential equations). It is however shown that a 6-order balanced realisation (207 systems of 6 ode) provides very high quality results. This implies a reduction of the calculating time from approximately 98%.

The paper addresses to linear models. However, the method should be extended to non-linear systems for sensitivity models remain linear and they share the same state, command and observation matrices. In contrast to the linear case, the coefficients of such matrices vary with time and special reduction techniques, as those proposed in [18], will then be required.

REFERENCES

[1] N. Rahni, Validation de modèles et variabilité des paramètres: Analyse de sensibilité et d'incertitude - Procédures d'optimisation. Application à des modèles thermiques du bâtiment, Ph.D. thesis, Université Paris 12, Paris, 1998.

[2] D.G. Cacuci, Sensitivity theory for non-linear systems. I Nonlinear functional analysis approach. J Math. Phys., vol. 22, pp. 2794-2802, 1981.

[3] K. el Khoury and A. Neveu, Analyse modale des systèmes thermiques en présence de transferts non-réciproques, Int. J. Heat and Mass Transfer, vol. 32, pp. 213-226, 1989.

[4] K. el Khoury, Formulation modale de problèmes thermiques de diffusion avec transport, Ph.D. thesis, École des Mines de Paris, Paris, 1989.

[5] E. Palomo, Résolution de problèmes thermiques de grande dimension. Méthodes de réduction, Ph.D. thesis, Université Paris 12, Paris, 2000.

[6] S.A. Marshall, An approximate method for reducing the order of a linear system, Control, vol. 10, pp. 642-643, 1966.

[7] G. Michailesco, J.M. Siret and P. Bertrand, R.A.I.R.O. Automatique/Systems Analysis and Control, vol. 13, pp. 159-170, 1979.

[8] A. Oulefky and A. Neveu, Réduction par amalgame modal d'un modèle thermique, J. Phys. III France, vol. 3, pp. 303-320, 1993.

[9] B.C. Moore, Principal components analysis in linear systems: controllability, Observability, and model reduction, IEEE Trans. of Automatic Control, AC-26 (1), pp. 17-32, 1981.

[10] A. Ait-Yahia and E. Palomo, Thermal systems modelling via singular value decomposition: direct and modular approach, Applied Mathematical Modelling, vol. 23, pp. 447-468, 1999.

[11] A. Ait-Yahia and E. Palomo, Numerical simplification method for state-space models of thermal systems, Numerical Heat Transfer Part B - Fundamentals, vol. 37, pp. 201-225, 2000.

[12] L. Arnold, Stochastic differential equations: Theory and applications, John Wiley & Sons, New York (1971).

[13] C.T. Mullis and R.A. Roberts, Synthesis of minimum Round off noise fixed point digital filters, IEEE Trans. Circ. & Sys., CAS-23, pp. 551-562, 1976.

[14] A.J. Laub, Computation of balancing transformation. Proc. 1980 Joint Automatic Control Conference, San Francisco, California, FA8-E, 1980.

[15] K. Glover, All optimal hankel-norm approximations of linear multivariable systems and their L_∞-error bounds, Int. J. Control, vol. 39, pp. 1115-1193, 1984.

[16] P. Girault and S. Delilles, Description of ETNA cells. Physical and geometrical configuration, Electricté de France Rept., Moret-sur-Loing, Ile de France, 1995.

[17] G. Lefèbvre, Modal-based simulation of the thermal behavior of a building: the M2m software, Energy and Building, vol. 25, pp. 19-30, 1997.

[18] S. Shokoohi, L.Mr. Silverman and P.Mr. van Dooren, Linear time-varying systems: balancing and model reduction, Trans IEEE. Automatic Control, Ac-28, pp. 810-822, 1983.

FIG. 1. ETNA building.

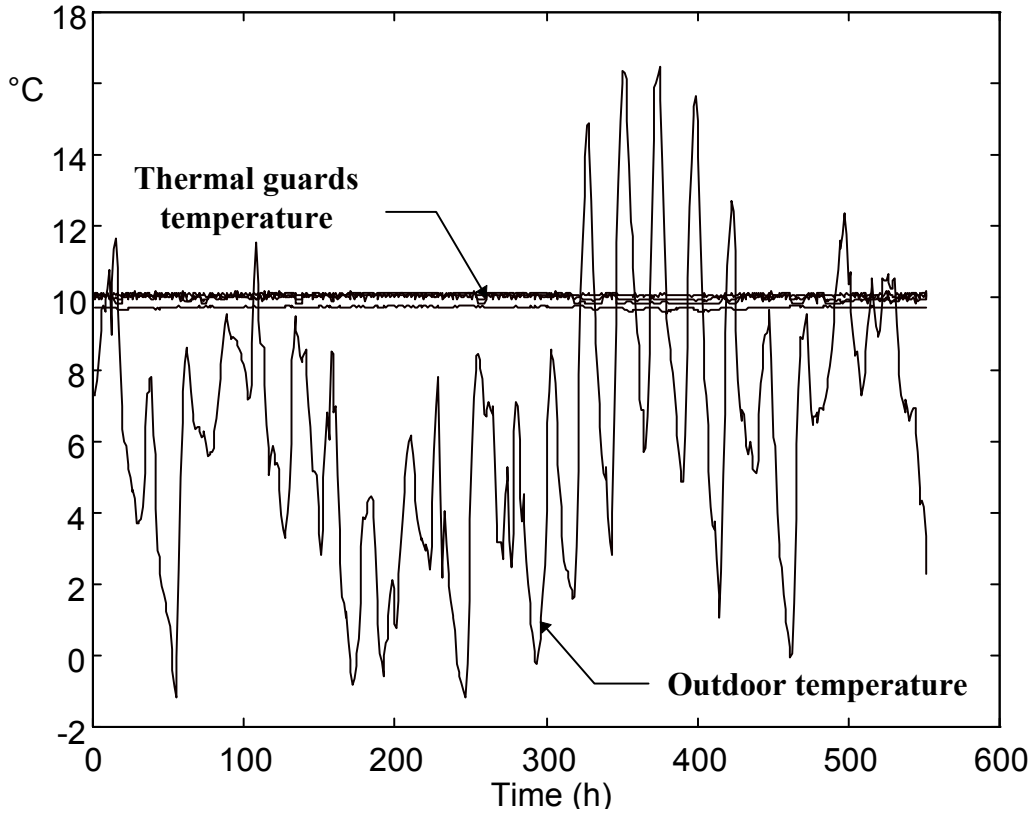

FIG.2. Time evolution of the outdoor air temperature and time evolution of the air temperature in the thermal guards.

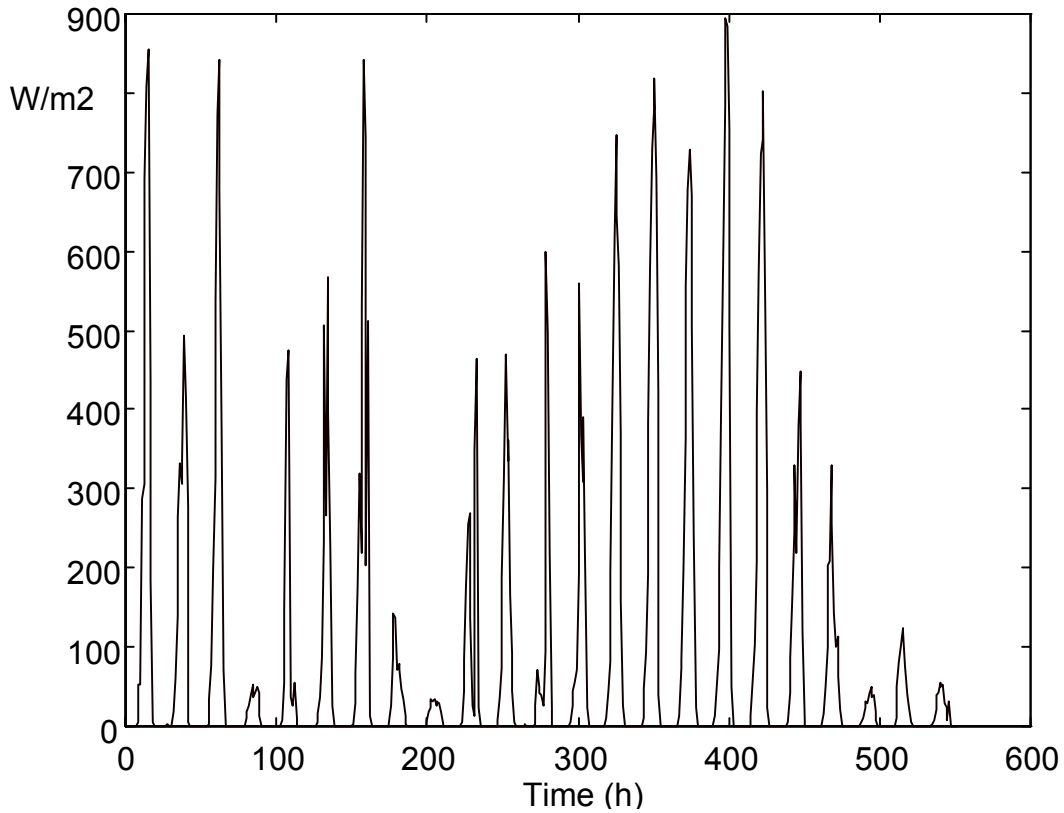

FIG. 3. Solar flux density on the south vertical facade.

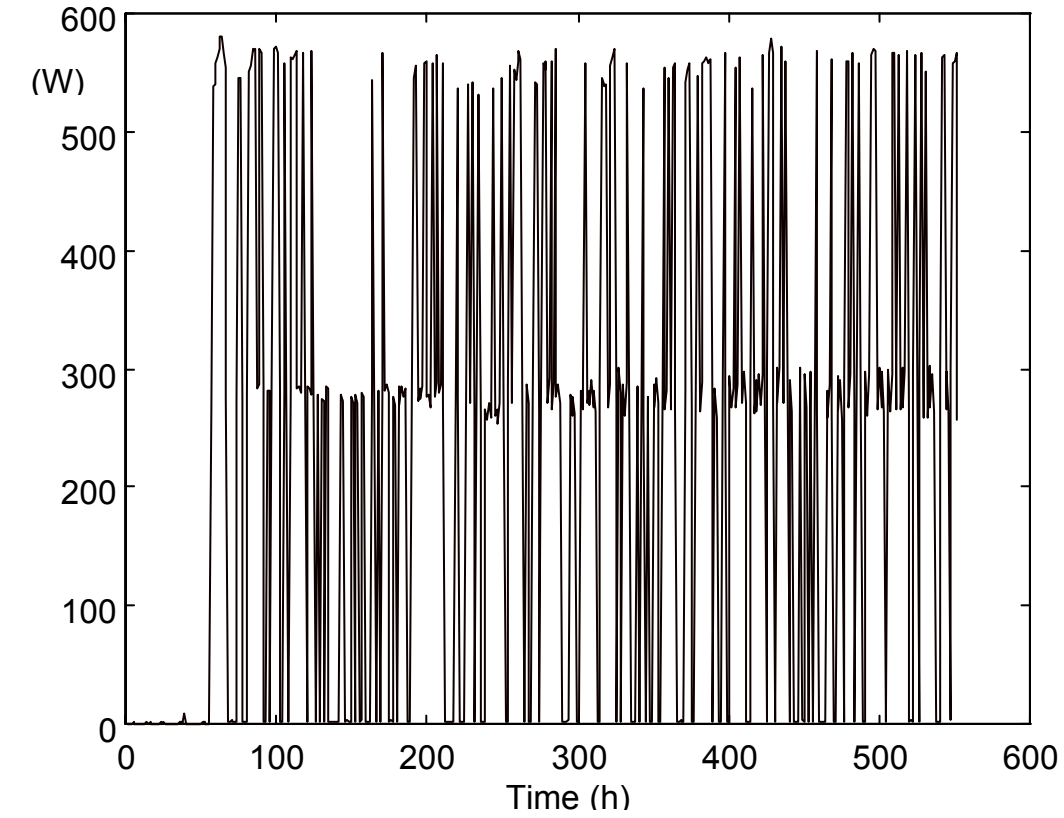

FIG. 4. Heat power supplied to the test cell.

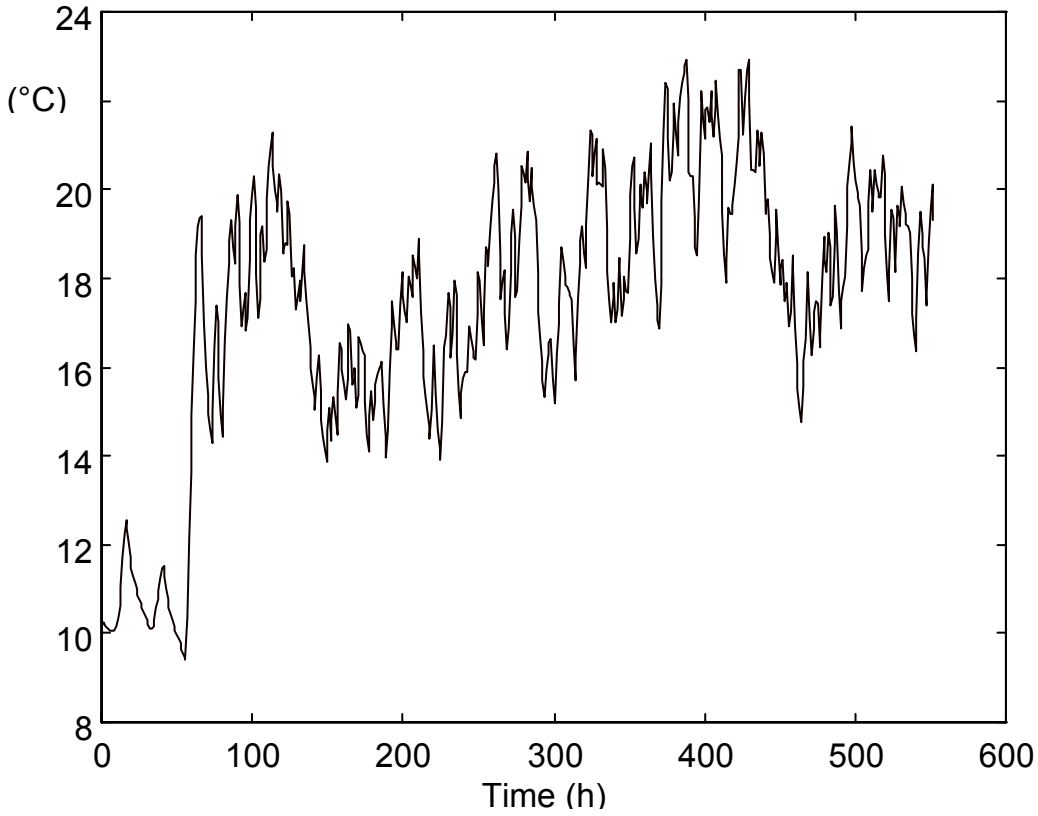

FIG. 5. Time evolution of the indoor air temperature (simulations from the nominal model.

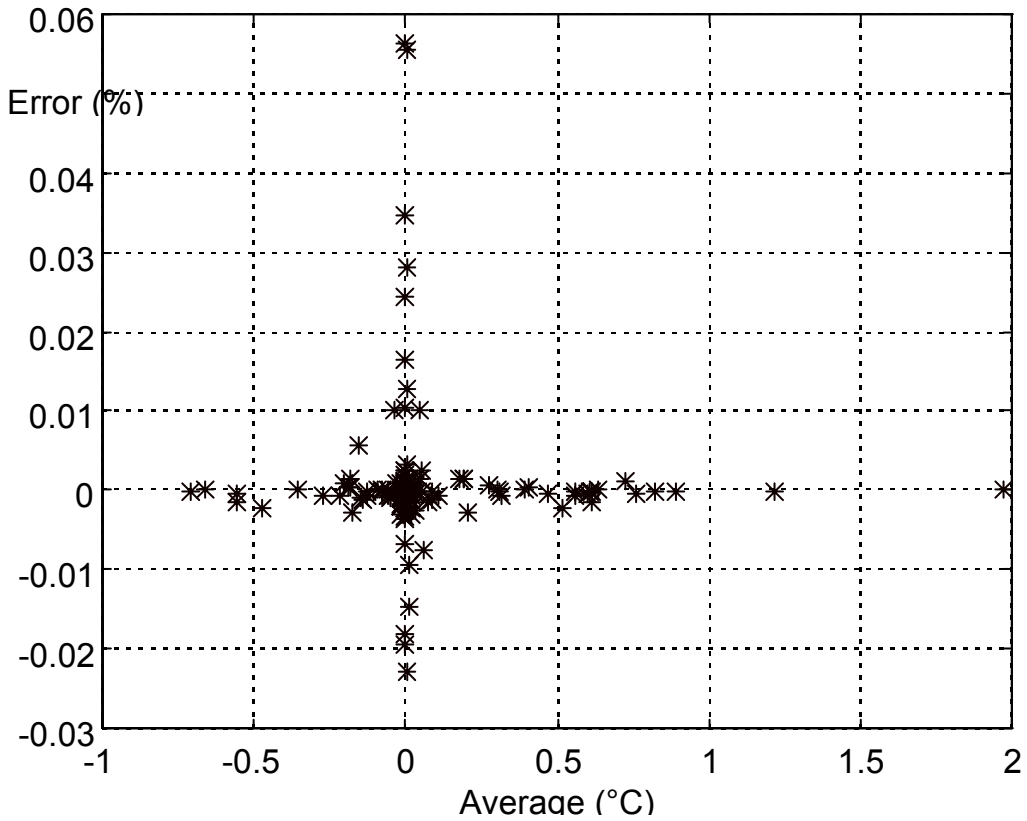

FIG. 6. Relative errors (%) on the sensitivity average value.

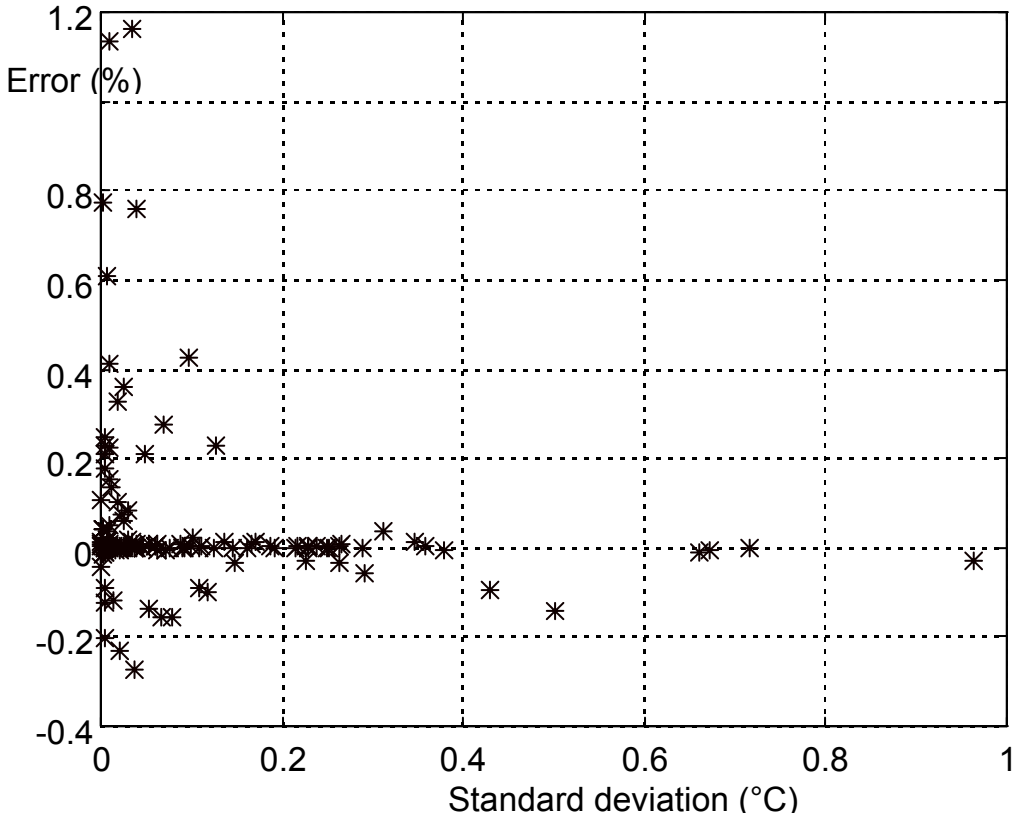

FIG. 7. Relative errors (%) on the sensitivity standard deviation.

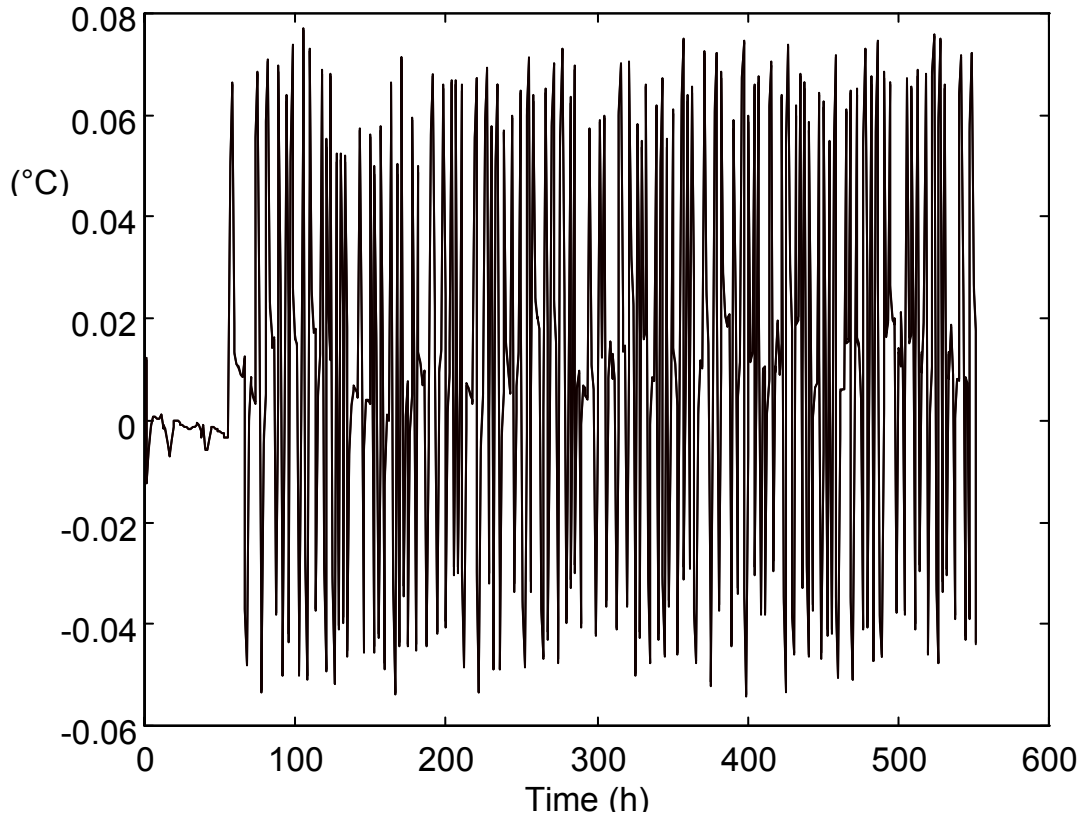

FIG. 8. Time evolution of the reduced sensitivity (worst case).

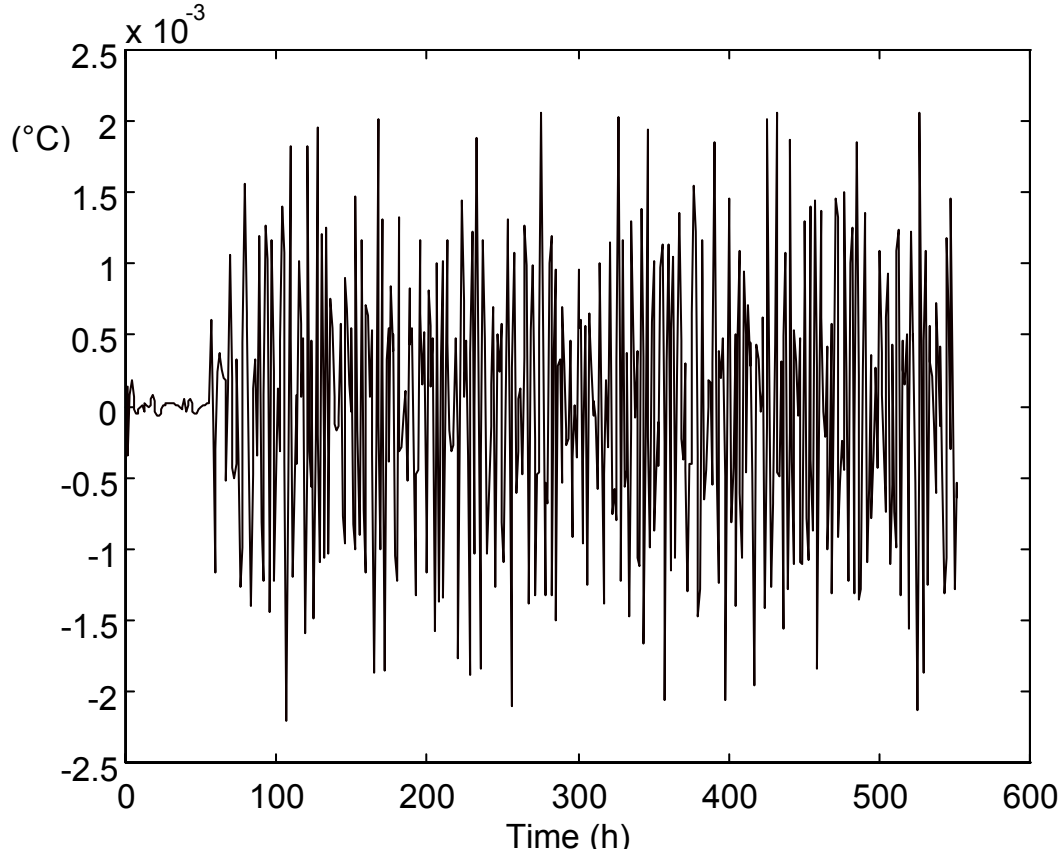

FIG. 9. Differences between the sensitivity calculated from the full-dimension model and that which is obtained with the 6-order balanced realisation (worst case).

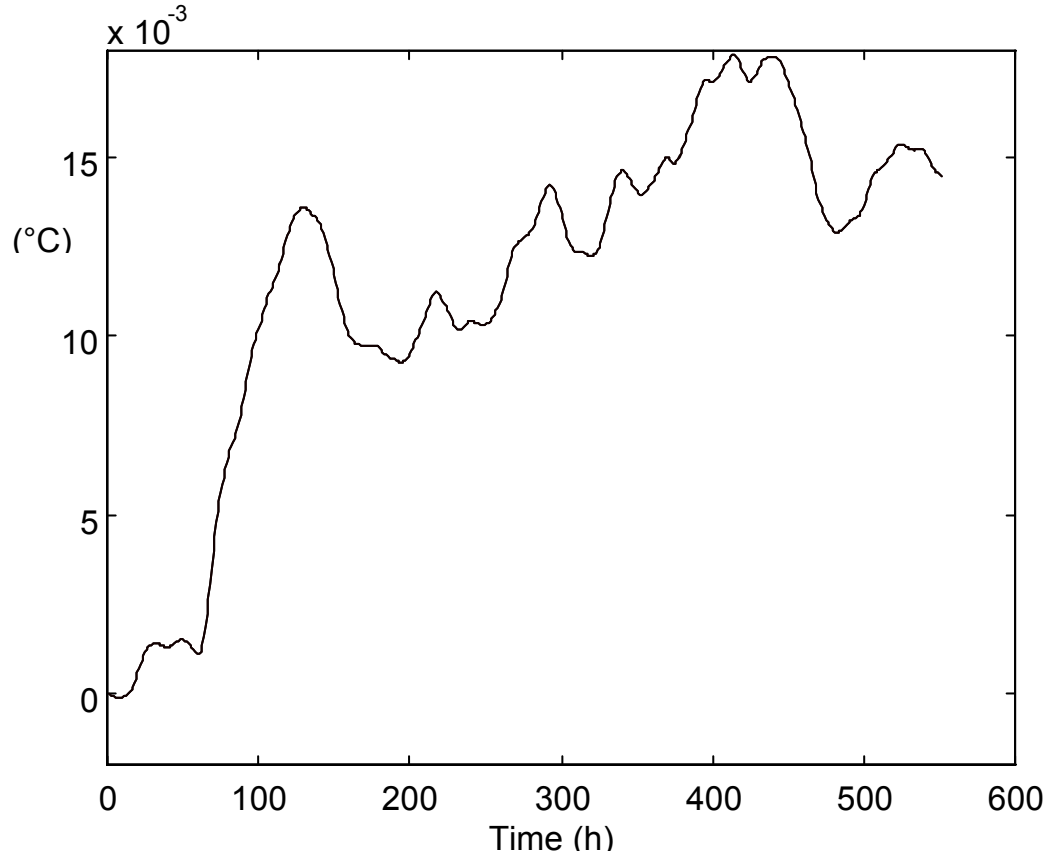

FIG. 10. Time evolution of the reduced sensitivity (best case).

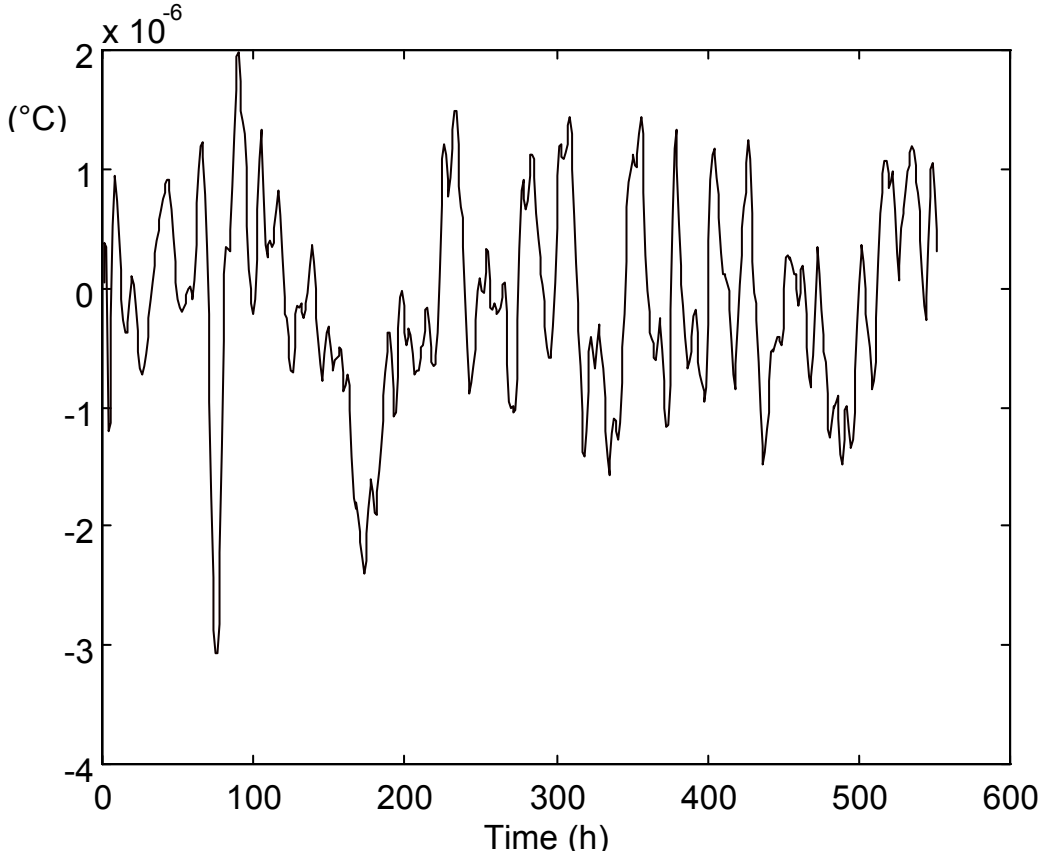

FIG. 11. Differences between the sensitivity calculated from the full-dimension model and that which is obtained with the 6-order balanced realisation (best case).

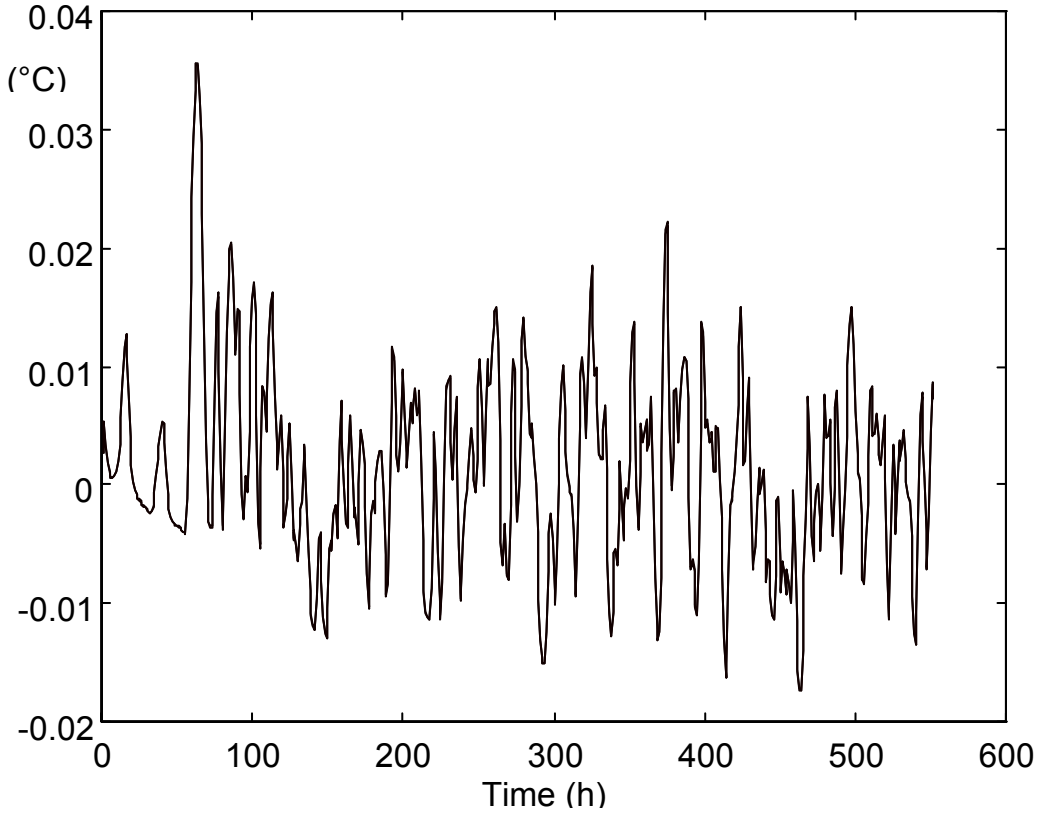

FIG. 12. Time evolution of the reduced sensitivity (intermediate case).

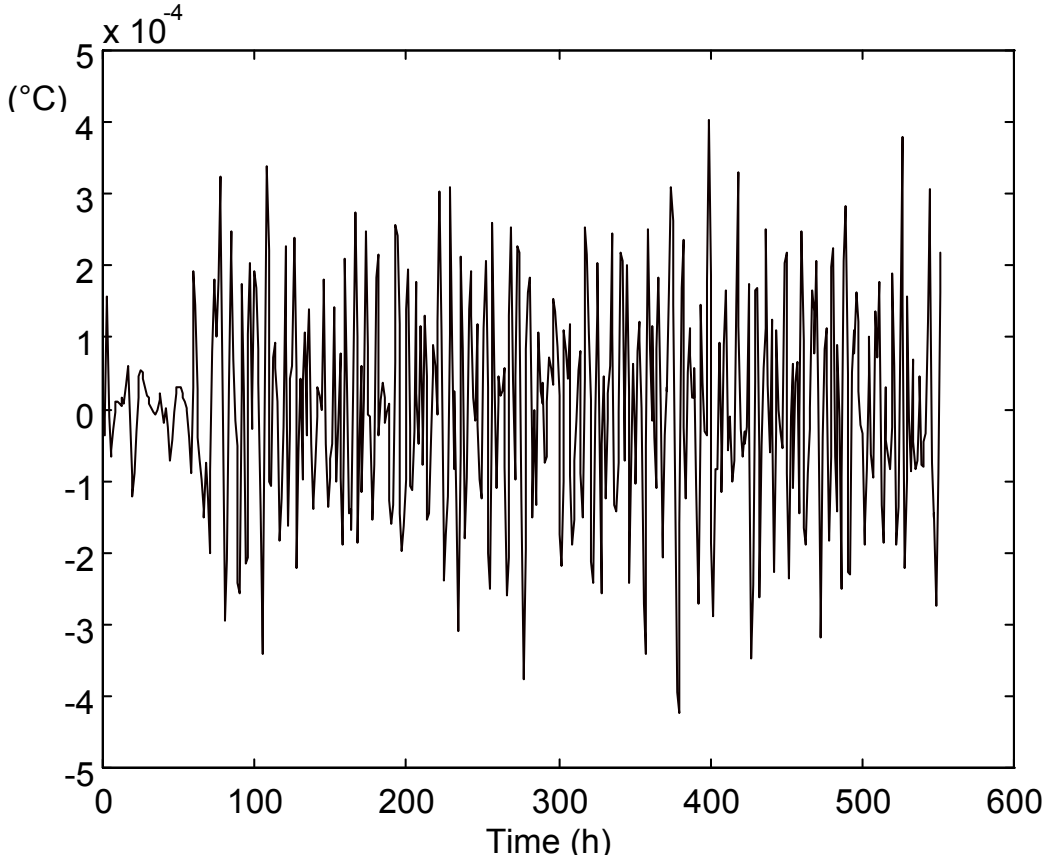

FIG. 13. Differences between the sensitivity calculated from the full-dimension model and that which is obtained with the 6-order balanced realisation (intermediate case).

Annex B

Validation of two French building energy programs: Part 2 – Parameters estimation method applied to empirical validation

Gilles GUYON
Electricité de France – Direction des Etudes et Recherches
Les Renardières BP 1, 77250 Moret-sur-Loing FRANCE
e-mail: gilles.guyon@edf.fr

Elena PALOMO DEL BARRIO
LEPT-ENSAM UMR 8508
Esplanade des Arts et Métiers, 33405 Talence Cedex FRANCE
e-mail: palomo@lept-ensam.u-bordeaux.fr

(Published in "ASHRAE, Vol. 105, SE-99-6-3, 1999")

Validation of Two French Building Energy Programs Part 2: Parameter Estimation Method Applied to Empirical Validation

Gilles Guyon, Ph.D. **Elena Palomo, Ph.D.**

ABSTRACT

Two French building energy programs were developed by the French utility company. The first one is intended to produce economic studies and be used as a research tool. The second one is more dedicated to engineering offices as a tool adapted to their constraints in thermal studies. To give confidence to the end-users and to ensure the quality of the software programs results, a validation procedure has been in place for many years. In Part 1, we presented the use of analytical tests with the first software. In this part, we focus on the empirical validation work proposed by the French team in the framework of a project led by an international organization dealing with energy savings. A new approximation based on parameter estimation methods has been proposed for purposes of modeling error diagnosis. It has been tested in providing a diagnosis to discrepancies between simulations and measurements in an actual building and has proved to be very efficient.

INTRODUCTION

A building energy software program (EDF/DER 1998) was developed by the French utility company and has been operational since June 1989. It allows the behavior of an entire building to be simulated. Its main objective is to produce economic studies, pertaining to energy balances over long periods, as well as more detailed physical behavior studies including nonlinear problems and varied dynamics. It can also be used for evaluating the efficiency of a new component, such as a heating system, ventilation system, or a new insulator, glazing, etc., because it is very easy to implement a new elementary model into it, reproducing numerically the physical behavior of the new component to be evaluated. This kind of software is one of the best means in terms of cost and time to evaluate a new building component.

The second software program (EDF/DER 1997), also developed by the French utility company, is dedicated to HVAC system comparisons. It is based on a building simulation program widely used in the USA (Klein and Beckman 1996), and a specific model library has been developed to simulate HVAC systems and allow easy comparisons between them. This software seems to be an answer to the problems of engineering offices, enabling analysis and accurate predictions of energy consumption in buildings within a relatively short time scale. This software also offers a three-step approach corresponding to the different levels of knowledge in a project—sketch, basic, and advanced.

It is necessary to show the end-users that these software programs are able to give good predictions. To do this, we have tried to develop a specific validation procedure. The aim of this validation work is to give confidence in the results produced by the code. In addition to that, it is obvious that, without any validation work, the simulated results will not be taken into account with great confidence by decision makers in a discussion more political than technical. This work was started at the beginning of the 1990s. In the Part 1 of this paper, we described the validation procedure used for the French software programs, with a conceptual idea of the validation and a presentation of the strengths and weaknesses of each stage in this procedure. The reader is invited to look at this part in order to see in which step of the validation procedure the empirical validation is included. We also presented the use of analytical verification tests with the first software and a comparison between analytical solution and simulated results.

Gilles Guyon is a research engineer in the Research and Development Division, Electricité de France, Moret/Loing, France. **Elena Palomo** is a researcher at l'Ecole Nationale des Ponts et Chaussées, Marne-la-Vallée, France.

Part 2 of this paper deals with empirical model validation matters. Empirical validation should, in principle, compare a true model derived from experiments with a computerized model. It is not, as is analytical validation, limited to isolated processes in simple constructions, but deals with real-world complexity comparable to situations encountered when the simulation code is used in design studies. Empirical validation is, therefore, the most widely used technique for validating transient simulation programs. Beyond any technical consideration, it provides a guarantee of user confidence and enables the modeler to improve his/her understanding of the system being modeled and to improve the model itself. The aim of empirical validation is twofold: First, one needs to detect if the model is able to describe correctly the observed reality, that is, to check whether the model satisfies some a priori validation criteria (checking model validity); and, second, the causes of the observed differences between measured and predicted values must be identified in order to improve the model if required (diagnosis). In this paper, attention is focused on methods of diagnosing modeling errors. It includes a brief presentation of the state of the art, a description of the methodology we are proposing, and an example of application based on the experiment carried out in the test cells owned by the French utility company that has developed both software programs (Girault and Delille 1995).

STATE OF THE ART

Two significant techniques using linear analysis tools have been proposed in the past for diagnosis of modeling errors in building thermal analysis.

The first one consists of a direct comparison of the system's global physical parameters (first time constant and static gains) estimated from measurements with the ones calculated by means of the analyzed model. To obtain such information from experimental data, identification techniques can be applied. A dynamic linear model, in state space form (Jensen 1993) or in a black-box form (Candau and Piar 1993), is identified on data and then reduced to its characteristic time constant and its static gains. To get such information from the knowledge model, the use of spectral decomposition techniques has been proposed in Candau and Piar (1993) and a different technique based on simulations in Jensen (1993).

The second technique deals with residuals (differences observed between measurements and simulations) analysis and was first proposed in Palomo et al. (1991). Because model simulation aims at reproducing the effect of the external influences that drive the experiment, one expects a part of the residuals to be sensitive to these inputs. Hence, the proposed technique seeks to quantify the contribution of each system input to the residuals. Such information helps modelers to sort the inputs and to target the one responsible for the major part of the error. Efforts to improve the model should then focus on the way the model takes into account this particular input.

The technique proposed in Palomo et al. (1991) and Jensen (1993) is based on nonparametric spectral analysis of residuals. The contribution of each input to the residuals is analyzed by means of the squared partial coherence functions. The squared partial coherence for the *i*th input is a normalized measure at frequency ω of the linear cross-correlation existing between residuals and input *i* after allowance is made for the effect of the other input variables. It takes values from 0 to 1. Zero values mean that no correlation exists between the *i*th input and the residuals, unity values mean that residuals could be completely recovered from this input, and values between 0 and 1 correspond to situations where residuals can be partially predicted from the *i*th input. Such information helps modelers to sort the inputs and to target the one responsible for the major part of the error over a given frequency area. This is the method reviewed and accepted in Ramdani (1994) and Ramdani et al. (1997), where spectra and partial coherence functions are simultaneously used to quantify the contribution of each model input to the residuals variance.

The technique proposed in Martin and Watson (1993) is slightly different, although it also deals with residuals analysis. A dynamical linear and stationary multiple inputs, single output (MISO) model is identified on the residuals/input data. Such a model is intended to predict the residuals time evolution, and it is then used to estimate the contribution of each model input to the total variance of the residuals. This error desegregation technique, dealing with the total residuals variance, does not allow separation of time scales (frequency ranges), and it does not provide as much information as the previous ones.

Residuals analysis techniques have been widely used in the 1990s, especially in the framework of a British-French collaboration between the French utility company that has developed the two software programs and a well-know British research center in the field of buildings. Although they appear capable of diagnosing some of the modeling errors (Tabary and Ramdani 1995), the authors believe them to suffer some limitations. The most important ones are:

1. They are based on linear analysis tool, and, consequently, they cannot be applied to diagnosis of errors in nonlinear models.

2. They are mainly based on analysis of the causal relationships between residuals and model inputs (black-box approximation). They give information about input-output relationships in the models but not about their structures. This is the reason why no clear indications of how to improve models are given often by means of residuals analysis techniques.

These limitations lead us to propose another kind of approximation to the model diagnosis problem, which is mainly based on parameter estimation techniques and is described and discussed in the next section.

MODELING ERRORS DIAGNOSIS VIA MODEL PARAMETERS SPACE ANALYSIS

The parameters are the closest elements to the model structure and to the underlying modeling hypothesis in a computerized model. The methodology we are proposing for diagnosis of modeling errors is then mainly based on analysis of the model parameter space. Its aim is to identify the amplitude of variation in parameters allowing residuals observed reduction. The comparisons of such results with the knowledge we have about the actual system and about the modeling hypothesis will help us to know the reasons for inadequate model behavior and to propose model improvements. The methodology involves three main steps:

1. *Parameter screening and grouping.* First, it allows one to identify the parts of the model that could really be tested with the available experiments (the ones related to the active model parameters) and, hence, to reduce the possible causes of discrepancies between measurements and simulations. Second, it allows parameter grouping for further estimation purposes.
2. *Parameter estimations.* This allows one to identify parameter vectors consistent with the model structure and data. Two different approaches are briefly presented and discussed. The first one involves standard Monte Carlo methods for searching the parameter vector that minimizes a certain objective function of the error. The second one looks for all the parameter vectors consistent with the observed error-bounded data, that is, leading to model outputs included in the measurements uncertainty bands.
3. *Diagnosis.* The possible causes of discrepancies between measurements and simulations are elucidated here. The comparison between the parameter values from step 2 with their nominal values should lead to known reasons for the observed modeling errors and to suggested model improvements.

Contrary to residuals analysis techniques, the approximation to modeling errors diagnosis based on parameter estimations can be applied to both linear and nonlinear models. In addition, it can supply very useful information concerning model structure faults. Methods and tools for each one of these task are briefly presented here.

Some Definitions and Notation

Thermal models for buildings can be usually described by finite-dimensional models of the general form

$$\dot{X}(t) = F(X(t), U(t), \theta)$$
$$\tilde{y}(t, \theta) = G(X(t), U(t), \theta)$$

where $X(t)$ is an n-dimensional vector containing the so-called state variable, $\tilde{y}(t,\theta)$ is a q-dimensional vector including the observation variables or outputs (for simplicity, we will assume that $q = 1$ in the following), and $U(t)$ is the inputs or excitations vector. θ is the p-dimensional vector of model parameters (geometric, optical, and thermophysical properties, convective coefficients, etc.), and F and G are two matrices of time-dependent nonlinear functions. A particular model thus corresponds to specification of functions in matrices F and G, as well as the parameters vector θ.

A keyword in empirical model validation is uncertainty. Uncertainty involves measured data, model parameters, or even the model structure:

- *Measurement uncertainty*: Data are always associated with some uncertainty, if only because of the finite precision of the sensors used to collect them. The approach most commonly used to characterize such uncertainty consists in assuming that data are corrupted by additive random noise, whose probability density function is known. While very popular, this approach is not immune to criticism. The probability density function assumed for the noise is not always based upon any sound prior information, and one does not necessarily have enough data to test it. Moreover, there are situations where the main contribution to error is not of a random nature and, therefore, not suitably described by random noise.

  An attractive alternative to the stochastic characterization of errors is characterization by upper and lower bounds only. Measured bounded-error data at time t are thus represented by the intervals $[y(t)] \equiv [y_{min}(t), y_{max}(t)]$.

  Most sensor manufacturers provide rules for computing the maximum and minimum possible measurement errors at any given range of operation, allowing $y_{min}(t)$ and $y_{max}(t)$ to be computed. Structural errors may, however, lead one to choose more pessimistic bounds than those obtained by this method. These bounds can then be viewed as the extreme values of the error between system and model outputs that are considered acceptable by the experimenter.
- *Model parameter uncertainty*: The uncertainty in model parameters is generally not of a random nature. It can reflect an imperfect knowledge of the system geometry or even composition; the lack of measured data for parameters; the uncertainty due to the finite precision of the sensors and methods used for measuring system properties; the uncertainty associated with the system exploitation, which is generally related to unpredictable behavior of the future users (Guyon 1997); and the imperfect knowledge we have about the physical processes taking place in the system.

  Hence, as for data before, model parameter uncertainties will be characterized by upper and lower bounds. Let $\theta = \{\theta_i,\ i = 1, ..., p\}$ be the p-dimensional vector of model parameters. Parameter uncertainty is thus described by the intervals: $\forall i \quad \theta_i \in [\theta_{min}, \theta_{max}]$, or, in a more compact way, by

$$\Theta = \prod_{i=1}^{p} [\theta_{i,\,min}\theta_{i,\,max}] = [\theta_{1,\,min}\theta_{1,\,max}]x\ldots x[\theta_{p,\,min}\theta_{p,\,max}]$$

which is the Cartesian product of the previous *p* intervals. (Normally, $\boldsymbol{X}$ would be used to describe the Cartesian product instead of Π.) The box Θ will be called parameters set.

When checking model validity, the intervals before generally represent parameter uncertainty due to the finite precision of the sensors and methods used to estimate them. For diagnostic purposes, they can be larger than the previous ones, as they represent the domain of variation where we are looking for suitable parameter values.

- *Model response uncertainty*: Model output uncertainty results from the uncertainties of the model parameters. The uncertainty in the model response at time *t*, associated with the parameter set Θ, can be characterized by the intervals

$$[\tilde{y}(t, \Theta)] \equiv [\tilde{y}_{min}(t, \Theta), \tilde{y}_{max}(t, \Theta)] ,$$

so that

$$\forall \theta \varepsilon \Theta, \quad \tilde{y}_{min}(t, \Theta) \leq \tilde{y}(t, \Theta) \leq \tilde{y}_{max}(t, \Theta)$$

A parameter vector θ is said to be consistent with the bounded-error data if it leads to model outputs included in the measurement uncertainty intervals:

$$\forall t, \quad y_{min}(t) \leq \tilde{y}(t, \theta) \leq y_{max}(t)$$

Similarly, a parameter set Θ is said to be consistent with bounded-error data if $\forall \theta \in \Theta$ the equation before is verified.

The Prior Parameter Set

The first step in the modeling error diagnosis methodology concerns the selection of the prior parameter set,

$$\Theta_o = \prod_{i=1}^{p} [\theta_{i,min} \quad \theta_{i,max}]$$

where $[\theta_{i,min}\ \theta_{i,max}]$ represents the allowed interval of variation for the parameter in the model. (Normally, $\boldsymbol{X}$ would be used to describe the Cartesian product instead of Π.)The prior parameter set definition involves grouping model parameters, selecting active model parameters, quantifying active parameter uncertainty, and testing the consistency of the resulting parameter set with the observed bounded-error data.

Grouping Model Parameters According to Identifiability Criteria. Two parameters showing no separable effects on the model outputs (parameters strongly correlated) are not identifiable separately and will thus be grouped in a unique parameter. Correlations between parameters depend both on the model structure (the way the parameters are involved in the model) and on the model input behavior. While it is not easy to anticipate correlations induced by the model inputs, correlations bound up with the way the parameters appear in the model are usually foreseeable. The easiest cases are those where two or more parameters are always grouped under arithmetic operations (i.e, products, additions, etc.) in the model equations.

Selecting Active Model Parameters. The objective of screening techniques is to identify model parameters to which the model predictions are really sensitive (active parameters). All the parameters in the model can potentially affect the model behavior, but generally only a small number of them are truly important or active. The reason is that not all the parts of the system are equally excited by the inputs and not all the physical processes taking place have a comparable effect on the quantities to be observed. The so-called active model parameters are those related to the dominant parts and processes in the model. It must, however, be noticed that such dominances are strongly influenced by the nature of the model inputs and the selected model outputs.

The interest of screening is twofold: it allows us to identify the part of the model that could be really validated with the available experiment and, hence, to reduce the field of possible causes of discrepancies between measurements and simulations and it allows to reduce the number of free model parameters for further identification purposes.

Commonly used screening techniques are:

a) Differential analysis based on calculation of the partial derivatives of the model outputs with respect to each parameter.

b) One-at-a-time design, which is an extension of the differential analysis method. It is based on changing a single parameter at a time, running the model, and observing the output variation.

c) Two-level experimental designs and regression analysis. Contrary to one-at-a-time design, this approach involves simultaneous variations of parameters, each of them taking two possible levels. It allows assessment of parameter effects by using a regression model or metamodel (Rahni 1998).

d) Group screening techniques (Walter and Piet-Lahanier 1990a, 1990b; Rahni 1998) that have been proposed for screening problems involving a large number of parameters, which generally act in a sequential way. First, they combine individual parameters into groups and experiment with these groups as individual parameters. Then, all parameters in the nonsignificant groups are eliminated and new groups are formed with the remaining parameters. The procedure continues until remaining parameters are few enough that we can analyze them in an individual way.

Quantifying Active Model Parameter Uncertainty. Zero-length intervals are assigned to nonactive model parameters; they are frozen to their assumed most likely values. On the contrary, intervals $[\theta_{i,min}\ \theta_{i,max}]$ for active parameters must be wide enough so that an inadequate modeling hypothesis could be identified (it is expected that values for parameters related to a phenomenon that is erroneously represented in the model change significantly when fitting the model to the data). For diagnostic purposes, the intervals describing parameter uncertainty define the domain where we are looking for parameter values allowing reduction of model residuals. For instance, we assume that convective and radiative exchanges

at the surface of a vertical wall can be represented by the Newton law with a unique and constant coefficient of exchange, h ($W \cdot m^{-2} \cdot K^{-1}$). Hence, reasonable values for h belong to [9, 10]. If, on the contrary, a joint representation of both kinds of phenomena is inadequate, parameter h, now representing convective fluxes only, will take very different values (3-4 $W \cdot m^{-2} \cdot K^{-1}$). To be able to test such a modeling hypothesis, a [3, 10] interval for h is required.

Preliminary Consistency Analysis. Parameter set consistency analysis involves two main tasks: estimating model output uncertainties associated with the parameter set under analysis (they are a measure of the influence of parameter uncertainty on model outputs) and testing consistency by comparisons between model output uncertainties and bounded-error data. If most of the time measurement uncertainty bands lie between the estimated upper and lower bounds for model outputs, the parameter set Θ_o hopeful includes parameter vectors, leading to good enough model behavior. No changes are a priori required, and parameter estimations can be carried out.

The most commonly used techniques for model output uncertainty calculations are differential sensitivity analysis and Monte Carlo methods. See Lomas and Eppel (1992) and Palomo (1994) for an analysis of their corresponding advantages and drawbacks. New techniques allowing a strong reduction of the required computation time have been recently proposed (Palomo and Guyon 1998).

Parameter Estimations

The main tool that we are proposing to guide modeling error diagnosis is based on parameter estimation techniques. If something in the model is clearly wrong, one would expect to find large parameter displacements when fitting the model on the measured data. The comparison between the estimated parameter values and their nominal values should lead to known reasons for the observed modeling errors and to suggest model improvements.

Problem Statement. The estimation problem can be stated in two different ways depending on the assumptions adopted concerning measured data.

- *First statement*. It assumes errorless data. Let

$$e(t, \theta) = y(t) - \tilde{y}(t, \theta)$$

be the residuals associated to the parameter vector $\theta \in \Theta$, and let

$$V^2(\theta) = \sum_{t=1}^{N} e^2(t, \theta)$$

be a quadratic measure of it. We are looking for the parameter $\theta^x \in \Theta$ that minimize the objective function $V(\theta)$. Solving such a problem means finding the global minimum, if it exists, of a generally complicated non-convex real-valued function.

- *Second statement*. Contrary to the previous one, it takes into account data uncertainty. The problem is no longer stated as "looking for $\theta^x \in \Theta$ that minimizes an objective function measuring the simulation error." Instead, we are looking for all $\theta \in \Theta$ providing simulation inside the uncertainty intervals of the measurements. In other words, we are looking for all $\theta \in \Theta$ so that

$$\forall t \quad \tilde{y}(t, \theta) \in [y_{min}(t) \;\; y_{max}(t)] .$$

Parameter Estimation Methods. Historically, methods to solve global optimization problems have been classified as either stochastic or deterministic. Stochastic methods evaluate the objective function at randomly sampled points from the parameter region of allowed variation. Deterministic methods, on the other hand, involve no elements of randomness.

All global optimization algorithms can also be partitioned into two classes—reliable and unreliable. Clearly, all stochastic methods, including simulated annealing, clustering, and random search, fall into the unreliable category. In fairness, however, efficiency is the strength of such methods. For now, large-scale problems may best be solved stochastically.

The class of deterministic algorithms, including branch and bound methods, covering methods, interval methods, tunneling, and enumerating, can be further partitioned into two categories—methods that compute objective function values at sampled points (point methods) and methods that compute function bounds over compact sets (bounding methods). This division further separates reliable from unreliable methods. Point methods are inherently incapable of reliably solving the global optimization problem. On the other hand, bounding methods, if properly implemented, can produce rigorous global optimization solutions.

Two different kinds of global optimization methods (GOM) have been implemented and tested in the framework of a project led by an international organization dealing with energy savings and model validation tools:

- *First GOM*. Two random search algorithms, a pure random one and a multistart algorithm, are used in association with the first statement of the minimization problem.

The pure random algorithm evaluates the objective function $V(\theta)$ at n randomly sampled points $\theta \in \Theta : V_1, V_2, ..., V_n$. The solution we are looking for is then estimated as θ^* so that $V(\theta)^* = \min(V_1, V_2, ..., V_n)$.

The multistart random search algorithm is a natural extension of the previous one. A number n of starting points belonging to Θ are selected at random, $\{\theta^{0i}\}_{i=1...n}$, and a random search algorithm for local optimization is applied from each one of these points. The set of all terminating points (local extrema, $\{\theta^{*i}\}_{i=1...n}$) hopeful includes the global minimum θ^*, which is estimated as $\theta^* = \arg \min(V(\theta^{*1}), V(\theta^{*2}), ..., V(\theta^{*n}))$.

As we said before, although unreliable, such methods are especially efficient for large-scale optimization problems.

- *Second GOM*. A reliable bounding method was developed in association with the second statement of the

optimization problem. A survey of techniques for estimating parameters from error-bound data can be found in Walter and Piet-Lahanier 1990a). Recently, new techniques, also allowing nonconnected parameters, are proposed in Walter and Piet-Lahanier (1990b), Moore (1992), and Jaulin and Walter (1993). The algorithm we have developed takes inspiration from the ones proposed in Moore (1992) and Jaulin and Walter (1993). It allows exploration of disconnected subsets in Θ in a systematic way. It proceeds by deleting parts of the initial parameter set Θ, which cannot contain feasible parameter vectors, leaving a list of subsets whose union still contains the set of all feasible parameters. Such a list of subsets in the algorithm is technically a *queue*. At iteration *k*, the algorithm performs as follows:

1. Unlist the first box $\Theta^{(k)}$ in the queue and bisect it in the coordinate direction of maximum with $\Theta^{(k)} = \Theta_1^{(k)} \cup \Theta_2^{(k)}$.
2. Test $\Theta_1^{(k)}$ consistency; if consistent, save it as making part of the global solution; if inconsistent, delete it; otherwise list $\Theta_1^{(k)}$ at the end of the queue.
3. Test $\Theta_2^{(k)}$ consistency; if consistent, save it as making part of the global solution; if inconsistent, delete it; otherwise list $\Theta_2^{(k)}$ at the end of the queue.

As a result, the widest box remaining in the queue is always the first one. If it is narrower than the prescribed tolerance, then so are all the rest and the iteration loop is terminated. We note Θ^* the parameter subset including solutions.

We remember that consistency analysis of parameter sets (subsets), Θ, involves (a) calculation of the upper and lower bounds for the model outputs, $[\tilde{y}(t, \Theta)]$, and (b) comparison with bounded-error data, $[y(t, \Theta)]$. The parameter set Θ is consistent with data when $\forall t \quad [\tilde{y}(t, \Theta) \subset y(t, \Theta)]$; it is inconsistent if $\exists t$ so that $[\tilde{y}(t, \Theta)] \cap y(t, \Theta)] = \varnothing$; otherwise, it is said to be ambiguous.

The methods allowing model output bounds estimations without code modifications that are commonly used (Monte Carlo methods and differential sensitivity analysis techniques) make the parameter estimation method unusable due to the computing time required. Special techniques, such as the one proposed in Palomo and Guyon (1998), that take inspiration from interval arithmetic are thus required.

Advantages and Drawbacks. The main advantages of the second GOM method are related to both the nature of the data and the nature of the models.

1. The method takes into account data uncertainty, as well as their nonrandom nature. Stating the problem as *looking for* $\theta^x \in \Theta$ *that minimizes an objective function* implies the assumption of uncorrupted data.
2. It allows nonconnected parameter set identification. Dynamic thermal models are based on differential equations whose outputs are nonlinear in their parameters, even if the model itself is linear. One of the major consequences of this nonlinearity is that Θ^* may no longer be connected. This may result from the fact that the model is not uniquely identifiable but may also be due to other factors not so easily detected (Palomo and Guyon 1998). This is especially important when the parameters to be estimated have a physical meaning or when decisions have to taken on the basis of their numerical values, as it is the case for diagnostic purposes.

Others advantages are:

3. No additional work is required for estimating the uncertainty regions for the identified parameters; they come naturally from the procedure itself.
4. The solution proposed by the algorithm always includes the optimal parameter vector (reliable method). On the contrary, when using Monte Carlo methods, we are never sure of getting it. The quality of the proposed solution from Monte Carlo methods is measured in terms of probability.

Concerning stochastic methods, their main advantage is efficiency. For now, large-scale (in parameters) problems may best be solved stochastically.

Diagnostic

The last step in the methodology is diagnosis. It is based on the following.

- *A certain knowledge about the model*. Which phenomena are represented in the model and what parameters are involved in their representation is the main information required.
- *Modeling hypothesis formalization and analysis*. It involves a strictly structured way of stating modeling hypotheses, as well as some analysis concerning the consequences in terms of model parameters that inadequate hypotheses provoke. This means to determine foreseeable model parameter sets for each one of the hypotheses in the model, as well as for their corresponding negative statement. As, unfortunately, no rigorous methods exist at present, the modeling hypothesis analysis will be founded on the expert knowledge the modeler has on both the system and the model itself. This method could be simple and economic, but it is prone to large personal biases.
- *Parameter displacement analysis*.This involves comparisons between estimated and nominal model parameter values. Large differences are expected for parameters involved in phenomena that are not correctly represented in the model.

The combination of these elements of judgment should lead one to know reasons for the observed modeling errors and to suggest model improvements.

EXAMPLE OF APPLICATION

The methodology presented in the previous section is here applied to diagnose modeling errors in an actual building. The experimental device is shortly described in first subsec-

tion. The second subsection includes the test cell model description, with special attention on the modeling hypothesis. Results from a blind model validation are briefly discussed in the third subsection. The next subsections are focused on model parameter estimations and diagnosis.

Description of Empirical Validation Experiment

An experiment (Girault and Delille 1995) has been carried out in test cells (see Figure 1) to measure the difference between a realistic convector, located under a window, without stirring of the internal air, and a purely convective heat source in the center of the room, with stirring of air (when the source is on). The experiment was in a natural climate, i.e., the south wall was exposed to solar radiation and the others surfaces were connected to guard zones. In the REFERENCE cell, there was a purely convective heater, which is close to the modeling used in most software programs. In the MEASURE cell, a classical electrical convector commonly used in France is located under the south window. The aim is to compare the effect of energy distribution on the air temperature in the center of the room for the realistic convector and the academic source with stirring. The experiment began on February 25, 1995 and finished on March 19, 1995. During this experiment, the cell configuration was as follows: guard temperatures controlled at 10°C (50°F), no air infiltration, pseudo-random heating at a nominal value of 500 W, a black screen installed behind the window in the guard zone to obtain a temperature for longwave radiation identical to the guard temperature. For the REFERENCE cell, the air inside the test cell was stirred using a fan to guarantee temperature homogenization and the heating is done by a convective heater (heating fan). For the MEASURE cell, the air inside the test cell was not stirred, and the heating is done by a classic electrical convector (the most common type of heater used in France).

The following variables were recorded: global and diffuse solar radiation, outdoor dry-bulb temperature, air temperature in the thermal guards, heating power, and indoor air and radiant temperature. All data were measured at a five-minute time step, except solar radiation, which was measured at a one-minute time step. The data were then averaged and undersampled at a one-hour time step. The analysis in this section refers to the REFERENCE cell only.

The Test Cell Thermal Model

The main hypotheses in the test cell model are classified by physical phenomena as follows:

- *Hypothesis 1, heat conduction phenomena*. **H1.1** Heat conduction is considered as one-dimensional; thermal bridges are not modeled. An equivalent homogeneous multilayer wall is used for representing the floor and the ceiling. **H1.2** Constant thermophysical properties are assumed for all the materials. **H1.3** Perfect contact between layers is assumed. **H1.4** Heat conduction through the glazing and frameworks is assumed noncapacitive.
- *Hypothesis 2, thermal infrared radiation (TIR) exchanges and heat convective exchanges at the outdoor wall-air interfaces.* **H2.1** TIR exchanges are not explicitly modeled. The convective-radiative flux at the *k*th wall surface is estimated as $\phi^{(k)} = h^{(k)}(T^{(k)}_{surface} - T_{air})$ where $h^{(k)}$ is a constant exchange parameter taking into account both radiative and convective exchanges. **H2.2** Standard values are adopted for the global exchange parameter *h*.
- *Hypothesis 3, TIRexchanges and heat convective exchanges at the indoor wall-air interfaces.* **H3.1** TIR exchanges are explicitly modeled, although linearized. All the surfaces are assumed to be gray, with emissivity values equal to 0.9. The reference temperature for linearization is 280 K. **H3.2** Convective heat exchanges at the wall-air interfaces are estimated by means of the Newton law. **H3.3** Standard values are adopted for the exchange convective parameter *h*.
- *Hypothesis 4, indoor air and heating power treatment.* **H4.1** Indoor air temperature is supposed to be homogeneous. The air is represented by a single node in the model. **H4.2** Air infiltration is assumed to be zero. **H4.3** The output from the heater is assumed 100% con-

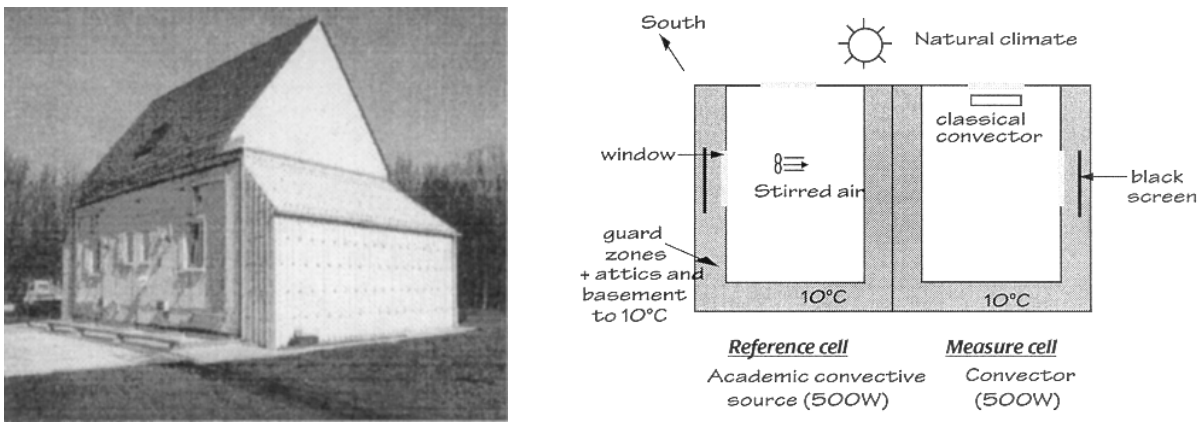

Figure 1 *Experimental sequence in test cells.*

vective. The electrical heating power is transmitted to the indoor air node. **H4.4** The heater inertia is neglected.

- *Hypothesis 5, solar radiation processor.* **H5.1** Solar irradiance on the vertical south facade of the test cell is calculated from the available horizontal global and diffuse irradiance data. Diffuse solar radiation is assumed to be isotrope, and the soil reflectivity is supposed to be 0.2. **H5.2** For transmitted solar flux through glazing calculations, no distinction is made between global and diffuse radiation. Window mask effects are, however, explicitly modeled. **H5.3** Constant optical properties for windows and walls are assumed. **H5.4** Incoming solar radiation is distributed among the wall indoor surfaces according to absorptance weighted ratios. The fraction of incoming solar radiation that is absorbed by any surface k is $\alpha_k A_k(\Sigma_j(1 - \rho_j)A_j)^{-1}$, where α_k is the solar absorptance of the surface and ρ_k its reflectance.

The model includes nine input variables and eight outputs. Input variables to the model are the outdoor air temperature, the horizontal global solar irradiance, the horizontal diffuse solar irradiance, the air temperature in the thermal guards (five inputs), and the heating power. The output variables are the indoor air temperature, the indoor mean radiant temperature, and the wall surfaces temperatures (six variables).

The model includes 110 potential free parameters. However, they can be reduced to 59 after grouping them according to identification criteria. As the objective of model parameter identification is modeling error diagnostics, it must be noticed that

1. optical parameters (17) could serve to test the hypothesis directly related to the solar radiation processor, mainly the one concerning the incoming solar radiation distribution (H4.4);
2. convective parameters (7) could be used to test the hypothesis concerning heat exchanges at the wall-air interfaces, the pertinence of using the Newton law for representing them (H3.1), and the validity of the assumed French standard values for the corresponding exchange coefficients (H2.2 and H3.3);
3. thermophysical parameters (34) can eventually be used, as well as the indoor surface areas, to test the hypothesis concerning heat conduction phenomena, mainly hypothesis H1.1;
4. finally, heating coefficients (radiative/convective ratio for the heater) could be used to test hypothesis H4.3.

Blind Model Validation

Simulations were performed using the model described above and the results were compared with measurements (Moinard et al. 1998). Residuals are defined as the difference between measurements and simulations, $e(t) = y_{measured}(t) - y_{simulated}(t)$. We will focus our attention on indoor air temperature predictions. Looking at the residuals time behavior (Figure 2, left) it can be seen that the model is not able to reproduce the static behavior of the test cell. The indoor air temperature is clearly overestimated. The mean value of the corresponding residuals is not satisfactory at all (–0.38°C). Similarly, the model shows a poor dynamic behavior, the main problems appearing at low frequencies (nonstationary behavior of the residuals). Residuals variance is 0.53°C^2.

The analysis of the residuals normalized cumulative spectrum (Figure 2, right) confirms these conclusions. It can be easily seen that most of the residuals variance is concentrated at low frequencies. The modeling error diagnostic method proposed in Palomo et al. (1991) is now applied. Because model simulation aims at reproducing the effect of the external influences that drive the experiment, one expects a part of the residuals to be sensitive to these inputs. Hence, the proposed technique seeks to quantify the contribution of each input to

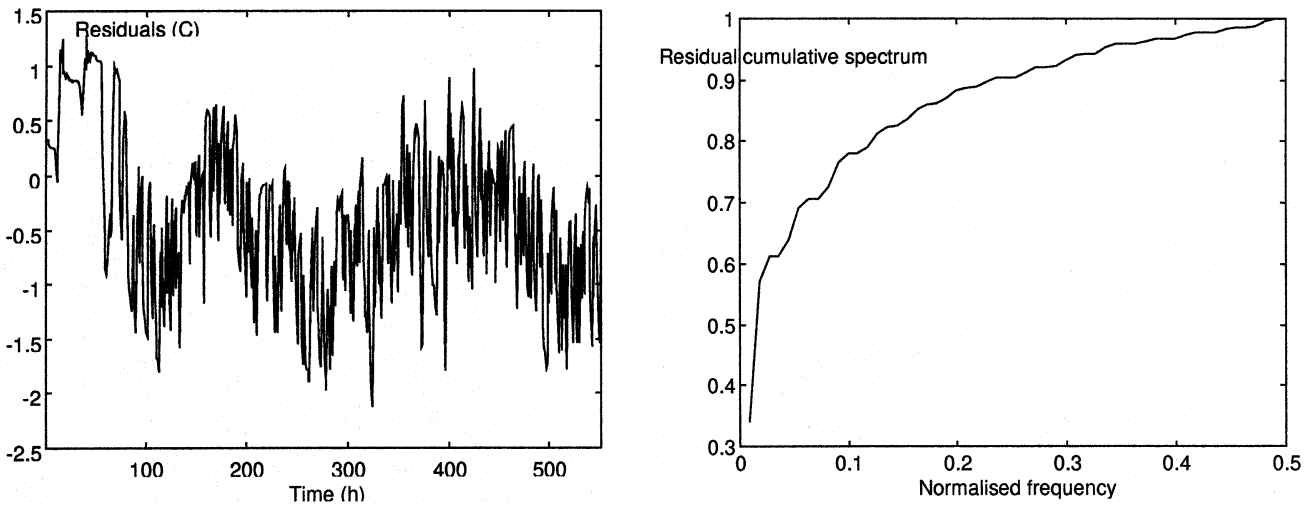

Figure 2 *Residuals from the nominal model (left) and cumulative spectrum (right).*

the residuals. Such information helps modelers to sort the inputs and to target the one responsible of the major part of the error. Efforts to improve the model should then focus on the way the model takes into account this particular input.

The contribution of each input to the residuals is analyzed by means of the squared partial coherence functions. The squared partial coherence for the *i*th input is a normalized measure at frequency of the linear cross-correlation existing between residuals and input *i* after allowance is made for the effect of the other input variables. It takes values from 0 to 1. Zero values mean that no correlation exists between the *i*th input and the residuals, unity values mean that residuals could be completely recovered from this input, and values between 0 and 1 correspond to situations where residuals can be partially predicted from the *i*th input. Figure 3 shows the estimated squared multiple and partial coherences for the indoor air temperature residuals. It can be seen that

- high values for the squared multiple coherency are obtained all over the frequency interval—this means that no strong structural modifications of the model will be required to improved it;
- the heating power is the input responsible for the major part of the error, but no conclusions on how to improve the model can be obtained from this observation because there are many possible sources of error in the model that could provoke strong correlations between the residuals and the heating power;
- some correlation is also detected with the solar radiation data—it seems clear that improving the solar radiation processor could lead to some improvement in model behavior.

Model Parameter Space Analysis

The methodology for modeling error diagnosis based on the analysis of the model parameter space is here applied

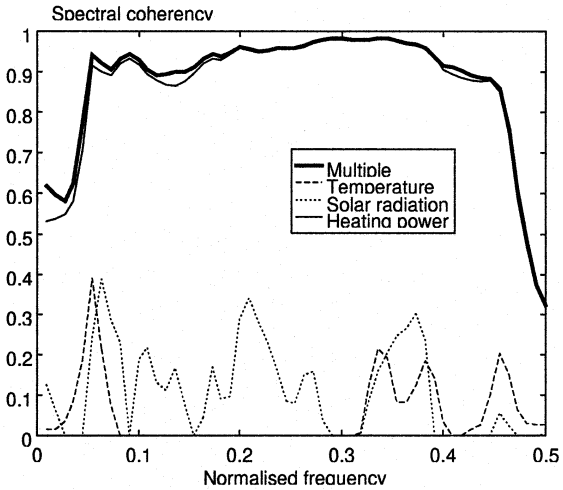

Figure 3 *Squared multiple and partial coherences. Residuals analysis of the nominal model.*

(Palomo and Guyon 1998). Its aim is to identify the amplitude of variation in parameters allowing observed reduction of residuals. The comparisons of such results with the knowledge we have about the actual system and about the modeling hypothesis will help us to know the reasons for inadequate model behavior and to propose model improvements. Parameter estimations involve selecting an acceptable prior parameter set, Θ_0; looking for parameter vectors consistent with the model structure and the data; and comparing results from the previous step with the assumed nominal values for the model parameters (diagnosis).

Prior Model Parameters Set. Two criteria have been used to select free model parameters. Free model parameters are those to which is associated a greater uncertainty (i.e., because related to critical modeling hypothesis) and the ones suggested by the previous residuals analysis (optical parameters). Resulting free model parameters are (a) the convective exchange coefficients (seven parameters), which allow one to test the pertinence of modeling hypotheses H2.2, H3.1, and H3.3; (b) the optical properties of glazing and wall surfaces (six parameters) that mainly allow one to test hypothesis H4.4; and (c) all the thermophysical properties (34 parameters). The unsatisfactory static behavior of the model could come both from the existence of unmodeled thermal bridges or from erroneous nominal values for the thermophysical parameters (it must be noted that they have not been measured but taken from the literature). Estimations of thermophysical parameters can give some elements of judgments in this respect. For instance, a clear augmentation of the conductivity and thermal capacity values could be generally interpreted as the existence of the unmodeled thermal bridges. On the other hand, an erratic modification of such parameters will lead one to conclude otherwise. The prior parameter set Θ_0 is then formed by 110 parameters; 63 of them are frozen to their nominal values, and the uncertainty associated to the remaining ones (47) is described by intervals whose length is chosen large enough so that critical modeling hypothesis can be tested. For instance, we will say that hypothesis H1 does not hold when large displacements in thermophysical parameters were required for model residual reduction.

Preliminary Consistency Analysis. The model output uncertainty due to the model parameter uncertainty described by Θ_0 has been calculated by a standard Monte Carlo procedure. It must be noted that the parameter intervals in Θ_0 do not represent parameter uncertainty due to the finite precision of the sensors and methods used to estimate them. Hence, the estimated model response uncertainty has nothing to do with the model precision. For diagnostic purposes, the intervals describing parameter uncertainty must be large enough so that critical modeling hypotheses can be tested. They define the parameter domain where we are looking for parameter values allowing model residual reduction. Consequently, it is not uncommon to get very large intervals for the model output uncertainty description. As can be seen in Figure 4 (left), most of the time measurements lie between the estimated upper and

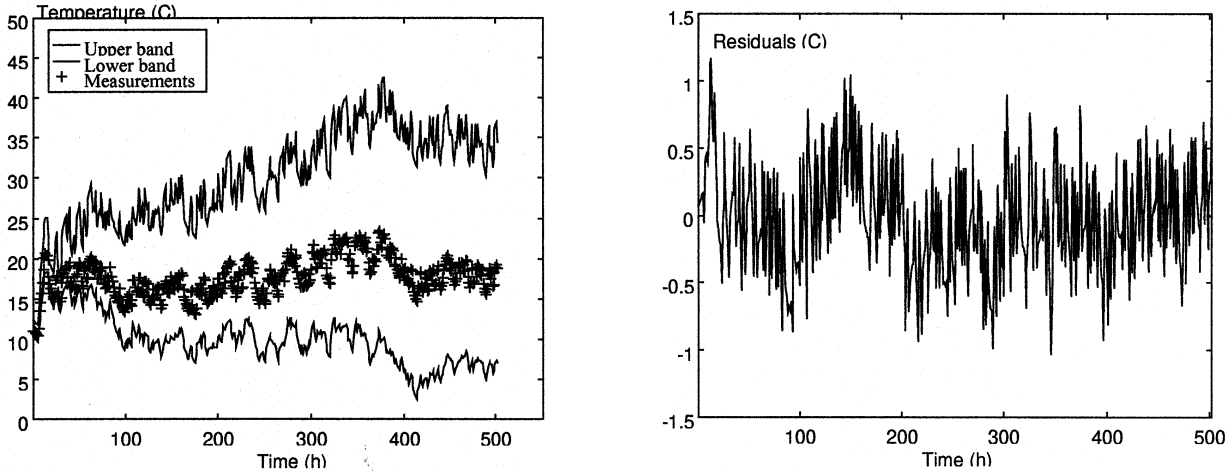

Figure 4 *Model output uncertainty bands (left) and residuals from the fitted model (right).*

lower bounds for model outputs. The parameter set Θ_o hopefully includes parameter vectors leading to good enough model behavior. No changes are a priori required.

Approximate Optimal Parameter Vector and Diagnosis. The parameter vector θ^* that minimizes the variance of the indoor air temperature residuals has been estimated by the multistart random search algorithm described in Palomo and Guyon (1998). Results are included in Tables 1 to 4. The third column in these tables is given by $(\theta_{i,o} - \theta_i^x)\theta_{i,o}^{-1}100$ %. Figure 4 (right) shows the time behavior of the indoor air temperature residuals associated with the fitted model. It can be seen that the identified model reproduces quite well the static behavior of the indoor air temperature (residuals mean value less than 0.1°C). It also shows a general dynamic behavior that is better than the one exhibit by the nominal model. Residuals variance is $0.15°C^2$ and low-frequency trends are damped out.

The main differences observed between the identified parameter vector and the nominal one are the following:

a) Indoor convective coefficients for the floor and the ceiling increase; their values are close to the ones of the indoor vertical walls. Taking into account that the air in the cell is stirred, this could be considered a reasonable result.

b) Outdoor convective coefficients for vertical walls are increasing too. Taking into account that the air in the thermal guards is removed with a fan, this result is also quite reasonable.

c) Solar absorptivity values are strongly reduced, indicating that the hypothesis concerning the incoming solar radiation distribution must probably be reviewed.

d) A clear general augmentation for conductivity values is observed, as well as for thermal capacities.

As we have noted before, such trends could be explained by the presence of unmodeled thermal bridges. Hence, clear suggestions for model improvement are to

- include thermal bridges in the model and use two-dimensional representations, if possible;
- review French standards for convective coefficients, introducing air velocity influence;
- review solar radiation processor, mainly incoming solar radiation distribution hypothesis.

Diagnosis Confirmation. The previous steps are repeated using another prior parameter set. The objective of this analysis is to get more confidence in the prior conclusions, especially with respect to thermal bridge effects. Hence, to the free model parameter set in the previous analysis, we add wall surface areas. If the effect of thermal bridges is really significant, it is expected that the wall surface area strongly increases when fitting the model on the measurements. Because they are more directly related to thermal bridges than thermophysical properties, no special trends are now expected in conductivities and heat capacity values. The resulting fitted model shows similar performance to the previous one. The estimated convective and the optical parameters show the same kind of trends as in the previous analysis. An erratic behavior is now observed in significant conductivity and thermal capacities values. However, a clear augmentation of the wall surface area appears. The nominal value for the indoor test cell area is 79.8 m^2, and the identified one is 85.8 m^2. This clearly suggests the presence of unmodeled thermal bridges. Parameter estimations have also been performed, leaving only convective and optical parameters as free model parameters. The identified values show the same displacements against nominal values as in the previous cases. However, the fitted model now shows poor static and dynamic behaviors. The major handicap of the nominal model, which concerns its unacceptable static behavior, can not be explained by errors in modeling convective exchanges or by faults in the solar processor.

TABLE 1
Convective Coefficient Values

	Results of parameter estimation method Convective coefficients values (W/m^2·K)		
	Identified	Initial value	Variation(%)
Indoor vertical	5.11	4.1	−24.6
Outdoor vertical	10.65	9.1	−17.0
Wind exposed	13.03	16.6	+21.5
Indoor floor	4.77	0.9	−430.5
Outdoor floor	6.77	5.9	−14.8
Indoor ceiling	1.16	6.1	+80.9
Outdoor ceiling	10.81	11.1	+2.6

TABLE 2
Solar Absorptivity(α) and Transmissivity (τ) Values

	Results of parameter estimation method Solar absorptivity (α) and transmittivity (τ) values		
	Identified	Initial value	Variation(%)
τ Glazing	0.77	0.675	−13.4
αGlazing	0.11	0.13	+13.2
αEast	0.322	0.9	+64.2
αNorth	0.434	0.9	+51.8
αWest	0.834	0.9	+7.4
αSouth	0.676	0.9	+24.9
αFloor	0.467	0.9	+48.1
αWest window	0.321	0.9	+64.3

TABLE 3
Thermal Capacity Values

	Results of parameter estimation method Thermal capacity values (J/kg·K)		
	Identified	Initial value	Variation(%)
Wallpaper	1033.8	938.0	−10.2
Plasterboard	557.8	680.0	+17.9
Polyestyrene	20.91	18.0	−16.1
Air layer	1.51	1.30	−16.2
Hollow blocks	1304.4	1140.0	−14.4
Concrete	1828.3	1957.0	+6.6
Styrodur	49.39	42.0	−17.6
Polyamide	1242.8	1200.0	−3.5
Floor eq. layer	1833.1	1695.1	−8.1
Honeycomb	30.59	34.90	+12.3
Facing	1610.6	1657.5	+2.8
Glass wool	9.82	8.80	−11.5
Planks	551.47	600.0	+8.1
Particleboards	879.56	840.0	−4.7
Air layer in ceiling	1.04	1.24	+15.9
Hollow door	297.83	275.0	−8.3

TABLE 4
Thermal Conductivities

	Results of parameter estimation method Thermal conductivities (W/m·K)		
	Identified	Initial value	Variation(%)
Wallpaper	0.168	0.14	−19.7
Plasterboard	0.382	0.35	−9.2
Polyestyrene	0.0387	0.043	+9.9
Air layer	0.0673	0.071	+5.1
Hollow blocks	1.051	1.052	+0.1
Concrete	1.52	1.39	−9.7
Styrodur	0.0333	0.029	−14.7
Polyamide	0.278	0.3	+7.2
Floor eq. layer	0.0402	0.0467	+14.0
Honeycomb	0.326	0.287	−13.6
Facing	1.207	1.15	−5.0
Glass wool	0.0445	0.042	−5.9
Planks	0.168	0.15	−12.1
Particleboards	0.196	0.17	−15.3
Air layer in ceiling	0.913	0.846	−8.0
Hollow door	0.106	0.09	-17.8

CONCLUSIONS

Residuals analysis shows that the major handicaps of the proposed test cell model are unacceptable static model behavior (temperatures are systematically overestimated) and poor dynamic behavior at low frequencies, the most important ones in building thermal analysis. It identifies heating power as the model input responsible for the major part of the observed differences between measurements and simulations. However, no conclusions on how to improve the model can be obtained from this observation because there are many possible sources of error in the model that could provoke strong correlations between the residuals and the heating power.

On the other hand, analysis of the model parameter space allows a better understanding of the possible causes for the residuals observed. It shows that the main differences observed between measurements and simulations can be explained by unmodeled thermal bridges, the adopted French standard for convective coefficients, and the modeling hypothesis concerning incoming solar radiation distribution. Parameter estimation techniques seems to be a useful and powerful tool for diagnosis.

ACKNOWLEDGMENTS

The authors would like to thank everyone who made this work possible, especially Mr. P. Dalicieux, who started this validation work at the French utility company, and Mr. P. Girault (EDF/DER), who carried out experiments in ETNA test cells.

REFERENCES

Candau, Y., and G. Piar. 1993. An application of spectral decomposition to model validation in building thermal analysis. *Int. J. of Heat and Mass Transfer*, (3) 645-650.

EDF/DER. 1998. *Catalogue des types formels de CLIM2000*, v 2.4, EDF.

EDF/DER. 1997. *Manuel utilisateur de CA-SIS 3.0*, EDF.

Girault, P., and S. Delille. 1995. Description of ETNA Cells, Physical and geometrical configuration. EDF report HE-14/95/053.

Guyon, G. 1997. Role of the model user in results obtained from simulation software program. *Proc. Building Simulation 97, Prague, Czech Republic*.

Jaulin, L., and E. Walter. 1993. Guaranteed nonlinear parameter estimation from bounded-error data via intervals analysis. *Mathematics and Computer in Simulations*, (2)123-137.

Jensen, S.O. 1993. Model validation and development. In Research Final Report, PASSYS: Part II, Commission of the European Communities DGXII.

Klein, T., and W.A. Beckman. 1986. TRNSYS v 14.2: Transient systems simulation program, SEL. University of Wisconsin, Madison.

Lomas, K.J., and H. Eppel. 1992. Sensitivity analysis techniques for building thermal simulation programs. *Energy and Buildings*, (19):21-44.

Martin, C.J., and D.M.J. Watson. 1993. Empirical validation of the model SERI-RES using data from test rooms. *Building and Environment*, (2) 175-187.

Moinard, S., G. Guyon, and N. Ramdani. 1998. Comparison between EDF ETNA and GENEC test-cells developed with AxBU, APACHE, CA-SIS, CLIM2000, DOE-2, SERI-RES, M2M, IDA and PROMETHEUS. IEA Task 22 Report.

Moore, R. 1992. Parameters sets from bounded-error data. *Mathematics and Computer in Simulations*, 7(34):113-119.

Palomo, E., J. Marco, and H. Madsen. 1991. Methods to compare measurements and simulations. In *Proc. IBPSA'91 Building Simulation Conference, Sophia-Antipolis, Nice, France*.

Palomo, E. 1994. Empirical whole model validation environment. Statistical evaluation methods. In, ed. S.O. Jensen, Validation of Building Simulation Programs, Part II. EUR-15116-EN, European Commision, DGXII.

Palomo, E., and G. Guyon. 1998. Application of parameters identification techniques to models errors diagnosis in building thermal analysis. IEA Task 22 Report, to be published.

Rahni, N. 1998. Validation des modèles et variabilité des parametres: Analyse de sensibilité et d'incertitude - Procedures d'optimisation, application à des modèles de thermique du batiment. Ph.D. thesis, Paris XII Univ., France.

Ramdani, N. 1994. Validation expérimentale et analyse des signaux: Développement d'une méthodologie de comparaison modèle/mesures en thermique du bâtiment. Ph.D. thesis, Paris XII Univ., France.

Ramdani, N., Y. Candau, S. Dautin, S. Delille, N. Rahni, and P. Dalicieux. 1997. How to improve building thermal simulation programs by use of spectral analysis. *Energy and Buildings*, 25: 223-242.

Tabary, L., and N. Ramdani. 1995. An error analysis method applied to a building simulation software: An example of applications and its results. *Proc. Building Simulation 95, Madison, Wisc., USA*.

Walter, E., and H. Piet-Lahanier. 1990a. Estimation of parameters bounds from bounded-error data: A survey. *Mathematics and Computer in Simulations*, (32):449-468.

Walter, E, and H. Piet-Lahanier. 1990b. Characterization of non-connected parameter uncertainty regions. *Mathematics and Computer in Simulations*, (32):553-560.